Medium-duty Electric Vehicle Infrastructure Planning and Operations in Urban Transportation Networks

by

Amir Davatgari
B.Sc., Sharif University of Technology , 2018
M.Sc., Purdue University, 2021

DISSERTATION

Submitted in partial fulfillment of the requirements
for the degree of Doctor of Philosophy in Civil Engineering
in the Graduate College of the
University of Illinois at Chicago, 2024

Chicago, Illinois

Defense Committee:
Abolfazl (Kouros) Mohammadian, Professor, University of Illinois Chicago, Chair and Advisor
Taner Cokyasar, Research Consultant, Argonne National Laboratory
Bo Zou, Associate Professor, University of Illinois Chicago
Jane Lin, Professor, University of Illinois Chicago
Kazuya Kawamura, Professor, College of Urban Planning and Policy, University of Illinois Chicago

This Dissertation is Dedicated to

Yalda Mohammadi

My beloved wife who has always been a compassionate friend and a supportive colleague throughout my PhD degree.

ACKNOWLEDGMENT

I would like to express my deepest gratitude to my advisor, Dr. Abolfazl (Kouros) Mohammadian, for his continuous support, guidance, and invaluable insights throughout my PhD degree. His expertise, encouragement, and commitment to my academic and professional growth have been instrumental in shaping the outcome of this research.

A heartfelt thank you also goes to Dr. Taner Cokyasar, whose mentorship has been an enriching part of this academic endeavor. His constant guidance, support, advice, and friendship throughout my PhD degree have been invaluable.

I extend my appreciation to the members of the committee, Dr. Jane Lin, Dr. Bo Zou, and Dr. Kazuya Kawamura, for their time, expertise, and thoughtful feedback that have strengthened the overall quality of this work.

I am also grateful to Argonne National Laboratory for funding my research and providing the data sources. This material is based upon work supported by the U.S. Department of Energy, Office of Science, under contract number DE-AC02-06CH11357. This material is sponsored by the U.S. Department of Energy (DOE) Vehicle Technologies Office (VTO) under the Systems and Modeling for Accelerated Research in Transportation (SMART) Mobility Laboratory Consortium, an initiative of the Energy Efficient Mobility Systems (EEMS) Program. Erin Boyd, a DOE Office of Energy Efficiency and Renewable Energy (EERE) manager, played an important role in establishing the project concept, advancing implementation, and provid-

ACKNOWLEDGMENT (Continued)

ing guidance. I would like to thank Aymeric Rousseau and Joshua Auld for their continued support.

Finally, I would like to express my sincere appreciation to my family for their unwavering support during my studies. To my parents, Nahid and Mohammad, thank you for consistently motivating me and being always positive about my work and research. To my lovely wife, Yalda, I extend my heartfelt gratitude for your love, support, motivation, guidance, and friendship. A special acknowledgment goes to my sister, Roya, who has always paved the way for me in all aspects of life. Her support and encouragement have been invaluable throughout my academic journey.

AD

CONTRIBUTIONS OF AUTHORS

In Chapter 1, the study plan and contribution of this research are introduced. Chapter 2 presents a paper (currently under review) authored by Amir Davatgari, Taner Cokyasar, Anirudh Subramanyam, Jeffrey Larson, and Abolfazl (Kouros) Mohammadian titled "Electric Vehicle Supply Equipment Location and Capacity Allocation for Fixed-Route Networks," in which I served as the primary author. The breakdown of contributions is as follows: Study conception and design were conducted by A. Davatgari, T. Cokyasar, and A. Subramanyam; data collection was performed by A. Davatgari; analysis and interpretation of results were carried out by A. Davatgari and T. Cokyasar; draft manuscript preparation involved A. Davatgari, T. Cokyasar, and J. Larson. All authors reviewed the results and approved the final version of the manuscript. This manuscript is available online on arXiv: `https://doi.org/10.48550/arXiv.2305.00806`.

Chapter 3 represents a paper (currently under review) authored by Amir Davatgari, Taner Cokyasar, Omer Verbas, and Abolfazl (Kouros) Mohammadian titled "Heuristic Solutions to the Single Depot Electric Vehicle Scheduling Problem with Next Day Operability Constraints," in which I served as the primary author. The contributions are as follows: Study conception and design were conducted by A. Davatgari and T. Cokyasar; data collection was performed by A. Davatgari; analysis and interpretation of results were carried out by A. Davatgari, T. Cokyasar, and Omer Verbas; draft manuscript preparation involved A. Davatgari, T. Cokyasar, and O.

CONTRIBUTIONS OF AUTHORS (Continued)

Verbas. All authors reviewed the results and approved the final version of the manuscript. This manuscript is available online on arXiv: `https://doi.org/10.48550/arXiv.2309.09707`.

Chapter 4 represents another paper (currently under review) authored by Amir Davatgari, Omer Verbas, Taner Cokyasar, and Abolfazl (Kouros) Mohammadian titled "Heuristic Solutions to the Single Depot Electric Vehicle Scheduling Problem with Next Day Operability Constraints," in which I served as the primary author. The contributions are as follows: Study conception and design were conducted by A. Davatgari and T. Cokyasar; data collection was performed by A. Davatgari; analysis and interpretation of results were carried out by A. Davatgari, T. Cokyasar, and Omer Verbas; draft manuscript preparation involved A. Davatgari, T. Cokyasar, and O. Verbas. All authors reviewed the results and approved the final version of the manuscript. Finally, Chapter 5 presents the conclusion, policy implications, and study limitations.

TABLE OF CONTENTS

TABLE OF CONTENTS (Continued)

CHAPTER **PAGE**

LIST OF TABLES

LIST OF FIGURES

SUMMARY

This dissertation focuses on the electrification of freight and transit vehicles as a sustainable solution to mitigate greenhouse gas emissions. The primary objectives of this dissertation focuses on efficiently addressing Electric Vehicle Supply Equipment Location and Capacity Allocation (EVSELCA) problems, optimizing Single Depot Electric Vehicle Scheduling Problem (SDEVSP) for urban transit systems, and optimizing the Electric Bus Scheduling and Charger Location (EBSCL). By addressing these objectives, this dissertation aims to contribute to the advancement of sustainable and environmentally responsible transportation in the context of heavy electric vehicles. In this regard, first, this dissertation introduces a mixed-integer linear programming (MILP) model for EVSELCA. This model optimizes the locations and number and type of chargers, aiming to minimize strategic investment costs. Second, the research proposes a two-step solution to SDEVSP. In the first step, an integer programming model generates blocks of consecutive trips. The second step introduces an MILP, which involves chaining these blocks to create efficient bus runs, optimizing recharging between blocks, and ensuring next day operability constraints are satisfied. Finally, the dissertation presents an integrated model that optimizes both electric vehicle scheduling and charger location. Each developed model undergoes computational performance analysis, and a comprehensive case study is designed to provide key managerial and policy insights, along with extensive sensitivity analyses aiming to identify crucial parametric levers.

CHAPTER 1

INTRODUCTION

1.1 Background and motivation

The widespread use of fossil fuels for meeting energy needs has long been associated with the generation of greenhouse gas (GHG) emissions, which exert detrimental effects on our climate and environment (Metz et al. 2007). Among the various sectors contributing to GHG emissions, the transportation sector stands out as a significant player, accounting for a substantial 27% of total emissions in the United States (US Environmental Protection Agency 2020). Within the transportation landscape, medium and heavy-duty vehicles, as well as buses, stand as pivotal contributors to the GHG challenge, further intensifying the environmental dilemma (Metz et al. 2007).

In particular, medium-duty (MD) and heavy-duty (HD) trucks have raised concerns, being responsible for a significant 26% of emissions within the transportation sector (US Environmental Protection Agency 2020). With the increase in e-commerce, the number of trucks and their total miles traveled are expected to grow, resulting in higher emissions from freight transportation (Hovland Consulting LLC 2020). This trend underscores the pressing need for sustainable alternatives in the freight industry.

Truck electrification is a promising solution that can help mitigate the negative impact of their GHG emissions (Talebian et al. 2018). By replacing conventional engines with electric

motors, the transportation sector can significantly reduce GHG emissions. While conventional trucks can cover long distances without refueling, a critical factor for electric trucks is their relatively shorter battery range (Hovland Consulting LLC 2020). The range of a typical HD/MD electric truck is around 130 miles (Lightning eMotors 2022), which limits their use in long-haul trucking. Additionally, the time required for recharging electric trucks can be another significant challenge: Depending on the charging method, it can take 20 minutes to 8 hours to fully recharge their batteries (Bennett et al. 2021). This can lead to significant downtimes for trucking companies, which affect their productivity and profitability. Therefore, efficiently solving electric vehicle supply equipment location and capacity allocation (EVSELCA) problems is crucial to making electric trucks a viable option for commercial transportation.

On a parallel track, the realm of public transit faces a different yet equally significant challenge. Public transportation plays a crucial role in cities by providing accessible, affordable, efficient, and equitable mobility options for travelers while helping to alleviate congestion. However, buses have taken center stage as primary contributors to carbon emissions in the transit sector, emitting an average of 0.643 lbs of carbon per passenger-mile traveled (FTA 2010). This figure is a staggering 76% higher than the emissions from the next highest transit mode, light-rail systems. Recognizing the urgency of reducing carbon emissions and improving air quality, the U.S. Department of Transportation (DOT) Federal Transit Administration has committed billions of dollars to achieve a net-zero emissions economy by 2050 (The White House 2022).

Similar to freight, within public transit, transitioning to electric vehicles (EVs) holds the promise of significantly reducing harmful emissions and enhancing local air quality (Muñoz et al. 2022). Nevertheless, the adoption of electric buses comes with its own set of challenges. One major concern is the higher upfront cost of EVs compared to conventional DVs (Muñoz et al. 2022). This cost disparity can impose financial barriers, particularly when there is a need to replace a large number of buses in existing fleets. Driving range, long charging time, and electricity grid impact of EVs are other issues to be tackled. Although technological advancements have improved battery capacity and charging speeds, EVs still have a shorter range and longer downtime compared to DVs. This can pose operational challenges, especially for longer routes that require long periods of operation. To overcome these challenges, one potential solution is to increase the number of buses in operation. However, the high cost of electric buses can be a hindrance. Therefore, optimizing EV scheduling becomes essential to minimize the bus fleet size and idle time, while ensuring sufficient recharging during idle periods. Additionally, there is the task of strategically placing charging locations to accommodate charging activities. The use of pantograph chargers, which supply power from the top of the bus through scissor-like arms, introduces issues related to space occupancy and cost Daliah (2023). A growing concern is the optimal placement of these chargers across the transit service network, including terminal garages, to ensure seamless electric vehicle operations.

1.2 Study objectives

The primary objective of this thesis is to strategically plan for the infrastructure required to support heavy electric vehicles. To achieve this goal, we have defined three key objectives,

each addressing critical aspects of electric vehicle deployment and operation within urban environments:

Objective 1: the first objective focuses on the efficient resolution of Electric Vehicle Supply Equipment Location and Capacity Allocation (EVSELCA) problems. This objective is pivotal in making electric trucks a viable and sustainable option for commercial transportation. The EVSELCA problem entails identifying optimal locations, quantities, and types of electric vehicle supply equipment, commonly referred to as "EV chargers." The primary aim is to minimize strategic investment costs while ensuring compliance with operational constraints. By tackling this challenge, we aim to pave the way for cost-effective and strategically located charging infrastructure that supports the seamless integration of electric trucks into commercial transport networks.

Objective 2: the second objective focuses on the optimization of electric vehicle scheduling, which is essential for minimizing bus fleet sizes and idle times, while ensuring sufficient recharging during idle periods. This objective primarily targets urban transit systems, where electric buses play a pivotal role in reducing emissions and enhancing sustainable mobility. Through advanced scheduling techniques, our aim is to enhance the operational efficiency of electric bus fleets, making them a more economically and environmentally viable choice for public transportation services.

Objective 3: the third objective focuses on the strategically locating chargers for electric buses, with a focus on minimizing strategic investment costs while adhering to operational constraints. While bus garages are primary locations for housing chargers, placing chargers

at trip end locations could facilitate charging activities. Regular recharging at these locations could make electric buses function similarly to conventional diesel-powered buses. Resolving this necessitates solving a facility location problem (FLP) to identify optimal locations from a candidate set for housing these chargers. FLP decisions often have strategic implications, as altering or retracting them can be challenging and costly. Identifying the candidate facility set requires consideration of vehicle schedules as well.

1.3 Organization of the Thesis

This thesis includes four chapters. Chapter 2: Electric Vehicle Supply Equipment Location and Capacity Allocation (EVSELCA). In this chapter, we introduce a mathematical model and propose a metaheuristic solution approach to address the intricate challenges related to the optimal deployment of charging infrastructure. Additionally, this chapter includes a thorough presentation and analysis of our research findings. Chapter 3: Single Depot Electric Vehicle Scheduling Problem (SDEVSP). Within this chapter, we provide a mathematical model and propose a heuristic solution approach designed to efficiently address the challenges associated with scheduling electric vehicles. Furthermore, we present and discuss the results obtained from two distinct urban areas, namely Chicago, IL and Austin, TX. Chapter 4: Electric Bus Scheduling and Charger Location (EBSCL). In this chapter, we formulate an MILP model. Our objective is to optimize electric bus schedules and strategically identify charging facilities, especially at trip end locations. We offer comprehensive insights into the utilized data, and present case studies to showcase the practicality of the proposed model. Finally, Chapter 5 presents the conclusion, policy implications, and study limitations.

CHAPTER 2

ELECTRIC VEHICLE SUPPLY EQUIPMENT LOCATION AND CAPACITY ALLOCATION

2.1 Introduction

In this chapter, we present a new approach to solve the EVSELCA problem by developing a mixed-integer linear programming (MILP) model that optimizes the locations and numbers of various types of chargers. The objective of the MILP model is to minimize strategic investment costs while satisfying operational constraints. To achieve this, our MILP model takes into account fixed-facility costs, charger costs, recharging energy costs, and value of time (VOT) costs. VOT costs account for the time spent traveling to a recharging station, waiting and recharging, and returning to service. By finding the optimal balance between these cost components, our model can aid in long-term EVSELCA planning. Because of the problem's complexity, we use a clustering approach that groups customers into clusters and allows recharging only after servicing these clusters. Moreover, we propose a metaheuristic solution method based on a genetic algorithm (GA) to generate near-optimal solutions within a reasonable time, enabling the model to be applied to large-scale instances.

Our study contributes to the EVSELCA literature through four crucial aspects. First, when designing EVSELCA for the freight transportation industry, it is important to consider fixed routes (Ghamami, Zockaie, and Nie 2016, Wang, Wang, and Lin 2016). The EVSELCA prob-

lem has often been modeled as an EV location routing problem (EVLRP), which solves both the strategic charging facility location (and allocation in some cases) problem and the routing problem Yang and Sun (2015), Hof, Schneider, and Goeke (2017), Schiffer and Walther (2017), Schiffer, Schneider, and Laporte (2018), Schiffer and Walther (2018). Although creating new routes for EVs may lead to better solutions (Shojaei et al. 2022), the convention in this industry is to use a fixed-route approach, usually electrifying existing routes that are shorter than an EV range. Second, the location and allocation decisions should be made jointly, with the numbers and types of chargers for each location serving as decision variables (Davatgari 2021, Ghamami et al. 2020, Londoño and Granada-Echeverri 2019). The type of charger impacts recharging time and infrastructure costs, while the number of chargers affects installation costs and waiting times for recharging. Thus, strategic planning requires a balance between waiting costs, recharging time, and infrastructure costs through the selection of appropriate types and numbers of chargers. Third, it is crucial to take into account the dynamic nature of charging demand over time since it plays a critical role, as highlighted by Ghamami, Zockaie, and Nie (2016) and Wang, Wang, and Lin (2016). If multiple recharging events happen simultaneously, the design would require an excessive number of chargers. By considering dynamic charging demand for recharging, however, it becomes possible to schedule these events in a way that uses fewer chargers, resulting in higher utilization rates. Therefore, the spatiotemporal aspect of the problem is conserved. Fourth, partial recharging is crucial and should be considered in the EVSELCA problem (Li, Huang, and Mason 2016). In some cases, electric trucks may be partially recharged because of operational time limitations, and a model without this con-

sideration may produce impractical solutions. Overall, the main contribution of our study is its comprehensive consideration of these four key aspects of the EVSELCA problem. While other studies in the literature have addressed these aspects, they modeled each aspect either individually or as a combinatorial subset that lacked one of the other aspects.

In Section 2.2 we first review studies that have used various approaches to tackle the EVSELCA problem. We provide a more comprehensive definition of the EVSELCA problem and clearly demonstrate the MILP in Section 2.3. Metaheuristic solution procedures are developed in Section 2.4. The setup and results of numerical experiments are presented in Section 2.5 using data from POLARIS, the Planning and Operations Language for Agent-based Regional Integrated Simulation developed at Argonne National Laboratory (Auld et al. 2016). In Section 3.6 we conclude the study and discuss potential future research directions.

2.2 Literature review

Many studies explore the strategic planning of EV charger placement (Ghamami et al. 2020, Zhu et al. 2016, Ghamami, Zockaie, and Nie 2016, Li, Huang, and Mason 2016, Wang, Wang, and Lin 2016, Davatgari 2021, Whitehead et al. 2021, Liu and Song 2018, Worley, Klabjan, and Sweda 2012, Speth et al. 2022, Londoño and Granada-Echeverri 2019). Most of these studies focus on light-duty (LD) vehicles rather than MD and HD vehicles (hereafter called trucks) (Ghamami et al. 2020, Zhu et al. 2016, Liu and Song 2018, Ghamami, Zockaie, and Nie 2016, Wang, Wang, and Lin 2016). For example, Davatgari (2021) develops a mixed-integer nonlinear programming (MINLP) model to solve the EVSELCA problem considering routing

for LD vehicles. Our study, in contrast, aims to solve the EVSELCA problem for trucks with fixed routes.

The planning of EV chargers for trucks is different from that of LD vehicles because trucks often require fast recharging due to the high value of time in the business world and because their larger batteries necessitate longer recharging times. Although fast-charging equipment can reduce recharging time, it is also more costly. Additionally, unlike LD vehicles, trucks typically have predetermined routes and operate with time limits enforced by law and regulations (Williams 2020). Given the differences, the EVSELCA problem for trucks is an area that has not been extensively explored in the literature, and this study aims to address this gap. The studies conducted on this problem generally can be classified into two categories based on their methodology: (1) a coverage-oriented approach (Whitehead et al. 2021, Speth et al. 2022) and (2) a demand-oriented approach (Worley, Klabjan, and Sweda 2012, Londoño and Granada-Echeverri 2019, Liu and Song 2018); our study falls into the second category.

Coverage-oriented approaches aim to maximize the geographical coverage of a recharging service. This approach often assumes that each charger location can meet the recharging demand of a circular area. The objective is then to maximize the coverage of a region while minimizing the number of circles, which represents the number of charger locations. Such approaches often do not consider demand intensity, the potential impact of queuing during recharging events, and other operational constraints such as the inability to recharge two vehicles simultaneously using one charger. For instance, Speth et al. (2022) model a coverage-oriented approach as a linear programming (LP) model to determine charger locations in order to minimize the num-

ber of chargers while maximizing the geographic coverage. After locating a charger, the model uses queuing to estimate the number of chargers in each EV charging facility. In contrast, our research focuses on locating EV chargers and optimizing the number of chargers using a demand-oriented approach that considers the impact of queuing during charging events.

Demand-oriented approaches aim to minimize strategic (e.g., infrastructure and charger) costs and operational (e.g., time and energy) costs subject to demand-conservation constraints that guarantee a certain level of service based on a deployment decision. This approach is often modeled as an EVLRP in the literature, which involves determining the allocation and location of EV chargers and solving the routing problem (Yang and Sun 2015, Hof, Schneider, and Goeke 2017, Schiffer and Walther 2017, Schiffer, Schneider, and Laporte 2018, Schiffer and Walther 2018). For example, Worley, Klabjan, and Sweda (2012) develop an MILP to determine charger locations that minimize travel time, recharging costs, and construction costs. While our study shares a similar objective, our approach differs in the vehicle routing aspect because we focus on fixed routes. Additionally, our study takes into account several important factors that were not considered in the aforementioned research, such as allocation, dynamic charging demand, and partial recharging. By taking into account these additional variables, we aim to provide a more accurate and comprehensive solution. Another study by Liu and Song (2018) uses a bilevel approach to model the EVLRP. In this approach, the upper level focuses on minimizing GHG emissions by determining the optimal location of chargers, while the lower level solves a mixed-traffic assignment of LD vehicles and trucks. Our study differs from this approach as well. Specifically, we use a fixed-route approach to minimize the costs associated

with charger placement, location, energy consumption, the value of time for recharging, and detouring. Additionally, like our previous example, we take into account allocation, dynamic charging demand, and partial recharging. Table I summarizes relevant studies and compares our study with their objectives, model types, and other features.

TABLE I: Summary of the existing literature on EVSELCA

Study	Vehicle	Objective	Model	(i)	(ii)	(iii)	(iv)	(v)	(vi)	(vii)	(viii)
Ghamami et al. (2020)	LD	Minimize infrastructure cost and users' detour, waiting, and charging delay	MINLP	✓	✓	✓	-	-	-	✓	N/A
Zhu et al. (2016)	LD	Minimize construction costs and station access cost	MILP	✓	✓	✓	-	-	-	-	N/A
Ghamami, Zockaie, and Nie (2016)	LD	Minimize infrastructure and battery costs, and recharging and queueing time	MINLP	-	✓	✓	-	✓	-	✓	-
Li, Huang, and Mason (2016)	LD	Minimize cost of construction and relocation of existing chargers	MILP	✓	✓	-	-	-	✓	-	N/A
Wang, Wang, and Lin (2016)	LD	Minimize operational and construction costs	MILP	-	✓	-	-	✓	-	-	✓
Davatgari (2021)	LD	Minimize total system travel time and construction cost of EV charging infrastructure	MINLP	✓	✓	✓	✓	-	-	-	N/A
Whitehead et al. (2021)	MD	Maximize coverage	MILP	✓	✓	-	-	-	-	-	N/A
Liu and Song (2018)	MD	Minimize emissions	MPCC	✓	✓	-	-	-	-	-	N/A
Worley, Klabjan, and Sweda (2012)	HD	Minimize transportation, recharging, and charging station placement costs	MILP	✓	✓	-	-	-	-	-	N/A
Speth et al. (2022)	HD	Maximize coverage	LP	✓	✓	-	-	-	-	-	N/A
Londoño and Granada-Echeverri (2019)	HD	Minimize energy consumption, charger installation, and routing costs	MILP	✓	✓	-	-	-	-	-	N/A
This study	MD/HD	Minimize charger, location, energy, value of time for recharging and detouring costs	MILP	-	✓	✓	✓	✓	✓	✓	✓

(i) Route choice, (ii) Location planning, (iii) Number of chargers, (iv) Charger type, (v) Dynamic charging demand over time in a day, (vi) Partial recharging, (vii) Queuing, (viii) Multiple fixed routes, MPCC: Mathematical programs with complementarity constraints, N/A: Not applicable.

2.3 Problem definition

We now formally describe the EVSELCA problem, which we model as an MILP. To ease reading, we use calligraphic letters to represent sets (e.g., $\mathcal{R}$), uppercase Roman letters for parameters (e.g., $\overline{T}$), lowercase Roman letters for variables and indices (e.g., y_f), and Greek letters (e.g., α) as superscripts to modify parameters and variables.

Let $\mathcal{C}$ denote a set of customers, and let $\mathcal{R}$ denote a set of trucks serving these customers with routes to be electrified while keeping their routes intact. (That is, regenerating routes from scratch due to electrification is not of interest.) We call these routes *EV routes*. The goal of the EVSELCA is to allow EVs to complete their daily operations at a minimum cost by planning recharging infrastructure and scheduling recharging activities. Although solving a strategic decision-making problem, the model respects operational limitations, such as total route time and charging capacities. Each EV route $r \in \mathcal{R}$ contains a subset of customers, denoted by the subset $\mathcal{C}_r = \{c_{0r}, c_{1r}, ..., c_{ir}, ..., c_{Nr}\}$ satisfying $\forall i \neq j, (i,j) \neq (0,N)$ by the order of visits: $c_{0r} \rightarrow c_{1r} \rightarrow ..., c_{N-1,r} \rightarrow c_{Nr}$, where $c_{0r} = c_{Nr}$ = depot of route $r \in \mathcal{R}$. A set of charger types $\mathcal{K}$ can be located at a set of candidate facilities $\mathcal{F}$. The optimization time is discretized into a set of time steps $\mathcal{T}$. Table II and Table III provide sets and parameters used in the model, respectively. Note that the definition of sets will be modified in Section 2.4.2 as we will cluster the customers to simplify the problem.

We now state our critical modeling assumptions (and note that some of these can easily be relaxed). We assume customer demand is deterministic, which means that the travel sequences in the routes remain unchanged over time except for accommodating on-route charging activ-

ities. Furthermore, the adoption of EV technology does not change the truck routes, and the customer visit sequences of a route are assumed to be the same as in conventional truck routes. Additionally, EVs are assumed to be identical. The amount of energy received from a charger type is assumed to be a linear function of recharging time, and the energy spent by EVs is assumed to be a linear function of travel time. Furthermore, we assume there is a fixed set of locations for possible EV charging facilities.

TABLE II: Sets used in the MILP.

Set	**Definition**
$\mathcal{C}$	set of customers, $\mathcal{C} = \cup_{r\in\mathcal{R}}\mathcal{C}_r$
$\mathcal{C}_r$	subset of customers in route $r \in \mathcal{R}$, $\mathcal{C}_r = \{c_{0r}, c_{1r}, ..., c_{ir}, ..., c_{Nr}\}$ satisfy $\forall i \neq j, (i,j) \neq (0,N)$ by continuation order of visit: $c_{0r} \to c_{1r} \to ..., c_{N-1,r} \to c_{Nr}$, where $c_{0r} = c_{Nr}$ = depot of route $r \in \mathcal{R}$
$\mathcal{C}_{rft}$	subset of customers in route $r \in \mathcal{R}$, after serving which the vehicle may visit $f \in \mathcal{F}$ for recharging at time step $t \in \mathcal{T}$, that is $\mathcal{C}_{rft} = \Big\{c \in \mathcal{C}_r \mid \sum_{j=0}^{i-1}\left[T^{\tau}_{c_{jr},c_{j+1,r}} + T^{\kappa}_{c_{jr}}\right] + T^{\kappa}_{c_{ir}} \leq D_t \leq \overline{T} - \sum_{j=i}^{N}\left[T^{\tau}_{c_{jr},c_{j+1,r}} + T^{\kappa}_{c_{jr}}\right]\Big\} \forall r \in \mathcal{R}, f \in \mathcal{F}, t \in \mathcal{T}$
$\mathcal{F}$	set of candidate EV charging facility locations
$\mathcal{F}_{c_{ir}}$	subset of candidate locations that the vehicle of $r \in \mathcal{R}$, after serving customer c_{ir}, may possibly visit for recharging, that is, $\mathcal{F}_{c_{ir}} = \Big\{f \in \mathcal{F} \mid T^{\tau}_{c_{ir}f} \leq \overline{B} \wedge T^{\tau}_{c_{ir}f} + T^{\tau}_{fc_{i+1,r}} \leq \overline{T} - \sum_{j=0}^{N-1}\left[T^{\tau}_{c_{jr},c_{j+1,r}} + T^{\kappa}_{c_{jr}}\right] + \min\{0, \frac{B^{\iota}_r - \sum_{j=0}^{N-1} T^{\tau}_{c_{jr},c_{j+1,r}} - B^{\omega}_r}{R_K}\}\Big\} \forall c_{ir} \in \mathcal{C}_r \setminus \{c_{Nr}\}, r \in \mathcal{R} \bigcup \Big\{f \in \mathcal{F} \mid T^{\tau}_{c_{Nr}f} \leq \overline{B} \wedge T^{\tau}_{c_{Nr}f} + T^{\tau}_{fc_{Nr}} \leq \overline{T} - \sum_{j=0}^{N-1}\left[T^{\tau}_{c_{jr},c_{j+1,r}} + T^{\kappa}_{c_{jr}}\right] + \min\{0, \frac{B^{\iota}_r - \sum_{j=0}^{N-1} T^{\tau}_{c_{jr},c_{j+1,r}} - B^{\omega}_r}{R_K}\}\Big\} \forall r \in \mathcal{R}$
$\mathcal{K}$	set of charger types, $\mathcal{K} = \{1, 2, 3, ..., K\}$
$\mathcal{R}$	set of routes
$\mathcal{T}$	set of time steps
$\mathcal{T}_{c_{ir}f}$	subset of time steps in the beginning of which the vehicle of $r \in \mathcal{R}$ after serving customer c_{ir} may possibly visit $f \in \mathcal{F}_{c_{ir}}$ for recharging, that is, $\mathcal{T}_{c_{ir}f} = \Big\{t \in \mathcal{T} \mid \sum_{j=0}^{i-1}\left[T^{\tau}_{c_{jr},c_{j+1,r}} + T^{\kappa}_{c_{jr}}\right] + T^{\kappa}_{c_{ir}} \leq D_t \leq \overline{T} - \sum_{j=i}^{N-1}\left[T^{\tau}_{c_{jr},c_{j+1,r}} + T^{\kappa}_{c_{jr}}\right]\Big\} \forall c_{ir} \in \mathcal{C}_r, r \in \mathcal{R}, f \in \mathcal{F}_{c_{ir}}$

TABLE III: Parameters used in the MILP.

Parameter	Definition
$\overline{B}$	maximum battery capacity in time unit
B_r^{ι}	initial battery capacity of EV route $r \in \mathcal{R}$
B_r^{ω}	desired final battery capacity of EV route $r \in \mathcal{R}$
C^{ρ}	value of time spent for recharging and driving to recharging facility
C_k^{ξ}	energy cost of recharging per time unit with charger type $k \in \mathcal{K}$
C_k^{ν}	cost of installing charger type $k \in \mathcal{K}$ per time unit
C_f^{ϕ}	fixed charging facility cost at candidate location $f \in \mathcal{F}$ per time unit
D_t	actual time associated with time step $t \in \mathcal{T}$, that is $D_t = tT^{\Delta}$
$\mathbb{M}$	an adequately large number, e.g., $\mathbb{M} > 2\overline{B}$
R_k	recharging amount received from charger type $k \in \mathcal{K}$ per time unit
$\overline{T}$	maximum allowed operational time for each EV route
T^{Δ}	duration of time steps
$T_{c_{ir}c_{jr}}^{\tau}$	travel time from customer $c_{ir} \in \mathcal{C}_r$ to customer $c_{jr} \in \mathcal{C}_r$ by EV route $r \in \mathcal{R}$
$T_{c_{ir}f}^{\delta}$	detour travel time from customer $c_{ir} \in \mathcal{C}_r$ by EV route $r \in \mathcal{R}$ to $f \in \mathcal{F}$
$T_{c_{ir}}^{\kappa}$	time spent for serving customer $c_{ir} \in \mathcal{C}_r$ by EV route $r \in \mathcal{R}$

We let the binary variable $x_{c_{ir}fkt} = 1$ denote that the EV of route $r \in \mathcal{R}$ recharges at $f \in \mathcal{F}$ using charger type $k \in \mathcal{K}$ at time step $t \in \mathcal{T}$ immediately after serving customer $c_{ir} \in \mathcal{C}_r$; $x_{c_{ir}fkt} = 0$, otherwise. To ensure $x_{c_{ir}fkt}$ represents the desired value, we keep track of the start and end time for recharging an EV for c_{ir}, f, and k with continuous variables $s_{c_{ir}fk}$ and $e_{c_{ir}fk}$. Let the binary variable $x_{c_{ir}fkt}^{\alpha} = 1$ indicate that the EV route $r \in \mathcal{R}$ is recharging at facility $f \in \mathcal{F}$ using charger $k \in \mathcal{K}$ after detouring from $c_{ir} \in \mathcal{C}_r$ for time steps, where the associated time D_t falls within the range $[0, s_{c_{ir}fk})$ (excluding $t \in \mathcal{T}$). On the other hand, let binary variable $x_{c_{ir}fkt}^{\beta} = 1$ denote that the EV route $r \in \mathcal{R}$ is recharging at facility $f \in \mathcal{F}$ using charger $k \in \mathcal{K}$ after detouring from $c_{ir} \in \mathcal{C}_r$ for time steps, where the associated time D_t falls within the range $[0, e_{c_{ir}fk}]$ (including $t \in \mathcal{T}$).

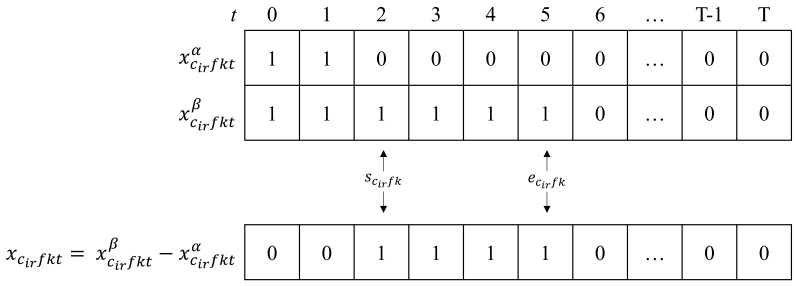

Figure 1: Example of how $x_{c_{ir}fkt}$ is maintained.

Figure 1 illustrates how our constraints ensure the variable $x_{c_{ir}fkt}$ takes the desired value. In this example, EV route $r \in \mathcal{R}$ starts recharging at facility $f \in \mathcal{F}$ using charger $k \in \mathcal{K}$ after detouring from $c_{ir} \in C_r$ at time $s_{c_{ir}fk}$, where the equivalent time step is 2 and ends at time $e_{c_{ir}fk}$, where the equivalent time step is 5. The binary variable $x^{\alpha}_{c_{ir}fkt} = 1$ for all time steps preceding and *excluding* time step 2, while the binary variable $x^{\beta}_{c_{ir}fkt} = 1$ for all time steps preceding and *including* time step 5. Consequently, utilizing the equation $x_{c_{ir}fkt} = x^{\beta}_{c_{ir}fkt} - x^{\alpha}_{c_{ir}fkt}$, the binary variable $x_{c_{ir}fkt}$ is 1 only for the expected time steps that are in the interval $[2, 5]$.

The binary variable $y_f = 1$ denotes $f \in \mathcal{F}$ is open; $y_f = 0$, otherwise. The variable $z_{fk} \in \mathbb{Z}_{\geq 0}$ denotes the number of charger type $k \in \mathcal{K}$ allocated to $f \in \mathcal{F}$. Refer to Table XVI for the definitions of all variables used in the model. The EVSELCA problem is formulated as follows:

TABLE IV: Variables used in the MILP.

Variable	Definition
$b'_{c_{ir}f}$	remaining battery capacity (in time units) before arriving $f \in \mathcal{F}$ for EV route $r \in \mathcal{R}$ after detouring from $c_{ir} \in \mathcal{C}_r$
$b_{c_{ir}}$	remaining battery capacity (in time units) before serving $c_{ir} \in \mathcal{C}_r$ of EV route $r \in \mathcal{R}$
$d_{c_{ir}}$	departure time from $c_{ir} \in \mathcal{C}_r$ of EV route $r \in \mathcal{R}$
$u_{c_{ir}fk}$	duration of recharging time EV route $r \in \mathcal{R}$ spends at $f \in \mathcal{F}$ using $k \in \mathcal{K}$ after detouring from $c_{ir} \in \mathcal{C}_r$
$w_{c_{ir}fk}$	duration of waiting time EV route $r \in \mathcal{R}$ spends to recharge at $f \in \mathcal{F}$ using $k \in \mathcal{K}$ after detouring from $c_{ir} \in \mathcal{C}_r$
$s_{c_{ir}fk}$	time that EV route $r \in \mathcal{R}$ starts recharging at $f \in \mathcal{F}$ using $k \in \mathcal{K}$ after detouring from $c_{ir} \in \mathcal{C}_r$
$e_{c_{ir}fk}$	time that EV route $r \in \mathcal{R}$ ends recharging $f \in \mathcal{F}$ using $k \in \mathcal{K}$ after detouring from $c_{ir} \in \mathcal{C}_r$
$q_{c_{ir}fk}$	$\begin{cases} 1 & \text{if EV route } r \in \mathcal{R} \text{ detours from } c_{ir} \in \mathcal{C}_r \text{ to } f \in \mathcal{F} \text{ to recharge using } k \in \mathcal{K} \\ 0 & \text{otherwise} \end{cases}$
$x^{\alpha}_{c_{ir}fkt}$	$\begin{cases} 1 & \text{if EV route } r \in \mathcal{R} \text{ is recharging at facility } f \in \mathcal{F} \text{ using charger } k \in \mathcal{K} \text{ after detouring from } c_{ir} \in \mathcal{C}_r \text{ for time steps where the equivalent time, } D_t, \text{ falls within the range } [0, s_{c_{ir}fk}) \text{ (excluding } t \in \mathcal{T}) \\ 0 & \text{otherwise} \end{cases}$
$x^{\beta}_{c_{ir}fkt}$	$\begin{cases} 1 & \text{if EV route } r \in \mathcal{R} \text{ is recharging at facility } f \in \mathcal{F} \text{ using charger } k \in \mathcal{K} \text{ after detouring from } c_{ir} \in \mathcal{C}_r \text{ for time steps where the equivalent time, } D_t, \text{ falls within the range } [0, e_{c_{ir}fk}] \text{ (including } t \in \mathcal{T}) \\ 0 & \text{otherwise} \end{cases}$
$x_{c_{ir}fkt}$	$\begin{cases} 1 & \text{if EV route } r \in \mathcal{R} \text{ is recharging at } f \in \mathcal{F} \text{ using } k \in \mathcal{K} \text{ at time step } t \in \mathcal{T} \text{ after detouring from } c_{ir} \in \mathcal{C}_r \\ 0 & \text{otherwise} \end{cases}$
y_f	$\begin{cases} 1 & \text{if a charging facility is located at } f \in \mathcal{F} \\ 0 & \text{otherwise} \end{cases}$
z_{fk}	number of charger type $k \in \mathcal{K}$ installed at $f \in \mathcal{F}$, $z_{fk} \in \mathbb{Z}_{\geq 0}$

$$\min \mathbf{C} = \sum_{\substack{c_{ir} \in \mathcal{C}_r, r \in \mathcal{R}, \\ f \in \mathcal{F}_{c_{ir}}, k \in \mathcal{K}}} \left[C^{\rho} \left(T^{\delta}_{c_{ir}f} q_{c_{ir}fk} + w_{c_{ir}fk} \right) + (C^{\rho} + C^{\xi}_{k}) u_{c_{ir}fk} \right] + \sum_{f \in \mathcal{F}} C^{\phi}_{f} y_f + \sum_{f \in \mathcal{F}, k \in \mathcal{K}} C^{\nu}_{k} z_{fk} \tag{2.1}$$

subject to,

$$x_{c_{ir}fkt} = x^{\beta}_{c_{ir}fkt} - x^{\alpha}_{c_{ir}fkt} \qquad \forall c_{ir} \in \mathcal{C}_r, r \in \mathcal{R}, f \in \mathcal{F}_{c_{ir}}, k \in \mathcal{K}, t \in \mathcal{T}_{c_{ir}f} \tag{2.2}$$

$$\sum_{c_{ir} \in \mathcal{C}_{rft}, r \in \mathcal{R}} x_{c_{ir}fkt} \leq z_{fk} \qquad \forall f \in \mathcal{F}, k \in \mathcal{K}, t \in \mathcal{T} \tag{2.3}$$

$$u_{c_{ir}fk} \leq T^{\Delta} \sum_{t \in \mathcal{T}_{c_{ir}f}} x_{c_{ir}fkt} \qquad \forall c_{ir} \in \mathcal{C}_r, r \in \mathcal{R}, f \in \mathcal{F}_{c_{ir}}, k \in \mathcal{K} \tag{2.4}$$

$$T^{\Delta} \sum_{t \in \mathcal{T}_{c_{ir}f}} x_{c_{ir}fkt} - u_{c_{ir}fk} \leq T^{\Delta} - \epsilon \qquad \forall c_{ir} \in \mathcal{C}_r, r \in \mathcal{R}, f \in \mathcal{F}_{c_{ir}}, k \in \mathcal{K} \tag{2.5}$$

$$z_{fk} \leq \mathbb{M} y_f \qquad \forall f \in \mathcal{F}, k \in \mathcal{K} \tag{2.6}$$

$$u_{c_{ir}fk} \leq \mathbb{M} q_{c_{ir}fk} \qquad \forall c_{ir} \in \mathcal{C}_r, r \in \mathcal{R}, f \in \mathcal{F}_{c_{ir}}, k \in \mathcal{K} \tag{2.7}$$

$$w_{c_{ir}fk} \leq \mathbb{M} q_{c_{ir}fk} \qquad \forall c_{ir} \in \mathcal{C}_r, r \in \mathcal{R}, f \in \mathcal{F}_{c_{ir}}, k \in \mathcal{K} \tag{2.8}$$

$$q_{c_{ir}fk} \leq \sum_{t \in \mathcal{T}_{c_{ir}f}} x_{c_{ir}fkt} \qquad \forall c_{ir} \in \mathcal{C}_r, r \in \mathcal{R}, f \in \mathcal{F}_{c_{ir}}, k \in \mathcal{K} \tag{2.9}$$

$$x_{c_{ir}fkt} \leq q_{c_{ir}fk} \qquad \forall c_{ir} \in \mathcal{C}_r, r \in \mathcal{R}, f \in \mathcal{F}_{c_{ir}}, k \in \mathcal{K}, t \in \mathcal{T}_{c_{ir}f} \tag{2.10}$$

$$\sum_{f \in \mathcal{F}_{c_{ir}}, k \in \mathcal{K}} q_{c_{ir}fk} \leq 1 \qquad \forall c_{ir} \in \mathcal{C}_r, r \in \mathcal{R} \tag{2.11}$$

$$b'_{c_{ir}f} \leq b_{c_{ir}} - T^{\tau}_{c_{ir}f} + \mathbb{M}(1 - \sum_{k \in \mathcal{K}} q_{c_{ir}fk}) \qquad \forall c_{ir} \in \mathcal{C}_r, r \in \mathcal{R}, f \in \mathcal{F}_{c_{ir}} \tag{2.12}$$

$$b'_{c_{ir}f} \leq \mathbb{M} \sum_{k \in \mathcal{K}} q_{c_{ir}fk} \qquad \forall c_{ir} \in \mathcal{C}_r, r \in \mathcal{R}, f \in \mathcal{F}_{c_{ir}} \tag{2.13}$$

$$b'_{c_{ir}f} + \sum_{k \in \mathcal{K}} u_{c_{ir}fk} \leq \overline{B} \qquad \forall c_{ir} \in \mathcal{C}_r, r \in \mathcal{R}, f \in \mathcal{F}_{c_{ir}} \tag{2.14}$$

$$b_{c_{i+1,r}} \leq b_{c_{ir}} - T^{\tau}_{c_{ir},c_{i+1,r}}(1 - \sum_{f \in \mathcal{F}_{c_{ir}}, k \in \mathcal{K}} q_{c_{ir}fk}) + \mathbb{M} \sum_{f \in \mathcal{F}_{c_{ir}}, k \in \mathcal{K}} q_{c_{ir}fk} \quad \forall c_{ir} \in \mathcal{C}_r, r \in \mathcal{R} \tag{2.15}$$

$$b_{c_{i+1,r}} \leq \sum_{f \in \mathcal{F}_{c_{ir}}} \left[b'_{c_{ir}f} + \sum_{k \in \mathcal{K}} \left(R_k u_{c_{ir}fk} - T^{\tau}_{f c_{i+1,r}} q_{c_{ir}fk} \right) \right] + \mathbb{M}\Big(1 - \sum_{f \in \mathcal{F}_{c_{ir}}, k \in \mathcal{K}} q_{c_{ir}fk}\Big) \quad \forall c_{ir} \in \mathcal{C}_r, r \in \mathcal{R} \tag{2.16}$$

$$b_{c_{0r}} = B^{\iota}_r \qquad \forall c_{ir} \in \mathcal{C}_r, r \in \mathcal{R} \tag{2.17}$$

$$b_{c_{Nr}} \geq B^{\omega}_r \qquad \forall c_{ir} \in \mathcal{C}_r, r \in \mathcal{R} \tag{2.18}$$

$$d_{c_{ir}} = \sum_{j=0}^{i-1} \left[T^{\tau}_{c_{jr},c_{j+1,r}} + \sum_{f \in \mathcal{F}_{c_{ir}}, k \in \mathcal{K}} (T^{\delta}_{c_{jr}f} q_{c_{jr}fk} + u_{c_{jr}fk} + w_{c_{jr}fk}) + T^{\kappa}_{c_{jr}} \right] + T^{\kappa}_{c_{ir}} \quad \forall c_{ir} \in \mathcal{C}_r, r \in \mathcal{R} \tag{2.19}$$

$$s_{c_{ir}fk} = d_{c_{ir}} + T^{\tau}_{c_{ir}f} q_{c_{ir}fk} + w_{c_{ir}fk} \quad \forall c_{ir} \in \mathcal{C}_r, r \in \mathcal{R}, f \in \mathcal{F}_{c_{ir}}, k \in \mathcal{K}, t \in \mathcal{T}_{c_{ir}f} \tag{2.20}$$

$$e_{c_{ir}fk} = d_{c_{ir}} + T^{\tau}_{c_{ir}f} q_{c_{ir}fk} + w_{c_{ir}fk} + u_{c_{ir}fk} \quad \forall c_{ir} \in \mathcal{C}_r, r \in \mathcal{R}, f \in \mathcal{F}_{c_{ir}}, k \in \mathcal{K}, t \in \mathcal{T}_{c_{ir}f} \tag{2.21}$$

$$s_{c_{ir}fk} \leq D_t + T^{\Delta} - \epsilon + \mathbb{M}\left(1 - q_{c_{ir}fk} + x^{\alpha}_{c_{ir}fkt}\right) \quad \forall c_{ir} \in \mathcal{C}_r, r \in \mathcal{R}, f \in \mathcal{F}_{c_{ir}}, k \in \mathcal{K}, t \in \mathcal{T}_{c_{ir}f} \tag{2.22}$$

$$s_{c_{ir}fk} \geq D_t + T^{\Delta} - \mathbb{M}(2 - q_{c_{ir}fk} - x^{\alpha}_{c_{ir}fkt}) \quad \forall c_{ir} \in \mathcal{C}_r, r \in \mathcal{R}, f \in \mathcal{F}_{c_{ir}}, k \in \mathcal{K}, t \in \mathcal{T}_{c_{ir}f} \tag{2.23}$$

$$e_{c_{ir}fk} \leq D_t - \epsilon + \mathbb{M}\left(1 - q_{c_{ir}fk} + x^{\beta}_{c_{ir}fkt}\right) \quad \forall c_{ir} \in \mathcal{C}_r, r \in \mathcal{R}, f \in \mathcal{F}_{c_{ir}}, k \in \mathcal{K}, t \in \mathcal{T}_{c_{ir}f} \tag{2.24}$$

$$e_{c_{ir}fk} \geq D_t - \mathbb{M}\left(2 - q_{c_{ir}fk} - x^{\beta}_{c_{ir}fkt}\right) \quad \forall c_{ir} \in \mathcal{C}_r, r \in \mathcal{R}, f \in \mathcal{F}_{c_{ir}}, k \in \mathcal{K}, t \in \mathcal{T}_{c_{ir}f} \tag{2.25}$$

$$d_{c_{Nr}} \leq \overline{T} \qquad \forall r \in \mathcal{R} \tag{2.26}$$

$$x_{c_{ir}fkt},\ x^{\alpha}_{c_{ir}fkt},\ x^{\beta}_{c_{ir}fkt},\ y_f,\ q_{c_{ir}fk} \in \{0,1\}, z_{fk} \in \mathbb{Z}_{\geq 0}, b_{c_{ir}},\ d_{c_{ir}},\ u_{c_{ir}fk},\ w_{c_{ir}fk} \in \mathbb{R}_{\geq 0}.$$

The objective function (2.1) minimizes the costs associated with detouring, waiting, recharging, energy consumption, charging facility, and charger installation. Note that all costs are minimized per time unit (e.g., one day). Constraint (2.2) defines the variable $x_{c_{ir}fkt}$ in terms of $x^{\alpha}_{c_{ir}fkt}$ and $x^{\beta}_{c_{ir}fkt}$. Constraint (2.3) ensures that the total number of trucks charging at a time step does not exceed the capacity of the charging facility. Constraint (2.4) satisfies that the recharging time does not exceed the total time occupied by a truck at a facility, and constraint (2.5) ensures that a truck does not occupy a charger while not recharging. Constraint (2.6) guarantees that if a charging facility is not located at f, a charger should not be allocated. Constraints (2.7) and (2.8) enforce the charging time $u_{c_{ir}fk}$ and waiting time $w_{c_{ir}fk}$ to be zero

when recharging does not occur. Constraints (2.9) and (2.10) ensure that if the truck recharges, the charger will be considered occupied at least in one time step. Constraint (2.11) ensures that a truck can recharge only at one facility using one charger type after serving a customer.

Constraints (2.12)–(2.16) define the remaining battery of trucks (in time units) after serving every customer ($b_{c_{ir}}$) and immediately before arriving at a charging facility ($b'_{c_{ir}f}$). Constraints (2.17) and (2.18) enforce the initial and desired final battery capacity to be equal to B_r^{ι} and B_r^{ω}, respectively. Constraint (2.19) defines the departure time of trucks after serving each customer. Constraints (2.22) and (2.23) define the variable $x^{\alpha}_{c_{ir}fkt}$. Similarly, constraints (2.24) and (2.25) define the variable $x^{\beta}_{c_{ir}fkt}$. Constraint (2.26) ensures that the total operational time cannot exceed the maximum allowed operational time for each EV route.

2.4 Metaheuristic solution approaches with clustering

We now present a metaheuristic solution procedure for solving the EVSELCA problem, as defined by Equations 2.1—2.26. We employ a metaheuristic approach because of substantial growth in solution space of the EVSELCA problem as the problem size increases. First, we adopt a clustering approach in Section 2.4.1 to simplify the problem. This involves redefining sets, parameters, and variables in the MILP so that it can be used with clusters, as shown in Section 2.4.2. Although clustering can help address the computational difficulty at a smaller scale, we further develop a metaheuristic solution method using the GA to tackle the EVSELCA problem in Section 2.4.3. Then, in Section 2.4.4 we describe a hybrid solution approach that combines the GA and MILP solvers.

2.4.1 Clustering

EVSELCA problems (Equations 2.1–2.26) can be complex, making solving them impractical for large-scale instances. To overcome this challenge, we adopt a clustering approach proposed by Cokyasar, Davatgari, and Mohammadian (2023). This approach simplifies the problem by grouping customers into clusters and limiting recharging to after the completion of service at these clusters. That is, rather than considering recharging after any customer, we create clusters of customers and assume recharging occurs only after completing service at these clusters.

The clustering method aims to identify the best cut-points with a given number of clusters to satisfy the following conditions:

i. All customers in a cluster must belong to a single route.

ii. The intersection of any two clusters must be empty.

iii. Customers in a cluster must follow the order of service.

iv. The distance traveled within a cluster must not exceed a certain threshold, such as a portion of the EV range.

This clustering method uses an optimization model that maximizes the spatial difference between clusters. In this model, the binary variable, $p_{nc_{ir}} = 1$ indicates cut $n \in \mathcal{n}$ is placed right after customer c_{ir}. The auxiliary binary variable $m_{nc_{ir}}$ regulates the order of cuts and conserves sequencing. Table V provides sets and parameters used in the clustering model. The clustering optimization model is formulated as follows.

$$\max \sum_{\substack{c_{ir} \in \mathcal{C}_r, r \in \mathcal{R}, \\ n \in \mathcal{n}}} T^{\tau}_{c_{ir}c_{jr}} p_{nc_{ir}} \tag{2.27}$$

subject to,

$$p_{nc_{ir}} = m_{nc_{ir}} - m_{nc_{i+1,r}} \qquad \forall c_{ir} \in \mathcal{C}_r, r \in \mathcal{R}, n \in \mathcal{n} \tag{2.28}$$

$$m_{nc_{i+1,r}} - m_{nc_{ir}} \geq 0 \qquad \forall c_{ir} \in \mathcal{C}_r, r \in \mathcal{R}, n \in \mathcal{n} \tag{2.29}$$

$$\sum_{c_{ir} \in \mathcal{C}_r, r \in \mathcal{R}} p_{nc_{ir}} = 1 \qquad \forall n \in \mathcal{n} \tag{2.30}$$

$$\sum_{n \in \mathcal{n}} p_{nc_{ir}} \leq 1 \qquad \forall c_{ir} \in \mathcal{C}_r, r \in \mathcal{R} \tag{2.31}$$

The objective function (2.27) maximizes the total travel time between clusters to ensure that clusters are sufficiently apart from each other. Constraints (2.28) and (2.29) conserve the order of cuts, preventing cut n from being placed after cut $n+1$. Constraint (2.30) ensures that every cut is positioned immediately after one specific point, while constraint (2.31) ensures that only one cut can be placed after a particular point. The model in Cokyasar, Davatgari, and Mohammadian (2023) also presents the within the cluster travel time constraints. As these constraints require more parametric definition, we refrain providing these constraints for simplicity.

With a predetermined number of clusters, the clustering method may not always guarantee a feasible solution because the travel time within clusters could exceed a preset threshold. In our analysis, we start with a small $|\mathcal{n}|$, solve the problem, and increment $|\mathcal{n}|$ by one until a feasible solution is obtained. Therefore, we find the minimum number of clusters ($|\mathcal{n}| > 0$) and

their partitioning. Note that such an approach sacrifices the solution quality to gain solution speed. Our analysis in the upcoming sections will be a product of this sacrifice, and a real case should better be handled with $|\mathcal{N}|$ large enough to obtain a higher quality solution.

TABLE V: Sets and variables used in the clustering model.

Set	**Definition**
$\mathcal{N}$	set of cut-points for clustering
Variable	**Definition**
$p_{nc_{ir}}$	$\begin{cases} 1 & \text{if cut } n \in \mathcal{N} \text{ is placed right after customer } c_{ir} \\ 0 & \text{otherwise} \end{cases}$
$m_{nc_{ir}}$	auxiliary binary variable regulating the order of cuts

2.4.2 Transformation

In switching from customer to cluster, the definition of some sets, parameters, variables, and constraints changes. It is straightforward to redefine $\mathcal{C}$ from being the set of individual customers to being the set of clusters of customers. We then define a new parameter $T^{\gamma}_{c_{ir}}$ to represent the total travel time based on the order of visits within the cluster for serving customers of cluster c_{ir} by the EV route r. Moreover, we redefine parameters $T^{\tau}_{c_{ir}c_{jr}}$ to be the travel time from the last customer of cluster c_{ir} to the first customer of cluster c_{jr} and $T^{\delta}_{c_{ir}f}$ to be the travel time from the last customer of cluster c_{ir} to the location of facility f.

With these changes, we redefine the subset $\mathcal{C}_{rft}$ in Definition 1.

Definition 1. *For a given $r \in \mathcal{R}$, $f \in \mathcal{F}$, and $t \in \mathcal{T}$,*

$$\mathcal{C}_{rft} = \Big\{ c \in \mathcal{C}_r | \sum_{j=0}^{i-1} \Big[T^{\tau}_{c_{jr},c_{j+1,r}} + T^{\kappa}_{c_{jr}} + T^{\gamma}_{c_{jr}} \Big] + T^{\kappa}_{c_{ir}} + T^{\gamma}_{c_{ir}} \\ \leq t \leq \overline{T} - \sum_{j=i}^{N} \Big[T^{\tau}_{c_{jr},c_{j+1,r}} + T^{\kappa}_{c_{jr}} + T^{\gamma}_{c_{ir}} \Big] \Big\}.$$

The definition of $\mathcal{C}_{rft}$ requires that an EV route can recharge only after serving the last customer of the cluster, rather than in the middle of the cluster. Therefore, $\mathcal{C}_{rft}$ refers to the subset of clusters on route $r \in \mathcal{R}$ that the vehicle must complete before it can visit $f \in \mathcal{F}$ for recharging at time step $t \in \mathcal{T}$.

Furthermore, we redefine $\mathcal{F}_{c_{ir}}$ and $\mathcal{T}_{c_{ir}f}$ due to the changes made to the definition of parameters. The updated $\mathcal{F}_{c_{ir}}$ denotes the subset of facilities that the vehicle of route $r \in \mathcal{R}$ can visit after serving customers of cluster c_{ir}, as defined in Definition 2. Similarly, $\mathcal{T}_{c_{ir}f}$ denotes the subset of time steps during which the vehicle of route $r \in \mathcal{R}$ can visit $f \in \mathcal{F}_{c_{ir}}$ for recharging after serving customers of cluster c_{ir}, as defined in Definition 3.

Definition 2. *For a given $c_{ir} \in \mathcal{C}_r \setminus \{c_{Nr}\}$ and $r \in \mathcal{R}$,*

$$\mathcal{F}_{c_{ir}} = \Big\{ f \in \mathcal{F} | T^{\tau}_{c_{ir}f} \leq \overline{B} \wedge T^{\tau}_{c_{ir}f} + T^{\tau}_{fc_{i+1,r}} \leq \overline{T} - \sum_{j=0}^{N-1} \Big[T^{\tau}_{c_{jr},c_{j+1,r}} + T^{\kappa}_{c_{jr}} + T^{\gamma}_{c_{jr}} \Big] \\ + \min\{0, \frac{B^{\iota}_r - \sum_{j=0}^{N-1} [T^{\tau}_{c_{jr},c_{j+1,r}} + T^{\gamma}_{c_{jr}}] - B^{\omega}_r}{R_K}\} \Big\} \\ \bigcup \Big\{ f \in \mathcal{F} | T^{\tau}_{c_{Nr}f} \leq \overline{B} \wedge T^{\tau}_{c_{Nr}f} + T^{\tau}_{fc_{Nr}} \leq \overline{T} - \sum_{j=0}^{N-1} \Big[T^{\tau}_{c_{jr},c_{j+1,r}} + T^{\kappa}_{c_{jr}} + T^{\gamma}_{c_{jr}} \Big] \\ + \min\{0, \frac{B^{\iota}_r - \sum_{j=0}^{N-1} [T^{\tau}_{c_{jr},c_{j+1,r}} + T^{\gamma}_{c_{jr}}] - B^{\omega}_r}{R_K}\} \Big\}.$$

Definition 3. *For a given $c_{ir} \in \mathcal{C}_r$, $r \in \mathcal{R}$, and $f \in \mathcal{F}_{c_{ir}}$,*

$$\mathcal{T}_{c_{ir}f} = \Big\{ t \in \mathcal{T} | \sum_{j=0}^{i-1} \Big[T^{\tau}_{c_{jr},c_{j+1,r}} + T^{\kappa}_{c_{jr}} + T^{\gamma}_{c_{jr}} \Big] + T^{\kappa}_{c_{ir}} + T^{\gamma}_{c_{ir}} \\ \leq t \leq \overline{T} - \sum_{j=i}^{N-1} \Big[T^{\tau}_{c_{jr},c_{j+1,r}} + T^{\kappa}_{c_{jr}} + T^{\gamma}_{c_{jr}} \Big] \Big\}.$$

Next, we replace the term *customer* with *cluster* wherever it is used in Table II, Table III, and Table XVI. Following the changes we have made to the sets, parameters, and variable definitions, we replace the constraints 2.12, 2.15, and 2.19 with 2.32, 2.33, and 2.34, respectively.

$$b'_{c_{ir}f} \leq b_{c_{ir}} - T^{\gamma}_{c_{ir}} - T^{\tau}_{c_{ir}f} + \mathbb{M}(1 - \sum_{k \in \mathcal{K}} q_{c_{ir}fk}) \qquad \forall c_{ir} \in \mathcal{C}_r, r \in \mathcal{R}, f \in \mathcal{F}_{c_{ir}} \tag{2.32}$$

$$b_{c_{i+1,r}} \leq b_{c_{ir}} - (T^{\tau}_{c_{ir},c_{i+1,r}} + T^{\gamma}_{c_{ir}})(1 - \sum_{f \in \mathcal{F}_{c_{ir}}, k \in \mathcal{K}} q_{c_{ir}fk}) + \mathbb{M} \sum_{f \in \mathcal{F}_{c_{ir}}, k \in \mathcal{K}} q_{c_{ir}fk} \\ \forall c_{ir} \in \mathcal{C}_r, r \in \mathcal{R} \tag{2.33}$$

$$d_{c_{ir}} = \sum_{j=0}^{i-1} \Bigg[T^{\tau}_{c_{jr},c_{j+1,r}} + T^{\gamma}_{c_{jr}} + \sum_{f \in \mathcal{F}_{c_{ir}}, k \in \mathcal{K}} (T^{\delta}_{c_{jr}f} q_{c_{jr}fk} + u_{c_{jr}fk} + w_{c_{jr}fk}) + T^{\kappa}_{c_{jr}} \Bigg] \\ + T^{\kappa}_{c_{ir}} + T^{\gamma}_{c_{ir}} \qquad \forall c_{ir} \in \mathcal{C}_r, r \in \mathcal{R} \tag{2.34}$$

2.4.3 The genetic algorithm

In this study we employ a tailored genetic algorithm to solve the EVSELCA problem. The GA is an evolutionary optimization search technique that has been widely used to solve MILPs (Katoch, Chauhan, and Kumar 2021). Algorithm 1 provides pseudocode for the approach; the functions used therein are detailed in the Supplementary Material. Key decision variables in the model are $q_{c_{ir}fk}$, $x_{c_{ir}fkt}$, y_f, and z_{fk}, which are the same as in Table XVI with the redefined $\mathcal{C}$. Among key variables, y_f and z_{fk} relate to strategic decision-making, while $x_{c_{ir}fkt}$ aids in

making an operational decision. At the tactical level, $q_{c_{ir}fk}$ plays an important role since it determines after which cluster to recharge, where to recharge, and what type of charger to use. To this end, we begin with exploring a solution for the tactical variable that implicitly impacts solutions to strategic variables and provides implied time bounds for the recharging time. That is, a solution to other variables can be derived for given solutions to $q_{c_{ir}fk}$. First, N^{pop} number of solutions for $q_{c_{ir}fk}$ is generated via the INITIALIZATION function as an initial population. In the initialization step we randomly select a number of clusters, following which a recharging is planned; and we select a facility for the recharging using a roulette wheel selection method (i.e., closer facilities have a higher chance of being selected). Once the *where* aspect of $q_{c_{ir}fk}$ is addressed, we randomly select a type of charger for those facilities that were just picked to be visited. This population is then passed into CROSSOVER and MUTATION functions to potentially find a better solution.

In Algorithm 1, T_r^{ρ} was used to represent the route travel time minus the time spent serving customers, recharging, and waiting, as defined in Definition 4.

Definition 4. *For a given $r \in \mathcal{R}$,*

$$T_r^{\rho} = \sum_{j=0}^{N-1} \left[T^{\tau}_{c_{jr},c_{j+1,r}} + \sum_{f \in \mathcal{F}_{c_{ir}}, k \in \mathcal{K}} T^{\delta}_{c_{jr}f} q_{c_{jr}fk} \right].$$

The value of z_{fk} is estimated to calculate the objective value for each given $q_{c_{ir}fk}$ in the initial population. For a given $q_{c_{ir}fk}$ equal to 1, z_{fk} can get values between 1 and $\sum_{c_{ir} \in C_{rft}, r \in \mathcal{R}} q_{c_{ir}fk}$ as Lemma 1 denotes. (See the Appendix for proofs of lemmas). The trade-off between the

waiting time and facility cost depends on z_{fk}. The maximum of z_{fk} ($\sum_{c_{ir} \in C_{rft}, r \in \mathcal{R}} q_{c_{ir}fk}$) implies zero waiting time as stated in Lemma 2 but high charger cost. We use a local search to find a suitable z_{fk} value. In this regard we first calculate the objective value ($\mathbf{C}$) for the upper and lower bounds of z_{fk}; if the former has a lower objective value, we update z_{fk} by subtracting chargers using zlUpdater (Algorithm A.7). Otherwise (i.e., the latter has a lower objective value), we increase the value of z_{fk} using zlUpdater (Algorithm A.8) until $\mathbf{C}$ reaches the minimum. The Evaluator function from (Algorithm A.5) updates the value of z_{fk}.

Lemma 1. *For a given $f \in \mathcal{F}$ and $k \in \mathcal{K}$, $z^*_{fk} \in [1, \sum_{c_{ir} \in C_{rft}, r \in \mathcal{R}} q_{c_{ir}fk}]$, if $\sum_{c_{ir} \in C_{rft}} q_{c_{ir}fk} > 1$; otherwise, $z^*_{fk} = 0$.*

Lemma 2. *For a given $f \in \mathcal{F}$ and $k \in \mathcal{K}$, $w_{c_{ir}fk} = 0$, if $z_{fk} = \sum_{c_{ir} \in C_{rft}} q_{c_{ir}fk}$.*

In each step of Evaluator, given $q_{c_{ir}fk}$ and z_{fk}, we calculate other variables using LowerLevelEvaluator (Algorithm A.6). In LowerLevelEvaluator, we first calculate the recharging time ($u_{c_{ir}fk}$) using uCalculation (Algorithm A.10). We assume that trucks recharge at a facility for a duration sufficient to complete the trip if it is less than the maximum battery capacity minus the battery's current level; otherwise, they recharge to full capacity. Next, we calculate the wait time ($w_{c_{ir}fk}$) using wCalculation (Algorithm A.11). To do so, we follow the first-come-first-served rule: that is, vehicles recharge at a facility in the order of their arrival times. Given $q_{c_{ir}fk}$, $u_{c_{ir}fk}$, $w_{c_{ir}fk}$, and z_{fk}, calculation of other variables and therefore $\mathbf{C}$ is straightforward.

Algorithm 1: Pseudocode for genetic algorithm

Input : $\mathcal{C}_r$, $\mathcal{F}$, $\mathcal{F}_{c_{ir}}$, $\mathcal{K}$, $\mathcal{R}$, $\overline{B}$, B^{ι}, B^{ω}, B^{ι}_r, B^{ω}_r, $C^{\alpha=0}$, C^{ρ}, C^{ξ}_k, C^{ν}_k, C^{ϕ}_f, $\underline{N}$, $\bar{N}$, N^{pop}, N^{iter}, $N^{parents}$, P^{mutate}, R_k, $\overline{T}$, T^{Δ}, T^{ρ}_r, T^{μ}_r, $T^{\tau}_{c_{ir}c_{jr}}$, $T^{\delta}_{c_{ir}f}$, $T^{\kappa}_{c_{ir}}$

Output: $Sols(1)$

Function GAMain():

- $Sols \leftarrow \{\}$;
- **for** $i \leftarrow 1$ **to** N^{pop}, **do**
  - $Sols(i) \leftarrow$Initialization($\mathcal{C}_r$, $\mathcal{F}_{c_{ir}}$, $\mathcal{K}$, $\mathcal{R}$, $\overline{B}$, B^{ι}, B^{ω}, $C^{\alpha=0}$, T^{μ}_r, $T^{\delta}_{c_{ir}f}$);
  - /* Create N^{pop} solutions using Initialization function. */
- **for** $iter \leftarrow 1$ **to** N^{iter}, **do**
  - **for** $i \leftarrow 1$ **to** N^{pop}, **do**
    - $\mathbf{C}(Sols(i)) \leftarrow$ Evaluator($\mathcal{C}_r$, $\mathcal{F}$, $\mathcal{K}$, $\mathcal{R}$, $\mathcal{T}$, $\overline{B}$, B^{ι}_r, B^{ω}_r, C^{ρ}, C^{ξ}_k, C^{ν}_k, C^{ϕ}_f, $\underline{N}$, $\bar{N}$, R_k, $T^{\tau}_{c_{ir}c_{jr}}$, $T^{\kappa}_{c_{ir}}$, $T^{\delta}_{c_{ir}f}$, T^{ρ}_r, $Sols(i)$);
  - Sort $Sols$ ascending based on $\mathbf{C}(Sols)$ and set $Sols$ to the first $N^{parents}$ of $Sols$;
  - $CrossoverSols \leftarrow \{\}$;
  - **for** $i \leftarrow 1$ **to** $N^{parents}$, **do**
    - **for** $j \leftarrow 1$ **to** $N^{parents}$, **do**
      - **if** $i \neq j$, **then**
        - $CrossoverSols(i) \leftarrow$ Crossover($Sols$, i, j);
  - $MutationSols \leftarrow \{\}$;
  - **for** $i \leftarrow 1$ **to** $N^{parents}$, **do**
    - $MutationSols(i) \leftarrow$ Mutation($Sols(i)$, P^{mutate});
  - **for** $i \leftarrow 1$ **to** $N^{parents}$, **do**
    - $\mathbf{C}(CrossoverSols(i)) \leftarrow$ Evaluator($\mathcal{C}_r$, $\mathcal{F}$, $\mathcal{K}$, $\mathcal{R}$, $\mathcal{T}$, $\overline{B}$, B^{ι}_r, B^{ω}_r, C^{ρ}, C^{ξ}_k, C^{ν}_k, C^{ϕ}_f, $\underline{N}$, $\bar{N}$, R_k, $T^{\tau}_{c_{ir}c_{jr}}$, $T^{\kappa}_{c_{ir}}$, $T^{\delta}_{c_{ir}f}$, T^{ρ}_r, $CrossoverSols(i)$);
    - $\mathbf{C}(MutationSols(i)) \leftarrow$ Evaluator($\mathcal{C}_r$, $\mathcal{F}$, $\mathcal{K}$, $\mathcal{R}$, $\mathcal{T}$, $\overline{B}$, B^{ι}_r, B^{ω}_r, C^{ρ}, C^{ξ}_k, C^{ν}_k, C^{ϕ}_f, $\underline{N}$, $\bar{N}$, R_k, $T^{\tau}_{c_{ir}c_{jr}}$, $T^{\kappa}_{c_{ir}}$, $T^{\delta}_{c_{ir}f}$, T^{ρ}_r, $MutationSols(i)$);
  - Merge $Sols$, $CrossoverSols$, and $MutationSols$ to form $newSols$;
  - Sort $newSols$ ascending based on $\mathbf{C}(newSols)$;
  - Replace $Sols$ with first N^{pop} of $newSols$;

2.4.4 A hybrid solution approach supported by the genetic algorithm

The GA initializes with estimating values for $q_{c_{ir}fk}$ variables. A hybrid solution approach can be formed by feeding these GA-generated $q_{c_{ir}fk}$ solutions into an MILP solver as a constraint set. Therefore, the hybrid approach finds optimal solutions for fixed $q_{c_{ir}fk}$ decisions. This is especially useful because many solutions can be investigated in parallel. In the following section, the performance of this solution approach will be compared with that of the GA.

2.5 Case studies

This section describes the details of our experimental design and data in Section 2.5.1, demonstrates the performance and limitations of the GA and the hybrid methods in Table XIV, illustrates the impact of the time step duration on system cost in Section 2.5.3, and provides key managerial and policy insights along with extensive sensitivity analyses aiming to identify crucial parametric levers in Section 2.5.4–Section 2.5.7.

2.5.1 Design of experiments

We conduct numerical experiments using the Chicago metropolitan area. E-commerce daily demand and road network data are obtained from POLARIS (Auld et al. 2016). We utilize the framework developed by Cokyasar et al. (2022) to form parcel delivery truck routes. For a given set of customer and depot locations and other parameters (e.g., the operational time during a day and vehicle capacity) the framework yields vehicle routes that are the sequences of customers to be visited. Customers in these routes are aggregated at clusters using the RCP solution model in Cokyasar, Davatgari, and Mohammadian (2023).

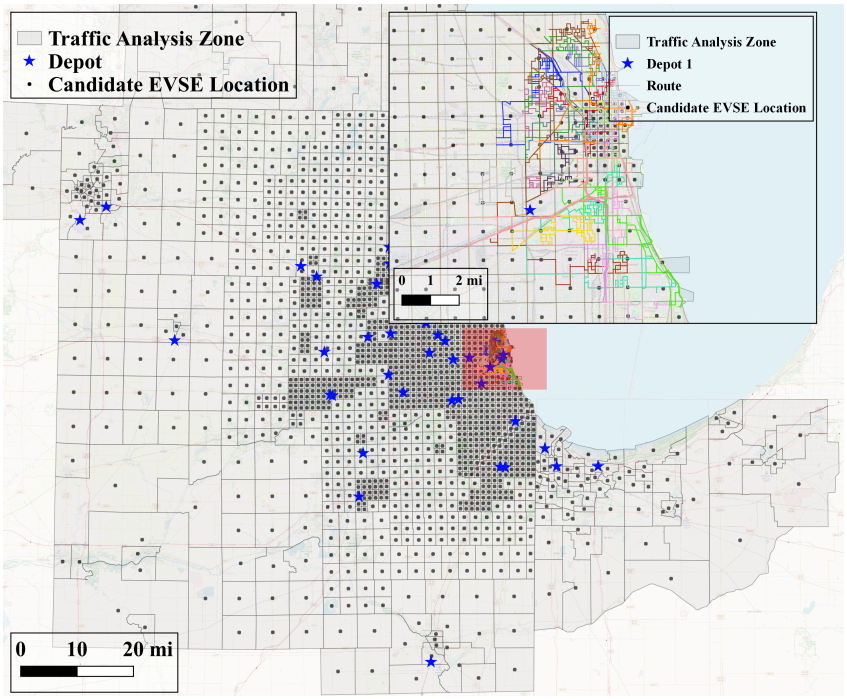

Figure 2: Illustrative EVSELCA problem instance in the Chicago metropolitan area. The main figure shows traffic analysis zones and depots used for e-commerce delivery in the area as well as candidate charging facility locations. The inset depicts the study region including links of routes and a depot of those routes. Links in the inset are color-coded, and each color indicates a specific route.

Figure 2 depicts an example problem layout. In this figure, the centroids of traffic analysis zones (TAZs), defined by metropolitan area organizations, represent candidate charging facility locations. In the experiments we use 20 routes depicted and their feeder depot, called depot 1. The depot serves 4,580 customers, and customers are aggregated at 89 clusters. Unless otherwise noted, in our experiments we consider four candidate locations, namely, the depot and the three closest centroids to the depot.

The problem parameters used, based on the literature (Electrify America 2022, Williams 2020, Ellis 2017, Davatgari 2021, Lightning eMotors 2022, Smith and Castellano 2015), are summarized in Table XIII. Aside from these parameters, we estimate $T^{\tau}_{c_{ir}c_{jr}}$, $T^{\kappa}_{c_{ir}}$, and $T^{\delta}_{c_{ir}f}$ using Manhattan distances and assuming a constant truck speed of 30 mph (Illinois State Police 2022). As with most studies in the literature, we consider three charger types with varying powers (Liu and Wang 2017, Yilmaz and Krein 2013). The average time required to power up a battery for 100 miles of range gain and charger installation costs are shown in Table VII, which are derived from the literature (Bennett et al. 2021). All costs in the objective function are converted to USD per day. To do so, the lifespans of chargers and facilities are set to 10 and 40 years, respectively (Bennett et al. 2021).

TABLE VI: Parametric values used.

C^{ϕ}_{f} (USD/day)	$T^{\kappa}_{c_{ir}}$ (minute)	$\overline{T}$ (hour)	$\overline{B}$ (minute)	B^{ι}_{r} (minute)	B^{ω}_{r} (minute)	C^{ξ}_{k} (USD/kWh)	C^{ρ} (USD/mile)
35	2	14	200	200	160	0.43	1.377

2.5.2 Computational performance of the GA and the hybrid methods

We analyze the computational performance of the GA and the hybrid methods and compare them with the MILP solved by Gurobi using $|\mathcal{R}|$ and $|\mathcal{F}|$ as problem size determinant levers. The three solution approaches are given the same clusters as an input to make the solutions

TABLE VII: Charger configuration.

Charger type	Power (kW)	Added driving range (mile)	Added driving charging time (minute)	Cost (USD×1000)
Basic	50	100	265	73
Moderate	180	100	88	157
Fast	360	100	29	228

comparable. A testbed of instances was generated utilizing simulated data from a depot in the Chicago metropolitan area serving e-commerce deliveries. As a baseline, the parametric design provided in Section 2.5.1 was utilized, and we selected three candidate charging facility locations closest to the depot and three random routes out of 20 that the depot serves. While keeping the three charging facility locations and the depot as candidates, a subset of routes $|\mathscr{R}| \in \{3, 6, 10, 15, 20\}$ were randomly (following a uniform distribution for the selection probability) selected to generate 20 problem instances for each number of routes. Another 20 instances for each of $|\mathscr{F}| \in \{3, 6, 10, 15, 20\}$ were generated such that the closest charging facility locations to the depot were chosen as candidates, and the three routes in the baseline were used. These 200 instances were then solved by using the three methods with a limit of 600 seconds of computational time per instance. Some of the instances were initially solved without a time limit to observe the impact of the time limit choice. After many compute hours, we did not observe considerable improvement in the solution quality compared to the solutions obtained at the time limit. In the GA, we solved each instance five times and provide statistics of the performances. All computations were carried out on an Intel® Xeon® Gold 6138 CPU @2.0

GHz workstation with 128 GB of RAM and 40 cores. Problem instances were solved by using the Python 3.8.8 interface to the commercial solver Gurobi 10.0 (Gurobi Optimization, LLC 2020).

Table VIII reports the computational performance of the MILP model solved via Gurobi, the GA, and the hybrid solution approaches. The first columns specify the scenario. The MILP columns denote the number of instances that could be solved (i.e., built and reported a feasible solution within 600 seconds) and the number of instances for which optimality was reached, respectively. In the GA, since each instance was solved five times, the maximum number of instances that could be possibly solved was 100 for each scenario. We see that all approaches were unable to produce a feasible solution within the time limit in some runs. GA columns indicate the minimum, maximum, average, and standard deviation of the percent gap between the best objective of the Gurobi-reported solution and the best solution found in the five GA runs. A negative average percent indicates that the GA's best solutions were better than that of the MILP. Hybrid columns follow a similar presentation approach for the hybrid approach.

In Table VIII, we observe that an increase in $|\mathcal{R}|$ impacts the problem difficulty more than does an increase in $|\mathcal{F}|$. Using the MILP through a solver can address only small problems. The GA performs better than the hybrid approach. Note that large gap percentages in the GA and the hybrid should not be a sign of poor performance because these percentages are based mostly on nonoptimal solutions obtained from the optimizer.

Figure 3 shows the solution time to the best solution per scenario and solution approach. The hybrid approach is the fastest in finding a solution in most scenarios. The time-to-solution

TABLE VIII: Summary of computational performance of the three solution approaches.

Scenario		MILP		GA					Hybrid				
		# Solved	# Opt	# Solved	Δ Gap (%)				# Solved	Δ Gap (%)			
					Min	Max	Avg	Std		Min	Max	Avg	Std
# Routes	3	20	19	92	0	19.9	2.1	5.3	17	7	30	19	9.7
	6	20	0	99	-0.5	30	6.6	7.6	12	4.1	18	9.7	4.8
	10	16	0	95	-6.7	6.7	0.8	3.7	3	-3	2.5	0.1	2.3
	15	6	0	94	-10	3.8	-3.5	4.5	1	-5.8	-5.8	-5.8	0
	20	4	0	89	-5.2	-3.2	-3.8	0.8	0	-	-	-	-
# Locations	3	20	19	88	0	19.8	1.3	4.5	17	8.5	29	21	7.3
	6	20	17	91	0	19.8	3.2	6.1	17	0	31	24	7.9
	10	20	8	90	-0.1	25	3.9	7.8	17	0	27	13	9.4
	15	20	1	94	0	11	1.1	2.5	17	0	10	5.9	2.9
	20	20	1	89	-1.4	15.5	1.9	3.4	17	0	26	5.4	5.6

Note: Δ Gap is calculated by one minus the division of the best solution obtained by the corresponding method to the best objective reported by the MILP solver.

comparison between an increasing number of routes and an increasing number of depots supports the claim that $|\mathcal{R}|$ is a key metric in problem difficulty. In Figure 3a supported by Table VIII, we can observe that 6–20 routes scenarios were not solved to optimality within 600 seconds. Figure 3a and Figure 3b show that the GA provides quick solutions that are indeed not far off from the MILP (see Table VIII for a quality comparison).

2.5.3 Impact of time step duration on system cost

The duration of the time step, T^{Δ}, discretizes the time and control charger availability. Understandably, it can have a considerable impact on the solution quality. It is clear that a large T^{Δ} could lead to a higher system cost as more chargers would be needed if an idle charger is shown to be occupied. For instance, $T^{\Delta} = 60$ minutes will label a charger unavailable for an hour even if a vehicle uses the charger for a portion of this time. To assess the impact of T^{Δ}

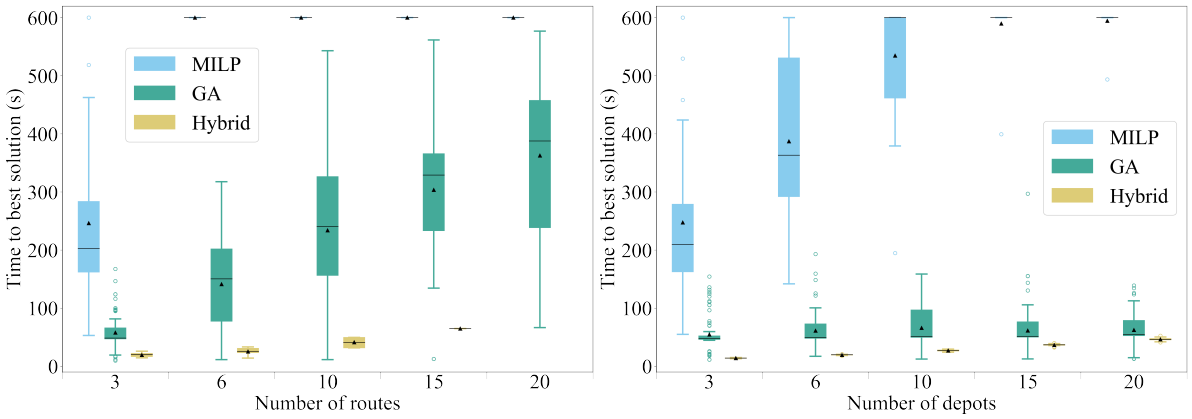

Figure 3: Time-to-best-solution statistics for the three solution approaches.

on $\mathbf{C}$, we consider 1, 5, 10, 15, 30, and 60 minutes as values for the time step duration, and we use the data from depot 1 and its 20 routes. Using the GA method with a time limit of 600 seconds, we solve each instance 20 times and retrieve the minimum $\mathbf{C}$. We assume $T^{\Delta} = 60$ as our baseline scenario by setting its $\mathbf{C} = 100$ and normalize $\mathbf{C}$ of other scenarios accordingly. The resulting comparison is demonstrated in Figure 4. We can observe that $T^{\Delta} = 1$ yields 12% lower $\mathbf{C}$ compared to that of $T^{\Delta} = 60$.

2.5.4 Impact of charger costs on system cost components

Because electrification is a relatively novel technology, charger costs are expected to decrease in the future. Therefore, we analyze the impact of C_k^{ν} on the cost components of the objective function (3.4) and the number of chargers allocated by type. To this end, we define *facility costs* by

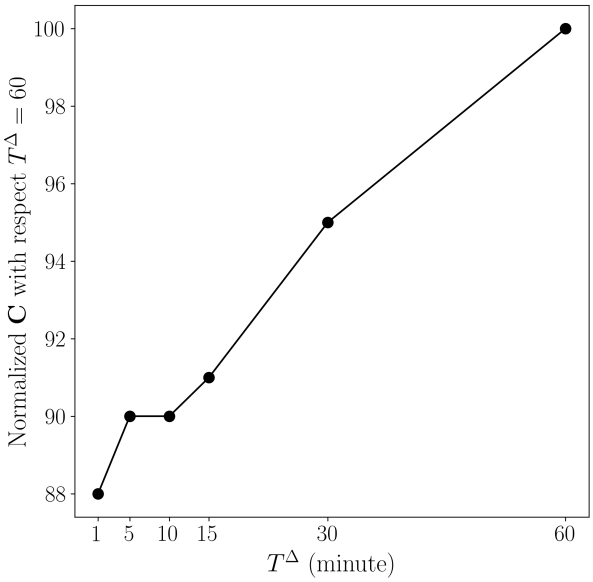

Figure 4: Impact of T^{Δ} on $\mathbf{C}$.

$$\sum_{f \in \mathcal{F}} C_f^{\phi} y_f,$$

charger costs by

$$\sum_{f \in \mathcal{F}, k \in \mathcal{K}} C_k^{\nu} z_{fk},$$

energy costs by

$$\sum_{c_{ir} \in \mathcal{C}_r, r \in \mathcal{R}, f \in \mathcal{F}_{c_{ir}}, k \in \mathcal{K}} C_k^{\xi} u_{c_{ir} f k},$$

and *VOT costs* by

$$\sum_{c_{ir} \in \mathcal{C}_r, r \in \mathcal{R}, f \in \mathcal{F}_{c_{ir}}, k \in \mathcal{K}} C^{\rho} (T_{c_{ir} f k} q_{c_{ir} f k} + w_{c_{ir} f k} + u_{c_{ir} f k}).$$

Five percentages of decrease in C_k^{ν} are considered: 0%, 20%, 40%, 60%, and 80%. We consider depot 1 and the 20 routes it serves by sampling $|\mathcal{R}| \in \{10, 12, 14, 16, 18, 20\}$ and $|\mathcal{F}| \in \{100\}$.

We use the GA method, limit the solution time per instance by 600 seconds, and solve each instance 20 times to obtain the best solution. We conducted 600 ($6 \times 5 \times 20$) runs for this analysis, and we report the statistics of the best solutions out of 20 GA runs by aggregating over $|\mathcal{R}|$ in Figure 5.

Figure 5a shows that the contribution of charger costs into (3.4) drops from 26% to 8% parallel to C_k^ν, while facility and energy costs substantially increase by 8% (from 24 to 32). Note that five tiers, i.e., -80, -60, -40, -20, and 0, indicate the percent change in charger costs, and these tiered representation is adopted for following subsections.

Figure 5b shows the decrease percent in C_k^ν versus the normalized cost. The normalized cost assumes $\mathbf{C} = 100$ when the decrease in C_k^ν is 0 and is calculated accordingly for other instances. In this figure we observe that a large decrease in C_k^ν increases the number of moderate and fast chargers, although there are fluctuations. The spikes can be a result of finding nonoptimal solutions through the GA and finding a better solution by swapping types of chargers along with a drop in C_k^ν. An example of the latter can be observed by seeing the number of chargers for basic and fast moving from 40% to 60%: that is, fewer fast chargers are equipped, while more basic chargers are utilized at 60% compared with 40%.

We note that an 80% decrease in C_k^ν results in a 25% drop in $\mathbf{C}$. This percentage will indicate the importance of C_k^ν compared with others analyzed in the following sections.

2.5.5 Impact of energy costs on system cost components

It is not certain how the wider adoption of EVs will impact energy prices. To analyze the impact of energy costs, we consider a percent change of -50, -25, 0, 25, 50, 75, and 100 in C_k^ξ.

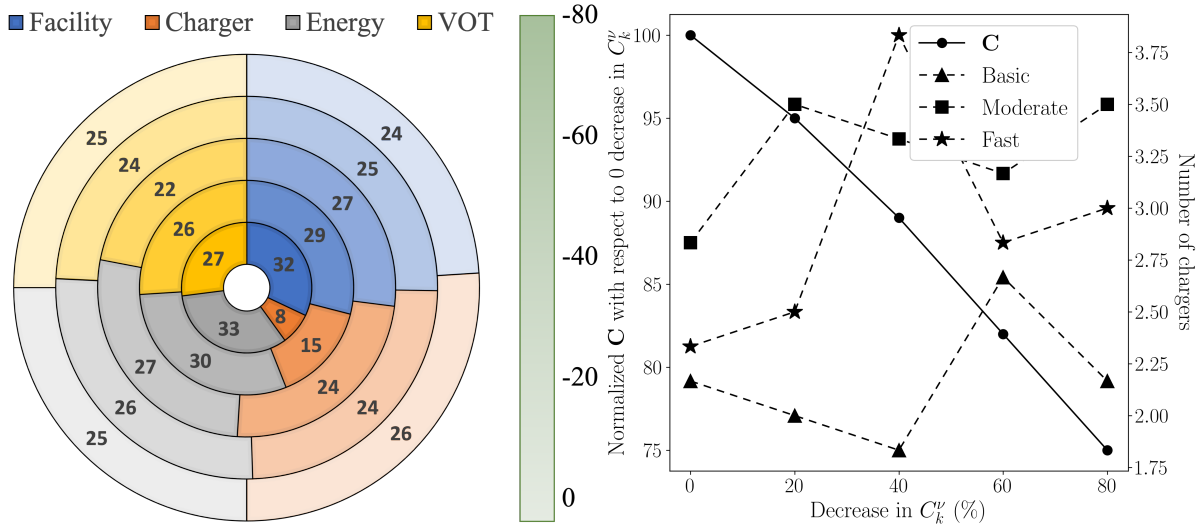

(a) Percent shares of cost components in **C**.

(b) Change in normalized cost and charger allocations.

Figure 5: Impact of percent decrease in charger costs.

The same settings as in the previous analysis are followed here and will be used in the upcoming sections. Therefore, 840 ($6 \times 7 \times 20$) runs were conducted, and Figure 6 provides the summary statistics.

Figure 6a shows a substantial jump in VOT costs along with an increase in C_k^ξ. In Figure 6b, moving from 0 to 100% increase in C_k^ξ, the number of fast chargers rises, while the numbers of other charger types reduce.

2.5.6 Impact of time value costs on system cost components

In some industries, VOT may be more important than others. Consumers may be willing to pay more for faster delivery. To analyze how a percent increase of 0, 20, 40, 60, 80, and 100

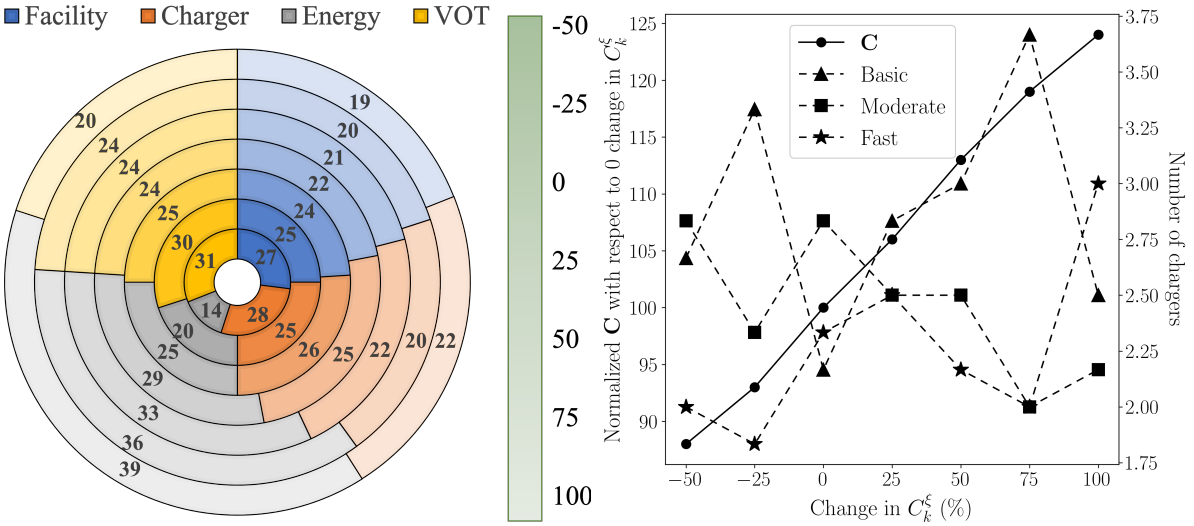

(a) Percent shares of cost components in **C**.

(b) Change in normalized cost and charger allocations.

Figure 6: Impact of percent change in energy costs.

in C^ρ impact the decisions, we conducted 720 ($6 \times 6 \times 20$) runs and report summary statistics in Figure 7.

Figure 7a illustrates how VOT costs can become dominant (by 40%) in Objective function (3.4) when C^ρ is doubled. From Figure 7b, we observe that the number of moderate and fast chargers increases as C^ρ doubles.

2.5.7 Impact of battery capacity on system cost components

EV technology is continuously improving, and advancements in battery technology enable longer vehicle ranges. In all analyses, we considered the low end of a 60–130 EV range reported (Lightning eMotors 2022) to be conservative. We now analyze EV ranges of 60, 90, 110, 130,

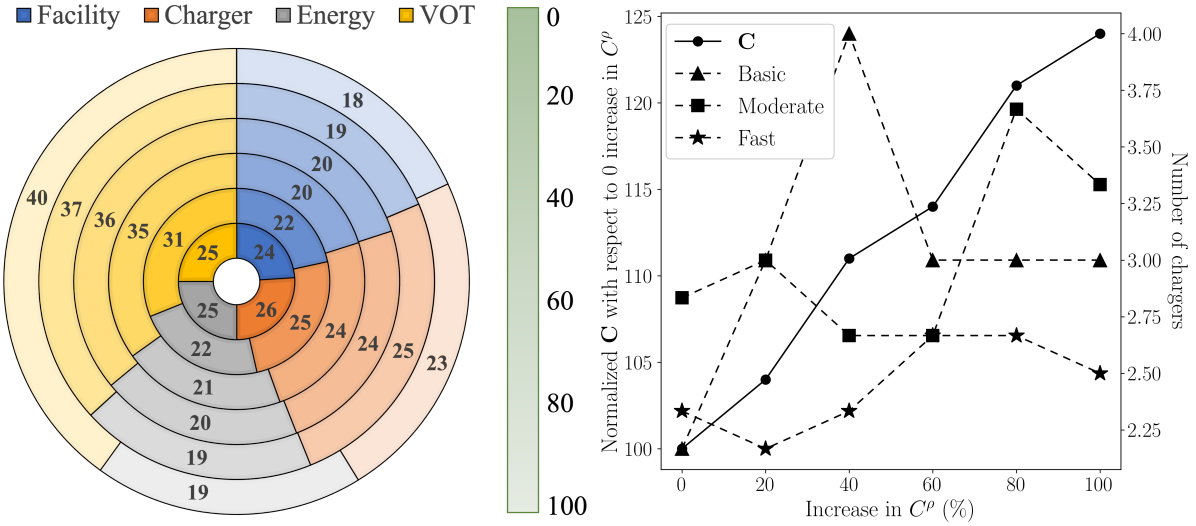

(a) Percent shares of cost components in **C**.

(b) Change in normalized cost and charger allocations.

Figure 7: Impact of percent increase in VOT costs.

and 250 miles. We conducted 600 ($6 \times 5 \times 20$) runs for this analysis, and the findings are illustrated in Figure 8.

Increasing the EV range reduces facility costs by enabling vehicles to recharge at more central locations, as shown in Figure 8a. Figure 8b demonstrates that a longer EV range decreases **C** up to a point. A similar finding was observed in a previous study (Cokyasar et al. 2022).

2.6 Conclusion

This research addresses some challenges in electrifying trucks, particularly in designing the necessary charging infrastructure. Indeed, infrastructure planning for large-scale electrification

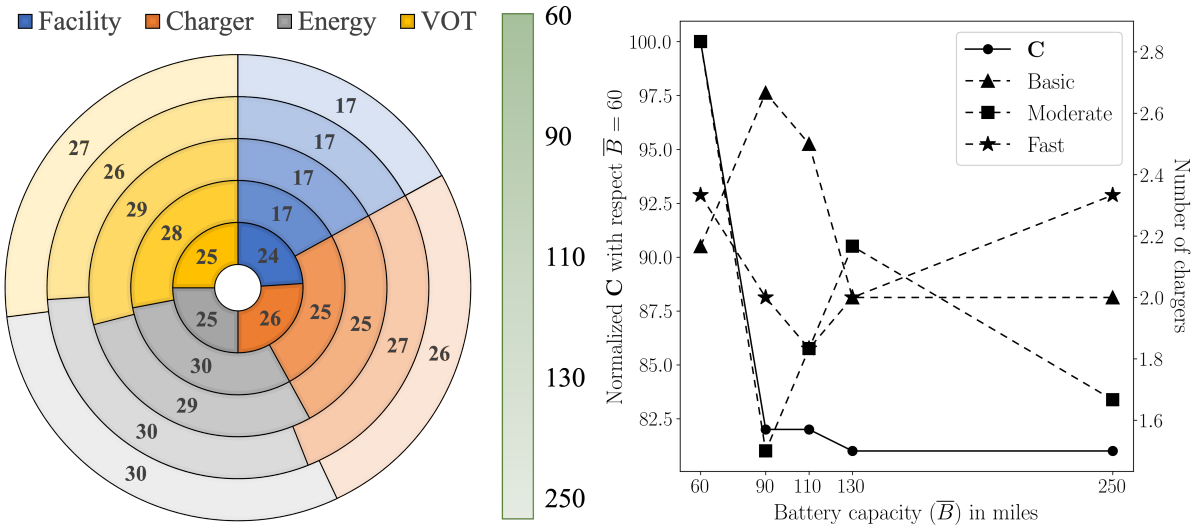

(a) Percent shares of cost components in **C**.

(b) Change in normalized cost and charger allocations.

Figure 8: Impact of battery capacity (in miles range).

projects can be complex because of factors including the placement of charging stations and the scheduling of recharging activities. While previous studies have focused on solving the EVLRP to address this issue, the freight industry has a different approach, where they make electrification decisions based on the characteristics of existing routes. However, by prioritizing routes shorter than the EV range and installing chargers only at depots, typically one charger for each EV, they forego the potential for cost savings that can be achieved by optimizing the charging activities. Exploiting and studying the limits of the associated economic opportunities is crucial, given the long-term impacts of strategic location-allocation decisions on short-term routing activities. Our paper seeks to address this gap by providing decision-making models

that combine the best of existing studies while also respecting the freight industry's philosophy of electrifying existing routes.

To that end, we formally describe the EVSELCA problem and construct an MILP model that focuses on fixed routes. The MILP model, solved through commercially available solvers that often use branch and bound as a solution method, faces scalability issues, making it impractical for larger-scale problems. To overcome this challenge, we propose a clustering approach that simplifies the problem by grouping customers into clusters and allowing recharging only upon completion of service at these clusters. Clustering is shown to partially address computational difficulties for small-scale problems, yet it is not adequate to fully address the issue. For this reason we develop a metaheuristic solution method using a GA. This approach generates near-optimal solutions within a reasonable time frame, making it possible to apply the model at a large scale. Combining the GA and MILP solvers, we introduce a hybrid solution approach.

We compare the computational performance of the GA and hybrid methods with the MILP model solved through Gurobi, using the number of routes and charging facility locations as problem-size-determinant levers. The results indicate that the GA outperforms the hybrid method in terms of solution quality, but the hybrid method is faster in finding solutions in most scenarios. The MILP model is suitable for small-scale problems. Overall, the GA provides quick solutions that are close in quality to the optimal solution. Moreover, the findings show that an increase in the number of routes has a greater impact on problem difficulty than does an increase in the number of charging facility locations.

We investigate the impact of four factors on the EVSELCA problem through a sensitivity analysis. These are charger costs (C_k^{ν}), energy costs (C_k^{ξ}), VOT (C^{ρ}), and battery capacity ($\overline{B}$). Our key findings are summarized as follows. An 80% decrease in C_k^{ν} results in a 25% cost reduction. A substantial reduction in VOT cost shares is observed as C_k^{ξ} increases. The number of moderate and fast chargers increases as C^{ρ} doubles. Longer EV ranges are beneficial in decreasing the overall cost up to a certain point. Beyond this threshold, longer EV ranges result in only a negligible decrease in the total cost. Our findings indicate that the objective function is the most sensitive to charger costs compared with other factors, while energy and VOT costs are less vital.

The proposed model is intricate and addresses critical concerns of determining the optimal time for EVs to visit charging facilities, selecting suitable facilities, allocating appropriate charging infrastructure, scheduling recharging activities to minimize wait times, and satisfying operational constraints. The strength of the MILP developed in this study is that it addresses all of these concerns. However, the model's dependency on the candidate locations for charging facility placement presents a challenge: that is, changing one candidate location may substantially alter the solutions and their interpretation. To address this, we plan to develop a tool that can mimic the MILP model to quickly find near-optimal solutions for any given set of candidate locations, reducing the time required to solve the problem.

CHAPTER 3

SINGLE DEPOT ELECTRIC VEHICLE SCHEDULING PROBLEM

3.1 Introduction

Public transportation plays a crucial role in cities by providing accessible, affordable, efficient, and equitable mobility options for travelers while helping to alleviate congestion. However, the use of conventional diesel vehicles (DVs) contributes to air pollution and carbon emissions, influencing air quality and public health (FTA 2010). Electrification of transit buses has emerged as a solution to address these environmental challenges. By transitioning to electric vehicles (EVs), cities can significantly reduce harmful emissions and improve air quality (Muñoz et al. 2022). (Note that the terms *vehicle* and *bus* are used interchangeably in this paper). Nevertheless, the adoption of electric buses comes with its own set of challenges. One major concern is the higher upfront cost of EVs compared to conventional DVs (Muñoz et al. 2022). This cost disparity can impose financial barriers, particularly when there is a need to replace a large number of buses in existing fleets. Driving range, long charging time, and electricity grid impact of EVs are other issues to be tackled. Although technological advancements have improved battery capacity and charging speeds, EVs still have a shorter range and longer downtime compared to DVs. This can pose operational challenges, especially for longer routes that require long periods of operation. To overcome these challenges, one potential solution is to increase the number of buses in operation. However, the high cost of electric buses can be

a hindrance. Therefore, optimizing EV scheduling becomes essential to minimize the bus fleet size and idle time, while ensuring sufficient recharging during idle periods.

The vehicle scheduling problem (VSP) involves the creation of *vehicle runs* (hereafter called runs) based on a set of timetabled service or revenue trips, called *trips*. These trips come with essential spatio-temporal information, including their origin (first stop), destination (last stop), start time, and end time. The objective of the VSP is to strategically organize these trips into bus runs that optimize the utilization of vehicles and ensure efficient transit operations. The Electric Vehicle Scheduling Problem (EVSP) extends beyond the VSP by not only strategically organizing these trips into bus runs but also facilitating the vehicle to recharge at the depot. This involves recharging during the day to serve the trips and also during the night to ensure the vehicle can serve runs in the upcoming planning horizons (often measured in days).

Figure 9 illustrates an example of an electric bus run. In this example, the bus run starts 6 AM on the current day and ends at 6 AM next day, with a planning horizon of 1 day. The nighttime recharging ends $\sim$ 7 AM. Subsequently, the bus remains at the depot until $\sim$ 9 AM and then *deadheads* to trip 1 (deadheading time refers to the duration spent traveling either from the final stop of one trip or from the depot to the initial stop of another trip, or back to the depot). In this example, after serving trip 4, the bus deadheads to trip 3 and arrives earlier than the trip start time. Consequently, it stays at the first stop of trip 3 for a while, defined as *intertrip layover*. Following the completion of trip 3, the bus deadheads to the depot. The bus uses *depot layover time* for *daytime recharging*. After daytime recharging at the depot, the bus

continues to serve the remaining scheduled trips. Upon completing the last trip, it returns to the depot for *nighttime recharging*.

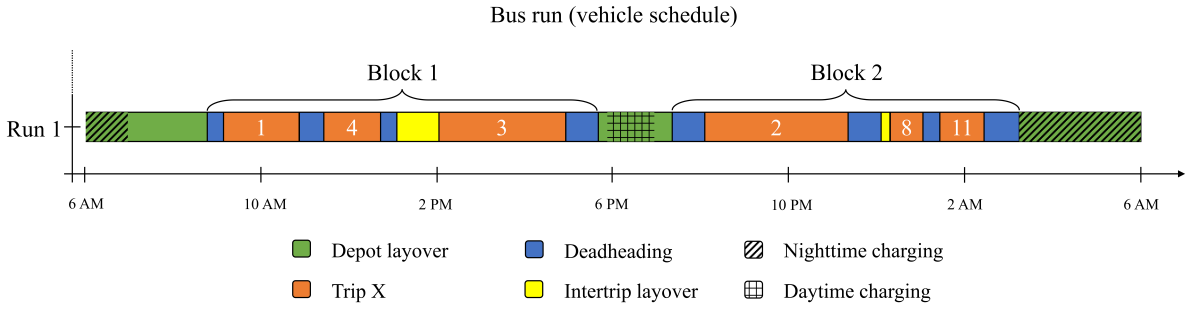

Figure 9: An example of a bus run.

The VSP has been extensively studied for many years, and various solution approaches have been proposed to address its complexity. See Bunte and Kliewer (2009) and Freling, Wagelmans, and Paixão (2001) for comprehensive reviews. However, with the emergence and early adoption of electric vehicles (EVs), there is a need to revisit the problem and adapt it to accommodate the unique characteristics and requirements of EVs. The EVSP can be classified into two main types based on the number of depots involved: single-depot EVSP (SDEVSP) and multi-depot EVSP (MDEVSP). In this study, we consider the SDEVSP. We develop an optimization-based scheduling framework using mixed-integer linear programming (MILP) that can generate bus runs with given trips. The framework ensures that each trip can be successfully completed

using DVs or EVs, and schedules recharging (when necessary). Moreover, we consider next day operability. Next day operability ensures each bus can serve at least one bus run the next day, and every scheduled bus run can be served by at least one bus. This means that during the night, when the buses are not in use, they recharge enough so they can serve bus runs the next day.

In this study, we propose a two-step solution approach for the SDEVSP. In the first step, solving an integer programming (IP) model, we generate *blocks* using the SDVSP model presented in Cokyasar, Verbas, and Auld (2023a). Each block is defined as a sequence of consecutive trips and has a designated depot as its starting and ending location. Blocks with a length shorter than EV range are considered electrifiable. Given the target EV deployment level (which is the ratio of number of electrifiable block to the total number of blocks), we adjust control parameters in the SDVSP model, allowing us to generate shorter or longer blocks to reach the target level. As the SDVSP with time or distance constraints is NP-hard (Bodin 1983), we do not impose hard constraints on block length or time to maintain computational feasiblity. This approach does not guarantee that all blocks are within the EV range since we do not have hard constraints. However, an *acceptable* or *targeted* share of within-range blocks can be obtained using this soft approach.

Once the blocks are generated, the subsequent step involves chaining them together to form a DV or EV schedules. This defines another set of problems: the block chaining problem (BCP) for DVs and EVs. The former problem chains diesel blocks while adhering to spatio-temporal conditions, while the latter adheres to both spatio-temporal and state-of-charge (SOC)

conditions. Additionally, the generated electric bus runs must satisfy the next day operability constraints, ensuring continuity of operations.

Figure 10 provides a visual representation of the study layout and the framework adopted for our solution approach. The reason behind designing this heuristic solution approach is two-fold. First, it aligns with the conventional practice employed by transit agencies, where bus blocks are initially created, followed by the utilization of these blocks to create DV schedules and crew schedules. Our approach is designed to resonate with this established method, facilitating its adoption within transit agencies. Transit agencies acknowledge that shorter blocks than that of DVs are needed to be created to electrify bus fleets, and these blocks can be chained to form EV schedules. Second, The SDEVSP is known to be NP-hard due to the presence of time or distance limitations (Bodin 1983). This implies that finding optimal solutions to large-scale problems is computationally infeasible within a reasonable time. Our solution approach adopts a two-step heuristic methodology, providing a practical and efficient means of resolving the complexity associated with the SDEVSP.

The motivation behind this study is threefold. First, our approach builds upon the widely adopted SDVSP modeling used by transit agencies to create schedules for conventional DVs. By leveraging this well-established method, we facilitate the adoption and implementation of our proposed solution framework, enabling transit agencies to seamlessly transition to electric bus fleets. Transit agencies acknowledge the necessity of creating shorter blocks to electrify bus fleets, and our approach allows for creating these blocks to form efficient electric vehicle (EV) schedules. Second, the SDEVSP is recognized as an NP-hard problem, making it analytically

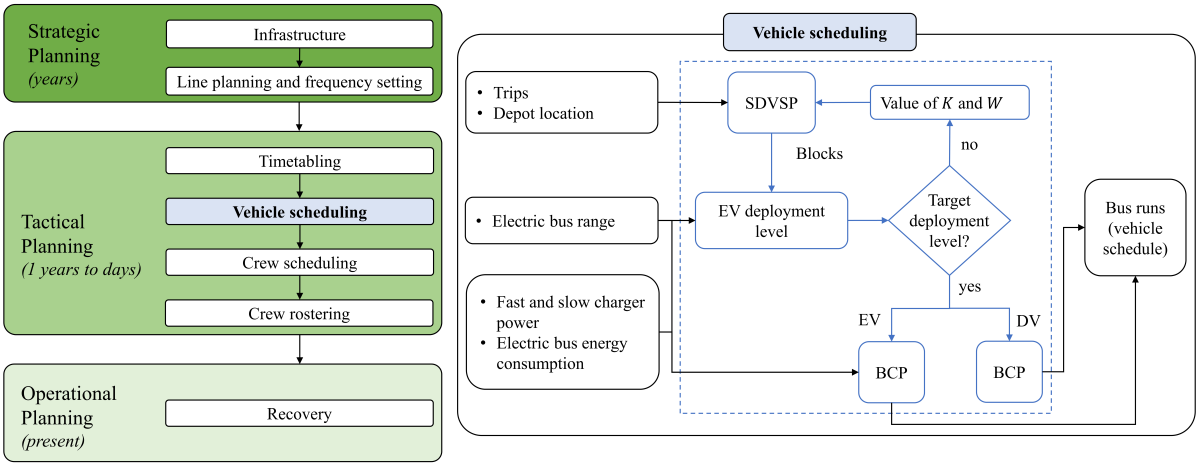

Figure 10: Study layout - SDEVSP framework. The left figure is adopted from Perumal, Lusby, and Larsen (2022a).

challenging to solve at a large-scale. By breaking down the SDEVSP into the SDVSP and the BCP, we effectively manage the challenges associated with large-scale instances of the SDEVSP. Third, our model incorporates next day operability constraints. This consideration ensures that the scheduling of bus blocks allows for their repetition on the following day, promoting efficient and reliable schedules. Our study considerably advances the SDEVSP literature by providing these contributions. Our practical and scalable solution approach enhances the feasibility and effectiveness of electric bus scheduling, supporting the transition towards more sustainable and environmentally friendlier public transportation systems.

In this study, we assume that we are given a predefined set of timetabled bus trips, with known start and end times as well as locations. Charging and discharging processes are assumed to follow linear profiles, simplifying the representation of energy transfer dynamics.

Furthermore, we assume that each depot is sufficiently large to accommodate new buses and the charging equipment. Moreover, there are as many slow and fast chargers as needed, resulting in zero waiting times for recharging. Moreover, We assume that during the day, vehicles use fast chargers because they need to recharge quickly and get back into service promptly. Slow chargers are not used during the day because the time between two bus blocks is limited, making slow charging impractical. For nighttime recharging, we assume slow chargers are used since they can recharge buses effectively during the night when buses are not in service. We assume fast chargers are not used at night to avoid overusing them as they are more expensive. This way, we balance the quick recharge needs during the day with the cost considerations, making sure the chargers are used efficiently.

In Section 3.2, we begin with providing a literature review on the SDEVSP. Section 3.3 formally describes the problem, the next day operability constraints, and the formulation of the MILP model. Section 3.4 outlines a heuristic approach to address the scalability concern in the BCP model. In Section 3.5, we detail the experimental design and the parametric choices, and demonstrate the results of numerical experiments conducted to evaluate the performance of the proposed solution approaches. Finally, Section 3.6 concludes the study by summarizing the key findings and discussing potential future research directions.

3.2 Literature review

Transit service design can be summarized as a sequence of five systematic decisions: Network design, frequency setting, timetabling, vehicle scheduling, and crew scheduling (Ceder and Wilson 1986). While many studies in the literature focus on solving these problems separately,

some select a subset and solve that selection jointly. See Guihaire and Hao (2008) for a thorough review on these problems. This study solely focuses on the vehicle scheduling problem, i.e. the route alignments, frequencies, and timetables are given and fixed. Similarly, crew scheduling that is solved either after or jointly with vehicle scheduling is also beyond the scope of this study. Table IX gives an overview of the existing relevant literature on the EVSP.

The existing literature on the electric VSP (EVSP) can be viewed in two main categories based on the number of depots included: SDEVSP and multi-depot EVSP (MDEVSP). While both variants are significant, recent studies have shown a growing interest in the MDEVSP (Wu et al. 2022, Liu and (Avi) Ceder 2020, Zhang et al. 2021, Yao et al. 2020, Diefenbach, Emde, and Glock 2023, Wen et al. 2016, Li et al. 2020). For instance, Wu et al. (2022) proposed a branch-and-price method for addressing the MDEVSP, incorporating time-of-use electricity tariffs and peak load risk. Similarly, Diefenbach, Emde, and Glock (2023) employed a branch-and-check method, considering non-linear charging and partial charging to minimize the electric vehicle fleet size in the MDEVSP context. However, in our research, we specifically concentrate on the single depot aspect of the EVSP. This decision is motivated by our understanding of the needs and requirements of large-scale transit agencies. Those agencies that operate out of multiple depots already have their blocks and runs assigned to certain depots by either solving an MDVSP, or by pre-assigning routes or trips to certain depots and solving multiple SDVSPs. In this study, we treat the existing assignment of trips to depots as initial conditions. By focusing on the SDEVSP, we aim to provide practical and applicable solutions that align with the operational context of these agencies. While the MDEVSP is undoubtedly an important

area of research, addressing the complexities associated with multiple depots falls beyond the scope and considerations of our study.

TABLE IX: Summary of the existing relevant literature.

Study	Objective	Model	(i)	(ii)	(iii)	(iv)	(v)	(vi)	(vii)	(viii)	(ix)	(x)
Wu et al. (2022)	Minimize the total operation cost.	MILP	✓	-	-	-	✓	-	-	-	-	-
Liu and (Avi) Ceder (2020)	Minimize the number of vehicles.	IP	✓	-	-	-	-	-	-	✓	✓	-
Zhang et al. (2021)	Minimize the vehicle purchasing cost and operation cost.	MILP	✓	-	-	✓	-	-	-	✓	✓	-
Yao et al. (2020)	Minimize the vehicle purchasing cost and operation cost.	IP	✓	-	✓	-	-	-	-	✓	-	-
Diefenbach, Emde, and Glock (2023)	Minimize the number of vehicles.	MILP	✓	-	-	-	-	-	-	✓	✓	-
Wen et al. (2016)	Minimize the number of buses and the total traveling distance.	MILP	✓	-	-	-	-	-	-	✓	-	-
Li et al. (2020)	Minimize the total cost of constructing and operating the electric bus system.	MILP	✓	-	-	-	-	-	-	✓	-	-
Xu, Yu, and Long (2023)	Maximize the difference between the profit from the bus fare and the operational cost.	IP	-	✓	-	-	-	-	-	-	-	-
Sistig and Sauer (2023)	Minimize the investment costs for vehicles and operational costs.	MILP	-	-	✓	-	-	-	-	-	-	-
Rinaldi et al. (2020)	Minimize the total operational cost.	MILP	-	-	-	✓	-	-	✓	-	-	-
Alwesabi et al. (2020)	Minimize the battery cost and charging infrastructure costs.	MIQCP	-	-	-	-	-	✓	-	-	-	-
Chao and Xiaohong (2013)	Minimize the capital investment for the electric fleet and the total charging demand.	MILP	-	-	-	-	-	-	-	-	-	-
Perumal et al. (2021)	Minimize the investment costs for vehicles and operational costs.	MILP	-	-	✓	-	-	-	-	-	-	-
This study	Minimize the number of vehicles and deadheading time.	MILP	-	-	-	-	-	-	-	✓	-	✓

(i) Multiple depots, (ii) Timetabling, (iii) Crew scheduling, (iv) Mixed fleet, (v) Power grid, (vi) Placement of charging infrastructure, (vii) Number of chargers, (viii) Partial charging, (ix) Non-linear charging, (x) Operational continuity, MIQCP: Mixed-integer quadratically-constrained program.

The SDEVSP has received limited attention in the existing literature, with a few studies dedicated to exploring its various aspects (Xu, Yu, and Long 2023, Sistig and Sauer 2023, Perumal, Lusby, and Larsen 2022a, Rinaldi et al. 2020, Alwesabi et al. 2020, Chao and Xiaohong 2013). For instance, Xu, Yu, and Long (2023) focused on jointly solving the electric bus timetabling and scheduling problem. They tackled this problem by employing the Lagrangian relaxation heuristic method as their solution approach. It should be noted that including timetabling introduced scalability challenges to their solution method. In our study, timetables are given and fixed, and we ensure that all the revenue trips are served by a vehicle. This deliberate choice ensures that our model is applicable to large-scale problems and can be effectively solved. Another related study conducted by Sistig and Sauer (2023) explored the integrated problem of electric vehicle and crew scheduling. To solve this problem, they employed a metaheuristic based on adaptive large neighborhood search (ALNS). Similarly, Perumal et al. (2021) also addressed the integrated electric vehicle and crew scheduling problem and utilized an ALNS as their solution approach. Our study does not consider the crew scheduling but considers the operational continuity. By focusing on operational continuity, our research aims to contribute to the field of sustainable electric vehicle scheduling. We recognize the importance of maintaining a consistent and efficient electric vehicle fleet, thereby enabling smoother and more reliable transportation services.

3.3 Problem definition

In this section, we provide a formal description of the SDVSP model as presented by Cokyasar, Verbas, and Auld (2023a). Next, we develop an MILP formulation to solve the

BCP. To ease reading, we adopt a specific notation convention where calligraphic letters denote sets, uppercase Roman letters represent parameters, lowercase Roman letters represent variables and indices, and lowercase Greek letters as superscripts modify parameters and variables.

3.3.1 Single Depot Vehicle Scheduling Problem (SDVSP)

The objective of SDVSP is to find optimal creation of bus blocks based on the given timetabled trips. Figure 11 illustrates an example solution for SDVSP. In this particular scenario, the SDVSP solution establishes three blocks based on the given trips. The connections between trips are decision variables for SDVSP, aiming to minimize the total intertrip layover time, deadheading time, and the number of blocks.

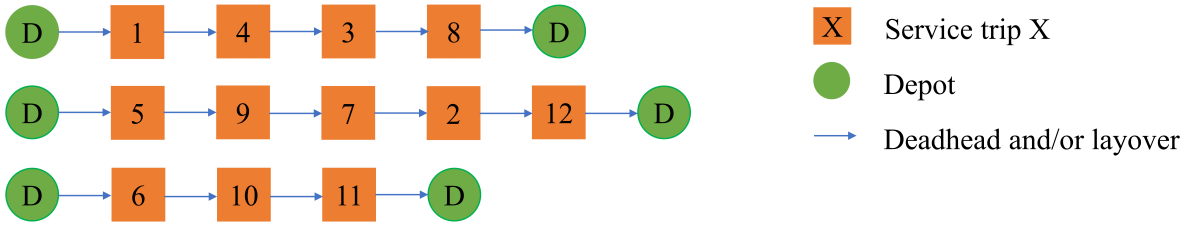

Figure 11: An example solution of SDVSP.

Let $\mathcal{T}$ represent set of timetabled bus trips with given origin O_i (first stop) and destination D_i (last stop). The tuple set $\mathcal{L}$ denotes all feasible arcs that connect bus trips, allowing them to be performed sequentially. Additionally, $\mathcal{R} = \mathcal{L} \bigcup (s \times \mathcal{T}) \bigcup (\mathcal{T} \times t)$ denotes set of all feasible

arcs, where s and t indices denote. We denote the deadheading time by T^{τ}_{ij}. The idle time spent between two consecutive trips is called *layover time*, denoted by T^{λ}_{ij}. Note that the layover time does not include the deadheading time but is the time spent after a bus finishes deadheading to the first stop O_j of trip j until the beginning of trip j. The block generation cost in time units is defined by K, and a unitless weight parameter W adjusts the balance between vehicle costs and layover time. The binary decision variable $l_{ij} = 1$ represents whether trip $j \in \mathcal{T}$ is served after trip $i \in \mathcal{T}$, and 0 otherwise. Table X denotes sets, parameters, and variables used in this section, and the mathematical model is as follows:

$$\min \sum_{(i,j)\in\mathcal{L}} (T^{\tau}_{D_iO_j} + WT^{\lambda}_{ij})l_{ij} + \sum_{j\in\mathcal{T}} \Big(K + T^{\tau}_{sO_j}\Big)l_{sj} + \sum_{i\in\mathcal{T}} T^{\tau}_{D_it}l_{it} \tag{3.1}$$

subject to,

$$\sum_{j:(i,j)\in\mathcal{R}} l_{ij} = 1 \qquad \forall i \in \mathcal{T} \tag{3.2}$$

$$\sum_{i:(i,j)\in\mathcal{R}} l_{ij} = 1 \qquad \forall j \in \mathcal{T} \tag{3.3}$$

$$l_{ij} \in \{0,1\} \qquad \forall\,(i,j) \in \mathcal{R}.$$

The objective function 3.1 is to minimize the weighted summation of the total non-revenue time (deadheading and weighted layover times) and the fleet size by adding an artificial time K to depot-to-trip travels. Constraints 3.2 and 3.3 guarantee that each trip follows exactly one preceding trip and is subsequently followed by exactly one subsequent trip. Adjusting the parameters K and W affect the block length. Increasing the value of K leads to longer blocks as the block generation cost becomes more significant, while increasing W results in shorter

blocks since the importance of layover time increases in relation to deadheading time and block generation cost.

TABLE X: Sets, parameters, and variables used in the SDVSP.

Set	**Definition**
$\mathcal{T}$	set of timetabled bus trips
$\mathcal{L}$	set of arcs connecting two consecutive trips
$\mathcal{R}$	set of all feasible arcs connecting two consecutive trips, $\mathcal{R} = \mathcal{L} \bigcup (s \times \mathcal{T}) \bigcup (\mathcal{T} \times t)$, where s and t indices denote the depot
Parameter	**Definition**
D_i	last stop of trip $i \in \mathcal{T}$
K	a big number representing the block generation cost in time units
O_i	first stop of trip $i \in \mathcal{T}$
T_i	start time of trip $i \in \mathcal{T}$
T_i^{ρ}	end time of trip $i \in \mathcal{T}$
T_{ij}^{τ}	deadheading time, the travel time from the last stop D_i of trip $i \in \mathcal{T}$ to the first stop O_j of trip $j \in \mathcal{T}$
T_{ij}^{λ}	layover time, the idle time spent between two consecutive trips $i \in \mathcal{T}$ and $j \in \mathcal{T}$ at the first stop O_j of trip $j \in \mathcal{T}$
W	weight factor for layover time between two consecutive trips
Variable	**Definition**
l_{ij}	$\begin{cases} 1 & \text{if trip } j \in \mathcal{T} \text{ is served after trip } i \in \mathcal{T},\ i \neq j \\ 0 & \text{otherwise} \end{cases}$

3.3.2 Block Chaining Problem (BCP)

The BCP is to find the optimal combination of bus blocks to be served consecutively by EVs that minimize the total depot layover time and the number of EVs, while making use of the depot layover time between blocks for recharging. Figure 12 illustrates an example solution

of the BCP. In this instance, the BCP solution combines two blocks into a single bus run and maintains the third block as an individual bus run. In the BCP, the connections between trips serve as decision variables determining whether to connect two blocks. This connection is contingent upon the layover time being sufficient for recharging the vehicle and preparing it for the next block. Additionally, the BCP ensures that the nighttime layover time is adequate for nighttime recharging, ensuring the vehicle's readiness to serve a bus run the next day. While adhering to these constraints, the BCP model aims to minimize both the total depot layover time and the number of bus runs (i.e., fleet size). Now, we formally describe an MILP formulation to solve the BCP, building upon the block results obtained from solving the SDVSP.

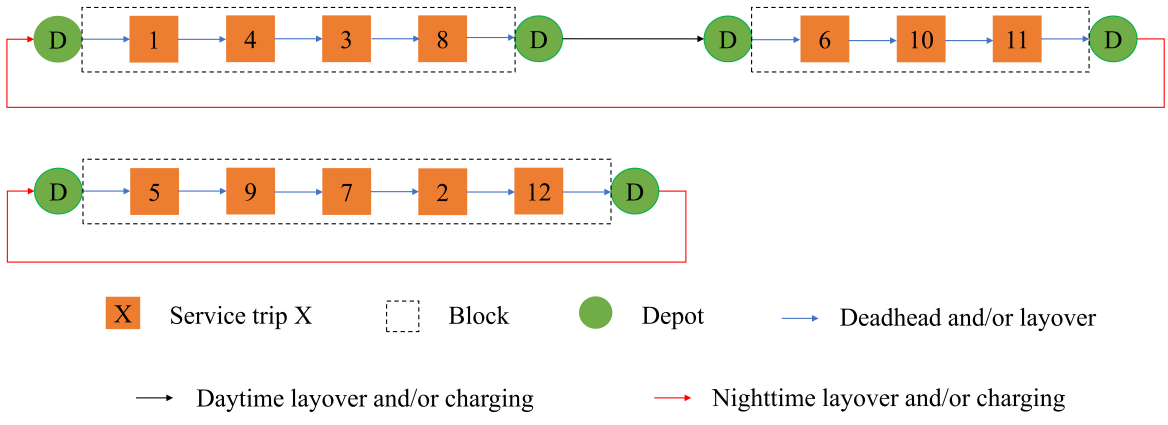

Figure 12: An example solution for the BCP.

The set of blocks that can be run by EVs (i.e., blocks meeting the range constraints) is denoted by $\mathcal{B}$. The tuple set $\mathcal{E}$ denotes all feasible arcs that connect bus blocks within the planning horizon. The tuple set $\mathcal{C}$ denotes all feasible arcs that connect bus blocks of consecutive horizons, that is each pair consists of a bus block from the current planning horizon and a bus block from the next planning horizon, and they can be combined in a sequential order. Furthermore, $\mathcal{A} = \mathcal{E} \bigcup (s \times \mathcal{B}) \bigcup (\mathcal{B} \times t)$ denotes set of all feasible arcs within a given horizon. Similar to the SDVSP, the indices s and t indicate the depot from which buses are dispatched and the depot to which they return, respectively. Table XV provides sets and parameters used in the MILP to solve the BCP.

The energy consumption required to operate block $i \in \mathcal{B}_i$ is represented by B_i and is measured in units of time. This energy consumption is assumed to be a linear function of the travel time for the block. The start and end times of block $i \in \mathcal{B}$, which are obtained by solving the SDVSP, are denoted by T_i^{α} and T_i^{β}, respectively. A recharging between consecutive blocks in the same planning horizon is considered to occur during the day, while recharging between consecutive blocks, one in the current and the other in the next planning horizon, is assumed to be overnight. The rate of recharge during the day is denoted by R^{δ}, while the rate of recharge overnight is denoted by R^{ν}. These recharge rates indicate the quantity of energy gained through recharging, measured in units of time per unit of time. The battery capacity, measured in units of time, is denoted by $\overline{B}$. This parameter represents the maximum amount of energy that the EV's battery can store, determining the maximum duration the vehicle can travel without recharging. The end time of the planning horizon, denoted by $\overline{T}$, establishes the

time limit or deadline for the scheduling of blocks. This parameter sets the boundary for the scheduling process, ensuring that all blocks are scheduled within the specified time frame. To control the layover time between consecutive blocks, we introduce the maximum and minimum layover time limits that are denoted by U and L, respectively. Weight parameters K' (in time units) and W' (unitless) represent the vehicle cost and importance of layover time against fleet size in the objective function, respectively. Lastly, $\mathbb{M}_1$ and $\mathbb{M}_2$ are adequately big numbers, where $\mathbb{M}_1 > \overline{B} + \max\left\{(\overline{T} + \max_{i\in\mathcal{B}} T_i^{\alpha})R^{\nu}, \max_{i\in\mathcal{B}} R^{\delta}T_i^{\alpha}\right\}$ and $\mathbb{M}_2 \geq \overline{B} + 2\mathbb{M}_1$.

Binary decision variable $y_{ij} = 1$ if block $j \in \mathcal{B}$ is served after block $i \in \mathcal{B}$, and $y_{ij} = 0$, otherwise. Binary decision variable z_{ij} takes a value of 1 if block $j \in \mathcal{B}$ on the next day can be served after block $i \in \mathcal{B}$ in the current day, and 0 otherwise. Decision variable $v_{ij} \in \mathbb{R}_{\geq 0}$ represents the state of charge (SOC) in time units at the beginning of block $j \in \mathcal{B}$ after serving block $i \in \mathcal{B}$. Decision variable $v'_{ij} \in \mathbb{R}$ represents the SOC in time units at the beginning of block $j \in \mathcal{B}$ on the next planning horizon after serving block $i \in \mathcal{B}$ in the current horizon. Decision variable $b_i \in \mathbb{R}_{\geq 0}$ denotes the SOC in time units at the beginning of block $i \in \mathcal{B}$. Decision variable $u_{ij} \in \mathbb{R}_{\geq 0}$ represents the amount of energy gained measured in time units during the layover time between two consecutive blocks. Additionally, we introduce two auxiliary binary variables: x_{ij} and n_{ij}. These variables are used to linearize the max and min functions, respectively. Table XVI provides variables and variable definitions used in the MILP. The mathematical model to solve the BCP is as follows:

$$\min \sum_{(i,j)\in\mathcal{E}} W'\left(T_j^{\alpha} - T_i^{\beta}\right) y_{ij} + \sum_{i\in\mathcal{B}} K' y_{si} \tag{3.4}$$

subject to,

$$\sum_{j:(i,j)\in\mathcal{A}} y_{ij} = 1 \qquad \forall i \in \mathcal{B} \tag{3.5}$$

$$\sum_{i:(i,j)\in\mathcal{A}} y_{ij} = 1 \qquad \forall j \in \mathcal{B} \tag{3.6}$$

$$v_{ij} = \max\left\{b_i - B_i - \mathbb{M}_1\left(1 - y_{ij}\right) + u_{ij}, 0\right\} \qquad \forall (i,j) \in \mathcal{A} \tag{3.7}$$

$$b_j = \sum_{i:(i,j)\in\mathcal{A}} v_{ij} \qquad \forall j \in \mathcal{B} \tag{3.8}$$

$$B_i \leq b_i \leq \overline{B} \qquad \forall i \in \mathcal{B} \tag{3.9}$$

$$u_{ij} \leq \left(T_j^{\alpha} - T_i^{\beta}\right) R^{\delta} y_{ij} \qquad \forall (i,j) \in \mathcal{E} \tag{3.10}$$

$$u_{it} = 0 \qquad \forall i \in \mathcal{B} \tag{3.11}$$

$$v'_{ij} = \min\left\{\overline{B}, v_{it} + \left(\overline{T} + T_j^{\alpha} - T_i^{\beta}\right) R^{\nu} - \mathbb{M}_1\left(2 - y_{sj} - y_{it}\right)\right\} \qquad \forall\,(i,j) \in \mathcal{C} \tag{3.12}$$

$$v'_{ij} \geq b_j - \mathbb{M}_2\left(1 - z_{ij}\right) \qquad \forall\,(i,j) \in \mathcal{C} \tag{3.13}$$

$$\sum_{i:(i,j)\in\mathcal{C}} z_{ij} = y_{sj} \qquad \forall j \in \mathcal{B} \tag{3.14}$$

$$\sum_{j:(i,j)\in\mathcal{C}} z_{ij} = y_{it} \qquad \forall i \in \mathcal{B} \tag{3.15}$$

$$y_{ij},\ z_{ij} \in \{0,1\}, b_i,\ u_{ij},\ v_{ij} \in \mathbb{R}_{\geq 0}, v'_{ij} \in \mathbb{R}.$$

The objective function 3.4 minimizes the total layover time between blocks and the number of vehicles. Constraints 3.5 and 3.6 guarantee that each block follows exactly one preceding

block or a depot block and is followed by exactly one subsequent block or a depot block, respectively. Constraints 3.7 and 3.8 determine the SOC at the start of block $j \in \mathcal{B}$ based on the SOC at the beginning of the preceding block $i \in \mathcal{B}$, the energy consumption during block i, and the energy gained between the blocks i and j. Note that $v_{sj} = b_s + u_{sj}$ when $y_{sj} = 1$ (that is for each run) in 3.7. Then, we know from 3.8 that $b_j = b_s + u_{sj}$. Therefore, initial SOC of each run can vary by artificially charging from s to the first block in the current horizon, and we can ensure that the initial SOC for each run is a variable. Constraints 3.9 ensure that the SOC does not exceed the maximum battery capacity, and EVs have adequate SOC to complete each block $i \in \mathcal{B}$ without running out of energy. Constraints 3.10 guarantee that the energy gained between two consecutive blocks does not exceed the maximum amount of energy that can be gained during the layover time between those blocks. Constraints 3.11 enforce that no daytime charging takes place if block i is the last block of the horizon.

The set of constraints 3.12 - 3.15 account for the feasibility of the next horizon's operations. Constraints 3.12 calculate the SOC at the beginning of block $j \in \mathcal{B}$ on the next horizon, after serving block $i \in \mathcal{B}$ on the current horizon. This calculation takes into account the SOC at the end of block i and considers the amount of energy gained between blocks i and j, where $(i, j) \in \mathcal{C}$. To establish the connection between block $j \in \mathcal{B}$ on the next horizon and block $i \in \mathcal{B}$ on the current horizon, we introduce constraint 3.13. This constraint ensures that if $z_{ij} = 1$, the SOC v'_{ij} at the beginning of block j is sufficient to serve that block. Constraints 3.14 ensure that each block j that start from the depot on the next horizon is preceded only

by one block i. Similarly, constraints 3.15 ensure that each block i that ends at the depot on the current horizon is succeeded by only one block in the next horizon.

Constraints 3.7 and 3.12 in their current form involve min and max functions with variables, which is quite straightforward to deal with by many commercial solvers without the need for linearization. However, it can still be useful to remove the non-linearity to possibly accelerate the solution. To this end, we replace constraints 3.7 with the set of constraints 3.16 - 3.18 and constraints 3.12 with the set of constraints 3.19 - 3.22.

$$v_{ij} \geq b_i - B_i + u_{ij} - \mathbb{M}_1 (1 - y_{ij}) \qquad \forall (i,j) \in \mathcal{A} \tag{3.16}$$

$$v_{ij} \leq b_i - B_i + u_{ij} - \mathbb{M}_1 (1 - y_{ij} - x_{ij}) \qquad \forall (i,j) \in \mathcal{A} \tag{3.17}$$

$$v_{ij} \leq \mathbb{M}_1 (1 - x_{ij}) \qquad \forall (i,j) \in \mathcal{A} \tag{3.18}$$

$$v'_{ij} \leq \overline{B} \qquad \forall (i,j) \in \mathcal{C} \tag{3.19}$$

$$v'_{ij} \leq v_{it} + \left(\overline{T} + T_j^{\alpha} - T_i^{\beta}\right) R^{\nu} - \mathbb{M}_1 (2 - y_{sj} - y_{it}) \qquad \forall (i,j) \in \mathcal{C} \tag{3.20}$$

$$v'_{ij} \geq \overline{B} - \mathbb{M}_2 n_{ij} \qquad \forall (i,j) \in \mathcal{C} \tag{3.21}$$

$$v'_{ij} \geq v_{it} + \left(\overline{T} + T_j^{\alpha} - T_i^{\beta}\right) R^{\nu} - \mathbb{M}_1 (3 - y_{sj} - y_{it} - n_{ij}) \qquad \forall (i,j) \in \mathcal{C} \tag{3.22}$$

$$x_{ij},\ y_{ij},\ n_{ij} \in \{0,1\}, b_i,\ u_{ij},\ v_{ij} \in \mathbb{R}_{\geq 0}, v'_{ij} \in \mathbb{R}.$$

TABLE XI: Sets and parameters used in the MILP for the BCP.

Set	**Definition**
$\mathcal{A}$	set of all feasible arcs connecting two consecutive blocks within the horizon, $\mathcal{A} = \mathcal{E} \bigcup (s \times \mathcal{B}) \bigcup (\mathcal{B} \times t)$, where s and t indices denote the depot
$\mathcal{B}$	set of timetabled bus blocks
$\mathcal{C}$	set of arcs connecting two consecutive blocks over night i (first, current horizon) and j (second, next horizon), $\mathcal{C} = \left\{ (i,j) \,\middle|\, i,j \in \mathcal{B} \wedge L \leq \left(\overline{T} + T_j^{\alpha} - T_i^{\beta}\right) \leq U \right\}$
$\mathcal{E}$	set of arcs connecting two consecutive blocks i (first, current horizon) and j (second, current horizon), $\mathcal{E} = \left\{ (i,j) \,\middle|\, i,j \in \mathcal{B} \wedge i \neq j \wedge L \leq \left(T_j^{\alpha} - T_i^{\beta}\right) \leq U \right\}$
Parameter	**Definition**
$\overline{B}$	battery capacity measured in time units
B_i	energy consumption of block $i \in \mathcal{B} \cup \{s\}$ measured in time units, and $B_s = 0$
K'	a big number representing the vehicle cost measured in time units
L	minimum admitted recharging time between two consecutive blocks
$\mathbb{M}_1$	big number, that is $\mathbb{M}_1 > \overline{B} + \max\left\{(\overline{T} + \max_{i \in \mathcal{B}} T_i^{\alpha})R^{\nu}, \max_{i \in \mathcal{B}} R^{\delta} T_i^{\alpha}\right\}$
$\mathbb{M}_2$	big number, that is $\mathbb{M}_2 \geq \overline{B} + 2\mathbb{M}_1$
R^{δ}	rate of recharge during day, i.e., energy (in time units) gained by recharging in one unit of time, e.g., R^{δ} minutes of driving range is gained by recharging a bus for one minute
R^{ν}	rate of recharge during night, i.e., energy (in time units) gained by recharging in one unit of time, e.g., R^{ν} minutes of driving range is gained by recharging a bus for one minute
$\overline{T}$	end of planning horizon in time units
T_i^{α}	start time of block $i \in \mathcal{B}$
T_i^{β}	end time of block $i \in \mathcal{B}$
U	maximum admitted recharging time between two consecutive blocks
W'	weight factor for recharging time between two consecutive blocks

3.4 Heuristic solution approaches

The SDEVSP is a known NP-hard problem, presenting a computational challenge for finding an optimal solution. To tackle this problem, we propose a two-step heuristic solution approach. In the first step, our objective is to identify suitable values for K and W that enable the generation of blocks where the service time for each block does not exceed the vehicle range. We use the method proposed by Cokyasar et al. (2023) to determine the suitable values for K and W, then we use the resulting blocks generated in the previous step and solve the BCP. The

TABLE XII: Variables used in the MILP for the BCP.

Variable	Definition
b_i	state of charge at the beginning of block $i \in \mathcal{B} \cup \{s\}$ measured in time units, $b_i \in \mathbb{R}_{\geq 0}$
n_{ij}	auxiliary binary variable used to linearize the min function, $(i,j) \in \mathcal{C}$
u_{ij}	energy gained between blocks i and j measured in time units on current horizon, $u_{ij} \in \mathbb{R}_{\geq 0},\ (i,j) \in \mathcal{A}$
v_{ij}	state of charge at the beginning of block j on current horizon after serving block i on current horizon measured in time units, $v_{ij} \in \mathbb{R}_{\geq 0},\ (i,j) \in \mathcal{A}$
v'_{ij}	state of charge at the beginning of block j on next horizon after serving block i on current horizon measured in time units, $v'_{ij} \in \mathbb{R},\ (i,j) \in \mathcal{C}$
x_{ij}	auxiliary binary variable used to linearize the max function, $(i,j) \in \mathcal{A}$
y_{ij}	$\begin{cases} 1 & \text{if block } j \text{ on current horizon is served after block } i \text{ on current horizon, } (i,j) \in \mathcal{A} \\ 0 & \text{otherwise} \end{cases}$
z_{ij}	$\begin{cases} 1 & \text{if block } j \text{ on next horizon can be served after block } i \text{ on current horizon, } (i,j) \in \mathcal{C} \\ 0 & \text{otherwise} \end{cases}$

BCP aims to generate an optimal schedule for electric vehicles based on the given blocks and their associated start and end times, taking into account charging requirements. Since the BCP is a variant of the SDVSP model with resource constraints, it is NP-hard. We introduce two solution algorithms to solve large-scale instances: A divide-and-conquer (DaC) algorithm and a greedy heuristic algorithm. In the following Sections 3.4.1 and 3.4.2, we elaborate on these solution algorithms in detail. Additionally, we present a computational analysis in Section 3.5.2, where we evaluate and compare the performance of the DaC and the greedy heuristic algorithm with an MILP solver.

3.4.1 Divide-and-conquer (DaC) algorithm

Divide and conquer (DaC) is well-known algorithm (Blahut 2010). The idea behind the DaC algorithm is to break down the large-scale BCP into smaller and manageable subproblems.

The subproblems at adequately small size (e.g., 20 blocks) can be solved independently using commercial solvers. Once the subproblems are solved, the solutions are combined to form an overall solution for the master problem. This combination step ensures that the solution obtained is feasible as Lemma 3 (see Appendix for proof) denotes.

Lemma 3. *Let $\mathcal{M}$ be the master problem and $\mathscr{P}$ be a set of subproblems, that $\mathcal{M} = \bigcup_{p \in \mathscr{P}} p$. If each subproblem $p \in \mathscr{P}$ has a feasible solution X_p, then $X_{\mathcal{M}} = \bigcup_{p \in \mathscr{P}} X_p$ is a feasible solution for $\mathcal{M}$.*

In order to break down the large-scale BCP into smaller subproblems, we employ the Kernighan-Lin (K-L) bisection algorithm, as introduced by Kernighan and Lin (1970). The Kernighan-Lin algorithm is a graph partitioning technique that optimizes the division of vertices into two sets, aiming to minimize the number of edges (cut size) connecting the sets. By iteratively swapping pairs of nodes between sets based on gain calculations, the algorithm efficiently refines the partition until reaching a locally optimal solution.

To apply the K-L bisection algorithm in the context of the BCP, we begin with representing the problem as a graph. Each block is represented as a vertex, based on the set $\mathcal{B}$, and the relationships between the blocks are captured as edges, based on the tuple set $\mathcal{E}$. The K-L bisection algorithm then aims to partition this graph into two subgraphs with the goal of minimizing the number of edges between the partitions while ensuring approximately equal number of vertices in each partition. This partitioning is achieved through an iterative process that involves swapping vertices between the two partitions to maximize the reduction in the

number of edges between them. Using this method, we attempt to minimize the optimality deviation caused by partitioning.

While the K-L algorithm is originally designed to partition a problem into two subproblems, we aim to divide the problem into a larger number of subproblems. To do this, we can repeat the K-L algorithm multiple times. In each iteration, the algorithm partitions a subproblem into two subproblems by dividing the corresponding graph representation. The first iteration applies the K-L algorithm to the original problem, resulting in two subproblems. Subsequent iterations apply the K-L algorithm to each subproblem from the previous iteration, dividing them into two subproblems each.

Let $|\mathcal{M}|$ represent the number of blocks in the master problem and $|p|$ represent the maximum number of blocks that can be solved using commercial solvers within a reasonable timeframe. The target number of subproblems is then $m = \frac{|\mathcal{M}|}{|p|}$. This would require $n = \lceil \log_2^m \rceil$ iterations, and in each iteration $k = 1, \ldots, n$ the number of partitionings is 2^{k-1} resulting in a total of $2^n - 1$ partitionings. The final number of subproblems would then be 2^n. Figure 13 illustrates an example of partitioning results. In this case, there are 12 blocks ($|\mathcal{M}| = 12$), and let's assume the largest problem size solvable by commercial solvers is 3 blocks, i.e., $|p| = 3$. Consequently, we need to divide the problem into $m = \frac{12}{3} = 4$ subproblems. This requires $n = \lceil \log_2 4 \rceil = 2$ iterations and results in $2^2 - 1 = 3$ partitionings. Note that, ideally, we divide the problem into a reasonably large number of subproblems to fully exploit the potential for parallelism and solution efficiency. However, dividing the problem into a larger number of

subproblems leads to a natural decrease in solution quality. Therefore, we carefully consider this trade-off to determine an appropriate value for m.

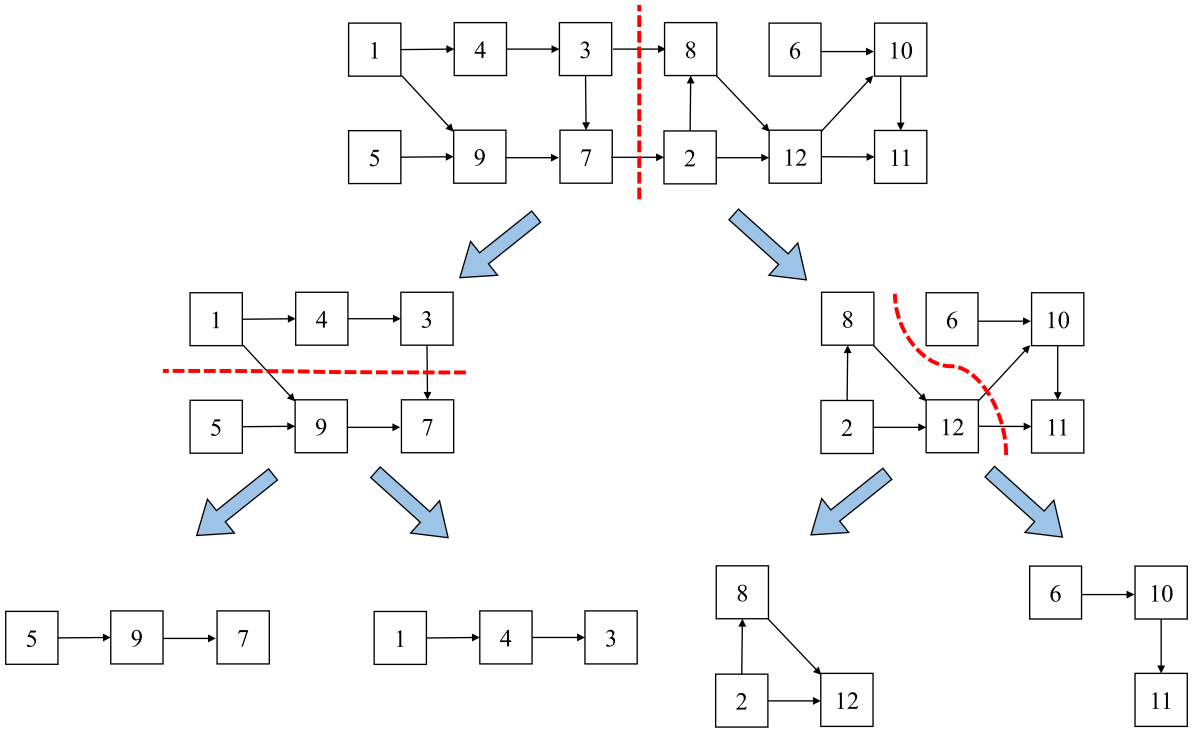

Figure 13: An example of partitioning a problem into subproblems.

3.4.2 Greedy algorithm

The greedy algorithm in Algorithm 2 iteratively assigns blocks to vehicles in a way that minimizes the number of vehicles needed. The algorithm follows a greedy strategy, making

locally optimal decisions at each step. It is one of the traditional methods to solve scheduling problems and is similar to the *earliest due date rule* presented in (Sule 2007, pp. 152). The algorithm begins with sorting the set of blocks $\mathcal{B}$, based on their start times T_i^{α}. We initialize various variables, including b_i, u_{ij}, and u'_{ij}, to zero. Additionally, we set $b_{\mathcal{B}(0)} = \overline{B}$.

Next, we define b_i^{ϕ} as the net energy consumption until the end of block i. It is computed by summing the consumption of all preceding blocks in the chain up to the previous block, and subtracting the sum of all charging values u_{ij} that occurred between those blocks. All b_i^{ϕ} values are initially set to zero. To begin, the algorithm generates the first vehicle $\mathcal{V}_0$ by adding the first block $\mathcal{B}(0)$ to the itinerary. The net energy consumption for this vehicle is set to the consumption of the first block, $B_{\mathcal{B}(0)}$. After removing the first block $\mathcal{B}(0)$ from $\mathcal{B}$, we initialize the vehicle counter, denoted as v, and the block counter, denoted as k, to zero.

The algorithm runs until all blocks are assigned to vehicles. Within the while loop, the first condition checks if a vehicle has at least one block already inserted. If not, the first block in the current set of blocks is inserted. For a given block i, which represents the last block in the current vehicle, and a block j currently under consideration for insertion, temporal conditions are evaluated. These conditions compare the start time of block j with the start time of block i to ensure chronological feasibility for both during the current horizon and also for the next horizon. Temporary variables u, b, u', and b^{ϕ}, are calculated. If the SOC conditions are met for these variables, indicating sufficient energy levels, the evaluated block is inserted into the current vehicle.

The first condition checks if the overnight charging u' is greater than or equal to the net energy consumption if the current block is inserted into the itinerary. This guarantees that there will be enough battery capacity for the next time period to continue the sequence of blocks. The second condition verifies that the SOC b_i of the last block in the vehicle is greater than or equal to the energy consumption B_i of that block. Lastly, the SOC level after completing block i (i.e., $b_i - B_i$) and charging the vehicle with u is checked to determine if it is sufficient to execute block j. If any of the SOC conditions are not satisfied, the block counter k or the vehicle counter v is incremented accordingly. When a block is successfully inserted, it is removed from the set of blocks $\mathcal{B}$.

3.5 Numerical Experiments

In this section, we provide an overview of our experimental design and data in Section 3.5.1, compare the performance and limitations of the Greedy, DaC, and the MILP solver methods in Section 3.5.2, and conduct case studies in Section 3.5.3 to reveal key takeaways on large-scale, real-world transit services.

3.5.1 Design of experiments

We conducted numerical experiments in Austin, TX and the Chicago Metropolitan Area transit networks. We utilized Capital Metropolitan Transportation Authority (CapMetro) network for Austin, and the Chicago Transit Authority (CTA) and the PACE Suburban Bus networks for Chicago through General Transit Feed Specification (GTFS) data (General Transit Feed Specification 2022). CapMetro operates 75 bus routes, and Chicago agencies collectively operate a total of 325 bus routes (Auld et al. 2016). The locations of these routes and depots

Algorithm 2: Greedy algorithm pseudocode

Input : $\mathcal{B}$, B_i, $\overline{B}$, $\mathcal{C}$, R^δ, R^ν, T_i^α, T_i^β, $\overline{T}$
Output: $\mathcal{V}$ ▷ A set storing blocks of vehicles.
Function GREEDY():
  SORT($\mathcal{B}$, T^α);
  $b_i, b_i^\phi \leftarrow 0\ \forall i \in \mathcal{B}$; $u_{ij} \leftarrow 0\ \forall (i,j) \in \mathcal{A}$; $u'_{ij} \leftarrow 0\ \forall (i,j) \in C$; $b_{\mathcal{B}(0)} \leftarrow \overline{B}$; $b_0^\phi \leftarrow B_{\mathcal{B}(0)}$;
  $\mathcal{V}_0 \leftarrow \{\}$;
  $\mathcal{V}_0 \leftarrow \mathcal{V}_0 \cup \{\mathcal{B}(0)\}$;
  $\mathcal{B} \leftarrow \mathcal{B} \setminus \mathcal{B}(0)$; ▷ Delete first block.
  $v \leftarrow 0$; ▷ Index of vehicle id.
  $k \leftarrow 0$; ▷ Counter for block indices of $\mathcal{B}$.
  while $\mathcal{B} \neq \{\}$, **do**
    if $|\mathcal{V}_v| \neq 0$, **then**
      $i \leftarrow \mathcal{V}_v(|\mathcal{V}_v|)$; ▷ Last block in $\mathcal{V}_v$ is i.
      $j \leftarrow \mathcal{B}(k)$; ▷ The k^{th} block in $\mathcal{B}$ is j.
      if $i \neq j$ and temporal conditions hold, **then**
        $u \leftarrow \min\left(\overline{B} - b_i + B_i, (T_j^\alpha - T_i^\beta)R^\delta\right)$;
        $b \leftarrow b_i - B_i + u$;
        $u' \leftarrow \min\left(\overline{B} - b + B_j, (\overline{T} + T^\alpha_{\mathcal{V}_v(0)} - T_i^\beta)R^\nu\right)$;
        $b^\phi \leftarrow b_v^\phi + B_j - u'$;
        if $u' \geq b^\phi \wedge b_i \geq B_i \wedge b \geq B_j$, **then**
          $\mathcal{V}_v \leftarrow \mathcal{V}_v \cup \{j\}$; $u_{ij} \leftarrow u$;
          $b_j \leftarrow b$; $u'_{ij} \leftarrow u'$; $b_v^\phi \leftarrow b^\phi$;
          $\mathcal{B} \leftarrow \mathcal{B} \setminus \{j\}$;
        else
          if $k + 1 < |\mathcal{B}|$, **then**
            $k \leftarrow k + 1$;
          else
            $v \leftarrow v + 1$; $\mathcal{V}_v \leftarrow \{\}$; $k \leftarrow 0$;
      else
        if $k + 1 < |\mathcal{B}|$, **then**
          $k \leftarrow k + 1$;
        else
          $v \leftarrow v + 1$; $\mathcal{V}_v \leftarrow \{\}$; $k \leftarrow 0$;
    else
      $\mathcal{V}_v \leftarrow \mathcal{V}_v \cup \{\mathcal{B}(0)\}$;
      $b_{\mathcal{B}(0)} \leftarrow \overline{B}$; $b_v^\phi \leftarrow B_{\mathcal{B}(0)}$; $\mathcal{B} \leftarrow \mathcal{B} \setminus \mathcal{B}(0)$;
  $\mathcal{V} \leftarrow \bigcup_{v' \in \{0,1,\ldots,v\}} \mathcal{V}_{v'}$;

used by these agencies are indicated in Figure 14. With the data provided, we identified 17 bus depots in Chicago and verified the number and locations through official websites of the agencies; however, we could locate four bus depots in Austin but could not verify neither the number

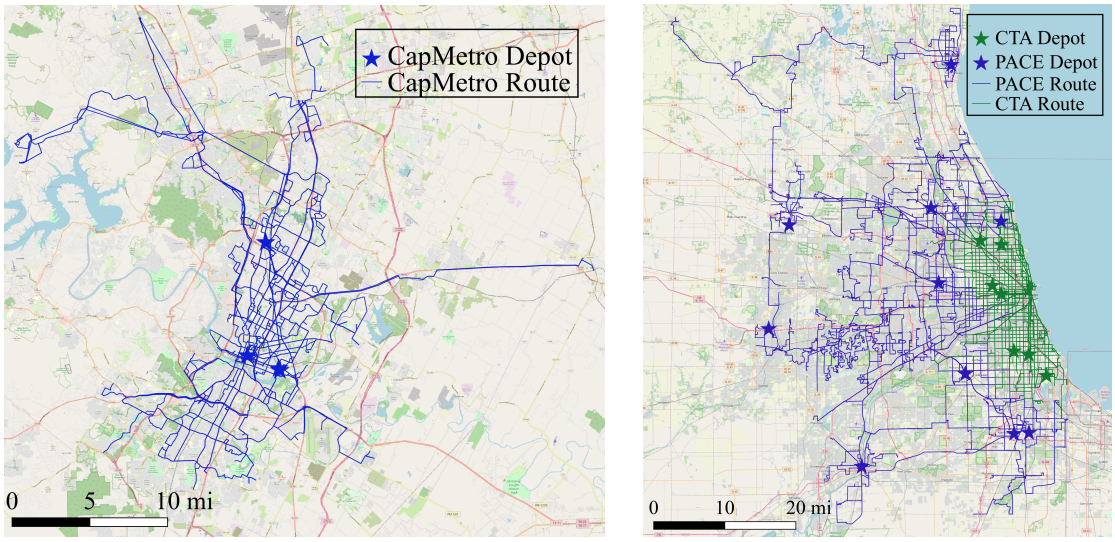

(a) Austin, TX. (b) Chicago metropolitan area.

Figure 14: Maps showing the case study regions and depot locations and routes of the three transit agencies.

nor the locations from other sources. To obtain the necessary trip schedule data, we referred to the GTFS. For CTA trips, we utilized the route-to-depot mapping information available in (ChicagoBus 2023) to assign trips to their respective depots. For CapMetro and PACE routes, we did not find any mapping information. Therefore, we computed the mid-point of each trip and assigned it to the closest depot.

The battery capacity $\overline{B} = 120$ minutes. The cost parameter $K' = 50,000$ seconds. The values of $\mathbb{M}_1 = 10^6$ and $\mathbb{M}_2 = 3 \times 10^6$. The planning horizon $\overline{T} = 86,400$ seconds, i.e., 24 hours. The weight factor for recharging time between consecutive blocks $W' = 1$. The revenue trip information, i.e. start and end times, and locations, are obtained from the GTFS data

(General Transit Feed Specification 2022). However, data for deadhead travel times is not available, so we assumed an average speed of 30 mph and used Manhattan distances as a basis for estimating deadheading travel times. The battery consumption B_i's are calculated as a summation of revenue trip and deadhead trip travel times within a block. For the parameters L and U, we set $L = 0$ and left the upper bound U unrestricted. For our analysis, we consider a 40-foot bus for both DVs and EVs. The assumed vehicle energy consumption rate $E = 220$ kW (Chicago Transit Authority 2022). To determine the EV battery capacity, we use the equation $R^{\kappa} = E\overline{B}$, which yields a battery capacity of 440 kWh for an EV range of two hours. The parameters are summarized in Table XIII.

Regarding the charging infrastructure, we considered both fast charging and slow charging. Overnight charging utilizes slow charging, while daytime charging utilizes fast charging. The power for fast charging is represented by $P^{\delta} = 450$ kW, while slow charging is represented by $P^{\nu} = 125$ kW. To determine the rates of recharge, we can apply the formulas $R^{\delta} = \frac{P^{\delta}}{E}$ and $R^{\nu} = \frac{P^{\nu}}{E}$. These calculations yield recharge rates of $R^{\delta} = 2.045$ and $R^{\nu} = 0.568$, respectively. In words, charging a bus for one minute overnight or during the day increases the SOC by 0.568 minutes or by 2.045 minutes, respectively.

TABLE XIII: Parametric values used.

$\overline{B}$ (minute)	K (\$)	M_1	M_2	R^{δ}	R^{ν}	$\overline{T}$ (minute)	W' (\$)
120	50000	10^6	3×10^6	0.568	2.045	86400	1

3.5.2 Computational performance of the heuristic methods

We conduct an analysis to reveal the computational performance of the Greedy and DaC methods, comparing them to the MILP solved by Gurobi using $|\mathcal{B}|$ as a problem size determinant lever. We utilized data from a depot located in the Chicago metropolitan area. The parametric design outlined in the previous section served as the baseline. We randomly selected a subset of trips from the available trips of this depot with $|\mathcal{B}| \in [10, 20, 30, 40, 50, 100, 200, 300]$ following a uniform distribution for the selection probability. A total of 2,230 instances were solved using the three methods, with a computational time limit of 1,200 seconds per instance.

In the Greedy method, it is assumed that all buses begin their daily trips with a fully charged battery. However, in the proposed MILP model, we allow the model to determine the required initial battery level dynamically. This assumption is made in the Greedy algorithm to simplify the model and enable it to handle large-scale problems more efficiently. To ensure a fair comparison between the Greedy, DaC methods, and the MILP solver, we change the proposed MILP model by incorporating an additional constraint. Constraint (3.23) ensures that the initial battery level of the buses is equal to their battery capacity.

$$v_{si} = \overline{B} y_{si} \qquad \forall i \in \mathcal{B} \tag{3.23}$$

All computations were performed on a workstation equipped with an Intel® Xeon® Gold 6138 CPU @2.0 GHz, 128 GB of RAM, and 64 cores. The Python 3.8.8 interface to the commercial solver Gurobi 10.0 (Gurobi Optimization, LLC 2020) was employed to solve the problem instances.

The computational performance of the MILP model solved with Gurobi, as well as the Greedy and DaC solution approaches, are reported in Table XIV. The first column specifies the number of trips, while the second column indicates the number of instances solved for a given number of trips. For the MILP approach, the first column represents the number of instances where optimality was achieved. The second column for the MILP shows the average MIP gap percentage, which measures the difference between the objective value of the best-known feasible solution found and the best lower-bound found. The Greedy column displays the average percentage Δ gap, indicating the difference between the solution reported by the solver and the solution found by the Greedy method. The DaC columns provide information on the number of times each scenario is divided into subproblems, m, as well as the average percentage Δ gap between the solution reported by the solver and the solution found by the DaC method. A negative average percentage indicates that the solutions obtained by the Greedy or DaC methods were superior to those achieved by the MILP approach. Note that in these instances, MILP actually did not reach an optimal solution.

In the analysis presented in Figure 15, it is evident that utilizing the MILP approach through a solver is only effective for handling small-scale problems. Comparatively, the DaC demonstrates slightly better performance compared to the Greedy approach with some exceptions reported on Table XIV. Furthermore, the results shown in Figure 15a indicate that as the number of subproblems (i.e., the number of times a problem is divided) increases, the quality of the solutions decreases. However, despite the increase in the number of subproblems, there is an improvement in solution quality for larger cases (e.g., 100, 200, and 300 trips) as shown in

TABLE XIV: Computational performance of the heuristic methods

# Trips	# Solved	MILP		Greedy	DaC	
		# OPTS	Avg. MIP gap (%)	Avg. Δ gap (%)	m	Avg. Δ gap (%)
10	1000	999	7.51E-06	11.69	2	9.13
20	500	497	4.69E-05	12.52	2	6.97
30	500	493	1.55E-04	13.35	4	17.76
40	100	98	1.97E-04	15.02	2	7.49
50	100	94	5.60E-04	16.20	4	15.81
100	10	8	0.035	15.39	2	8.00
200	10	0	15.5	3.65	4	-1.01
300	10	0	37.6	-21.74	4	-25.87

Figure 15b. This is because the solution quality of the Greedy and DaC approaches is compared to sub-optimal solutions obtained from the MILP solver.

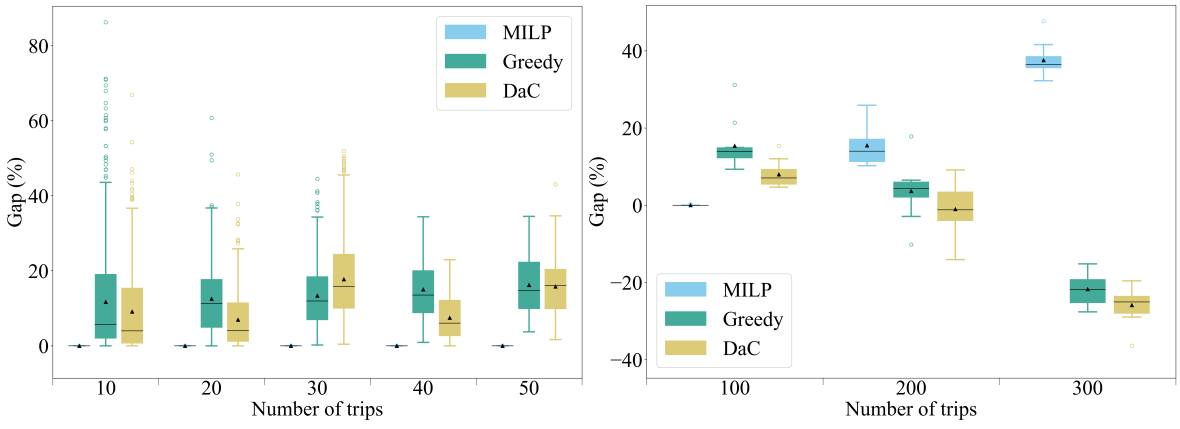

Figure 15: Gap statistics for the three solution approaches.

The solution times for the different approaches are visually represented in Figure 16a and 16b. These figures clearly demonstrate that the Greedy method consistently outperforms the other approaches in terms of solution time. The DaC method also shows a faster performance compared to the MILP solver, although it is slightly slower than the Greedy method. However, it is important to note that as the problem size, measured by the number of trips, increases, the solution time for the DaC method experiences a substantial increase.

Taking the problem size variability into account, each method exhibits its own strengths. The MILP solver performs well for small cases, where its optimal solutions can be effectively utilized. The DaC method proves to be effective for medium-sized cases, offering a balance between solution quality and computational efficiency. The Greedy method, on the other hand, excels in handling large cases by providing rapid solutions that are reasonably close to the solutions obtained by the MILP solver, for solution quality refer to Table XIV and Figure 15. This demonstrates the efficiency of the Greedy method in terms of both speed and solution quality. As the Greedy is the fastest approach for very large-scale instances and finds reasonable solutions, it is utilized in Section 3.5.3.

3.5.3 Large-scale case studies

Case studies were conducted to provide insights for key metrics, such as share of EVs, number of EVs per each DV replaced, and share of revenue trip time over the day. These studies also demonstrate the applicability of the proposed approach at large-scale problem instances. We adopted the CTA, PACE, and CapMetro data as explained previously. The number of revenue trips for CTA, PACE, and CapMetro are nearly 18,700, 7,300, and 5,400,

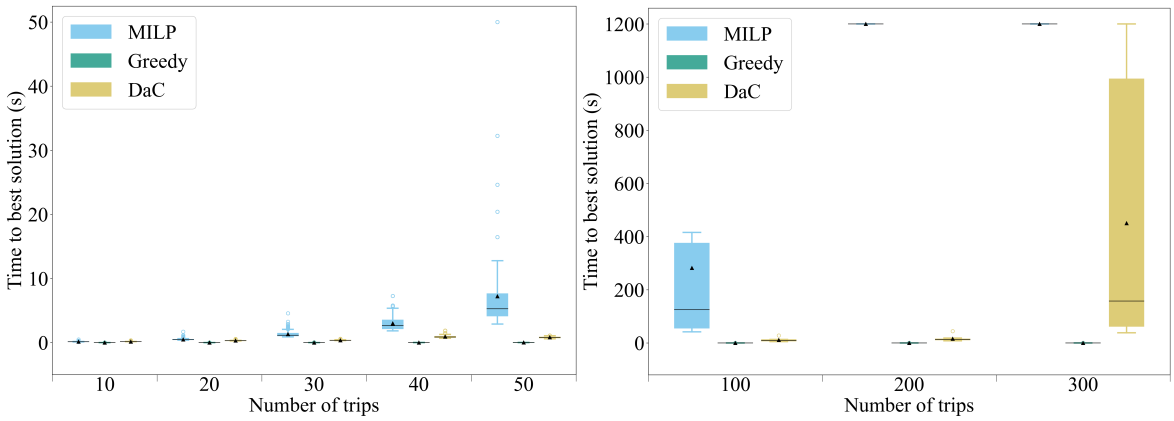

Figure 16: Time-to-best-solution statistics for the three solution approaches.

respectively. We consider three vehicle range lever: 60, 120, and 150 miles and three EV deployment target lever: Low, medium, and high. The deployment target is controlled through parameters K and W, which are described in the Section 3.3. We also ran a *DV only* scenario for each agency by solving the SDVSP allowing longer blocks followed by a version of the BCP without electrification constraints. Similarly, the leftover, longer than EV range, blocks in each electrification scenario are also chained into DVs using that version of the BCP.

Figure 17 presents the percent share of EVs and DVs (i.e., the fleet decomposition) on the left y-axis, and the total number of buses on the right one. Since our method does not implement hard constraints on the block length, 100% electrification is not guaranteed but as the results reveal, a near 100% electrification is possible at the expense of a substantial fleet size increase. These are 54%, 59%, and 58% for CTA, PACE, and CapMetro, respectively, in

the case of high deployment and 150-mile range compared to DV only. Note that "DV" on x-axis of Figure 17 and figures to be presented hereafter denotes the DV only scenario.

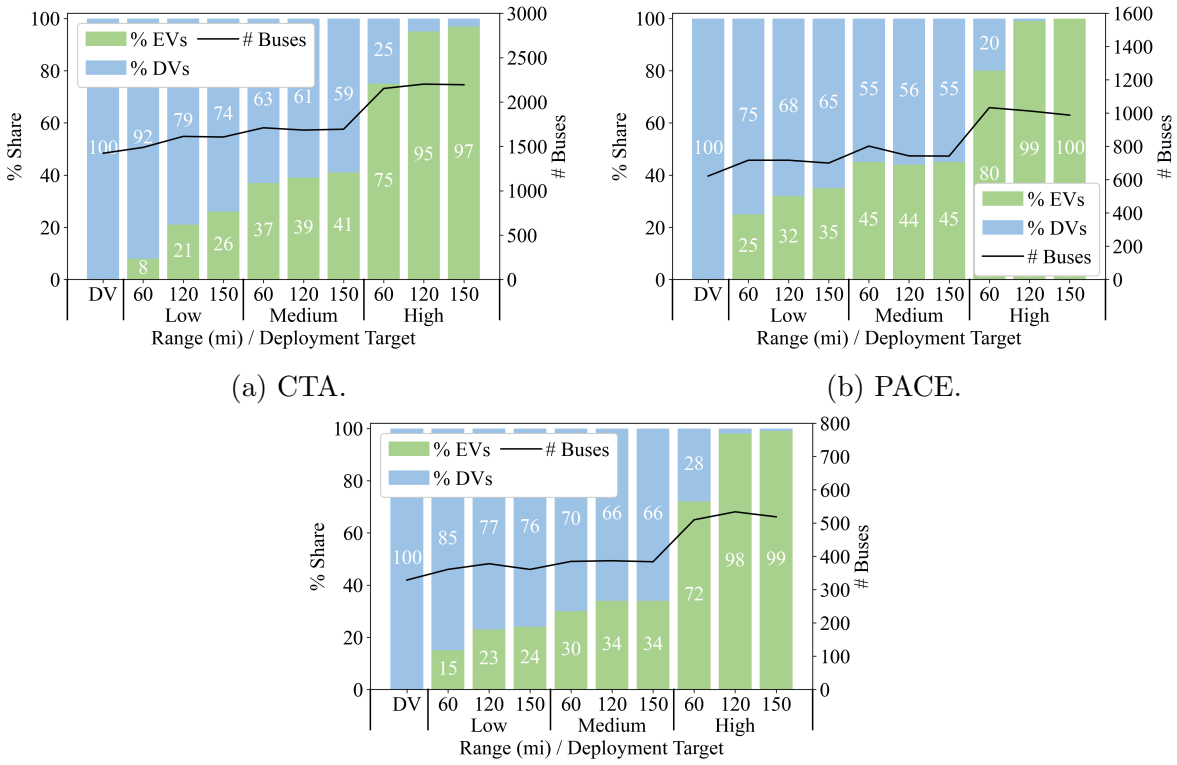

(a) CTA.

(b) PACE.

(c) CapMetro.

Figure 17: Percent share and number of buses.

Figure 18 presents the number of EVs replacing one DV. This metric is of particular interest to transit agencies as it informs on an expected fleet size with EV deployment targets. Number of EVs in a given scenario is divided by the difference of DVs in the DV only and the given

scenario to obtain this ratio. The ratio decreases as the EV range increases. This is intuitive because EVs become similar to DVs with increasing EV range. We do not observe such a strong relationship between deployment target and replacement ratio for a given EV range with the exception of 60-mile range, where there is a substantial decrease moving from low to medium.

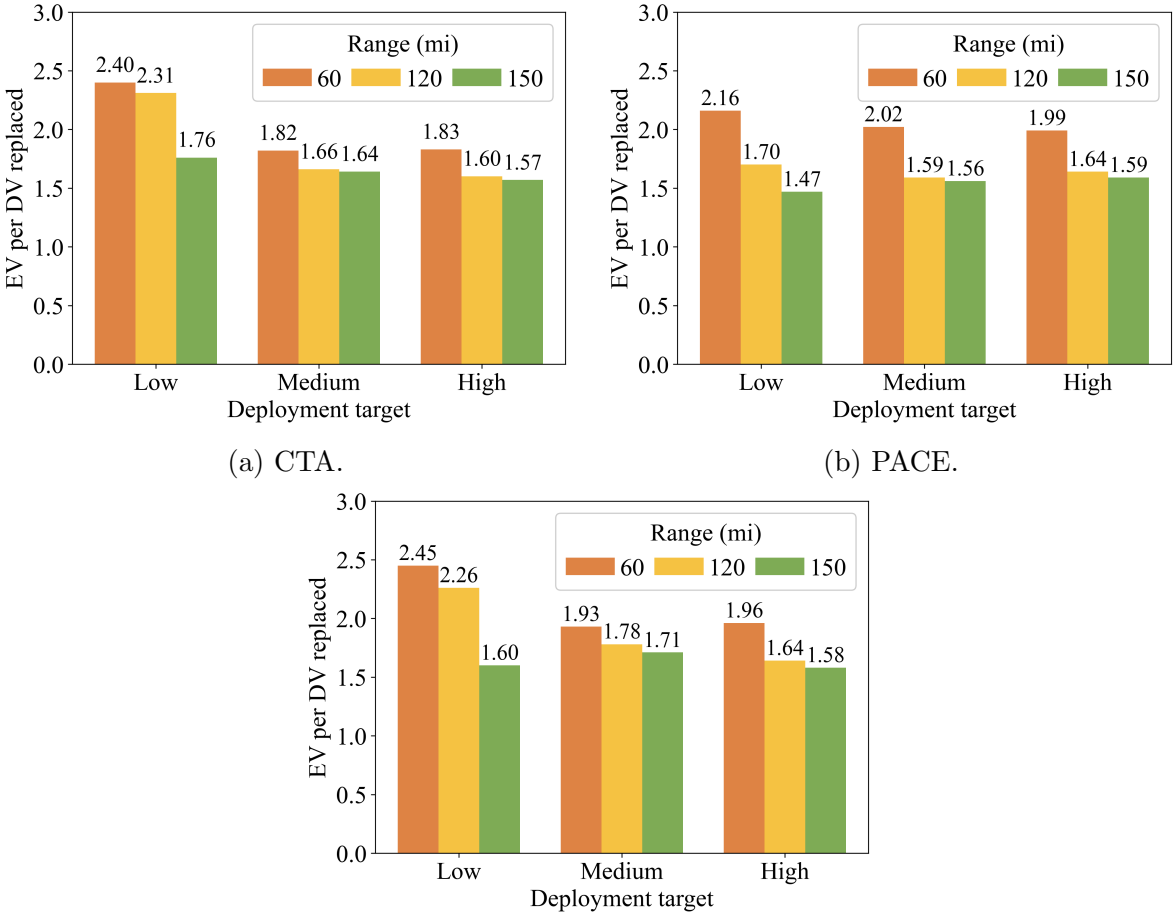

(a) CTA.

(b) PACE.

(c) CapMetro.

Figure 18: EV per DV replaced by deployment target.

The block efficiency is demonstrated in Figure 19 and is simply the ratio of revenue trip time to the entire block time. Comparing the high-deployment, 150-mile scenario to DV only, one observes an 18% reduction in the share of revenue trip time for CTA and CapMetro, whereas a 20% reduction is observed for PACE. Since blocks become shorter with higher EV deployment, there are more deadheading trips to and from the depot, which explains this change. Moreover, with higher EV deployment, there is more layover at the depots due to recharging, which is demonstrated in Figure 20. The vehicle schedule efficiency is calculated by dividing the revenue trip time to the entire horizon. In this case the efficiency decrease is by 35% for CTA, and 37% for PACE and CapMetro. Compared to the block efficiency, the drops are even more dramatic because there is also time loss due to recharging, and not only extra deadheading.

3.6 Conclusion

In this study, we proposed a two-stage solution framework to solve the SDEVSP. We solve the SDVSP to generate blocks in the first stage and then solve the BCP to form vehicle schedules. While we utilized traditional solution methods to solve the SDVSP, three solution approaches, namely MILP, DaC, and Greedy, were developed. An extensive computational experiments conducted to compare these methods revealed solution quality and computational time trade-off. We observed that the Greedy method can solve large-scale instances considerably fast, and its solution quality is comparable to that of the MILP within reasonable solution time limits.

Utilizing the greedy method, we conducted case studies for three transit agencies: CTA, PACE, and CapMetro. Near 100% electrification is possible with a replacement ratio of $\sim$1.6 EVs per DV and a 150-mile range. However, vehicle schedule efficiency would decrease by

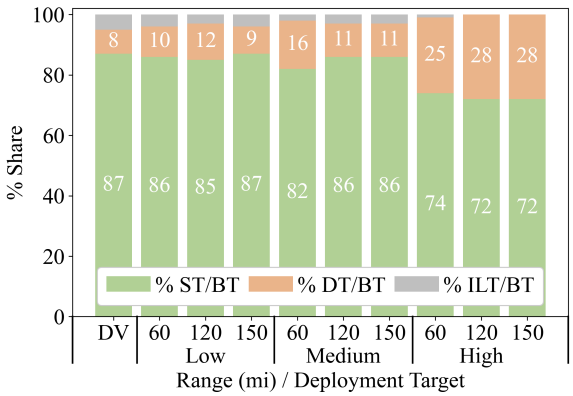

(a) CTA.

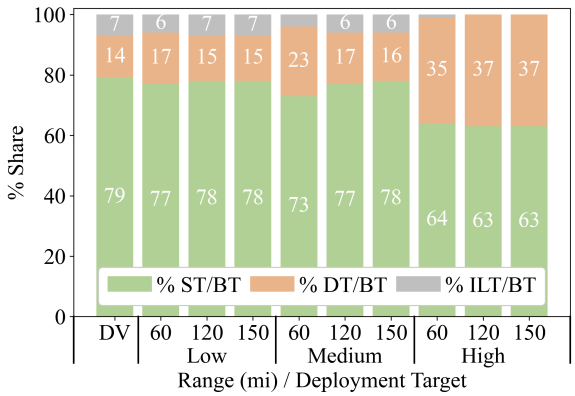

(b) PACE.

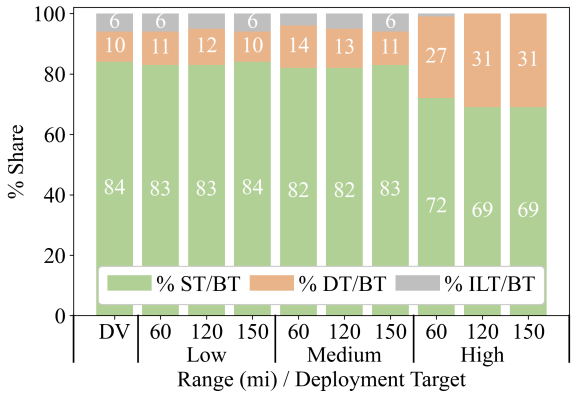

(c) CapMetro.

Figure 19: Block efficiency statistics. BT: Block time, ST: Service time, DT: Deadhead time, ILT: Intertrip layover time.

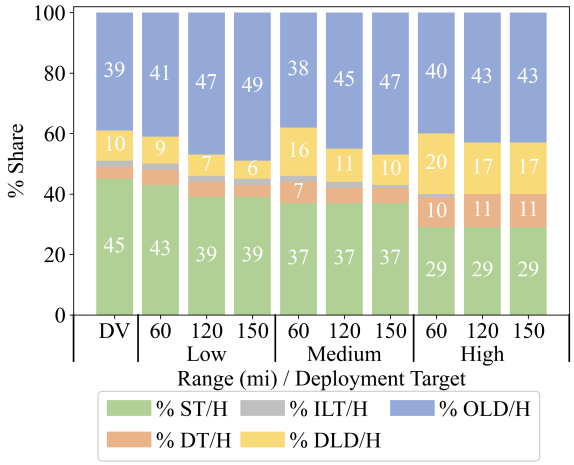

(a) CTA.

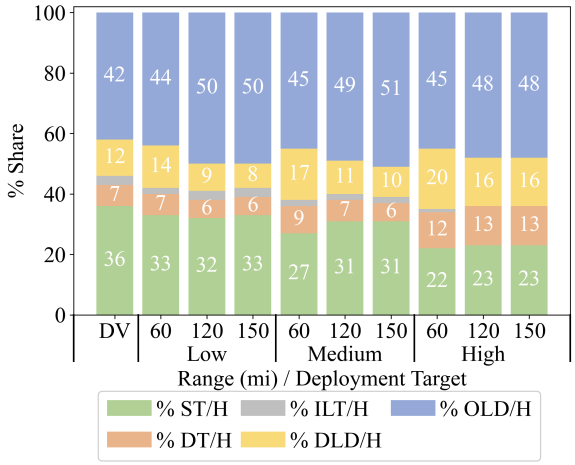

(b) PACE.

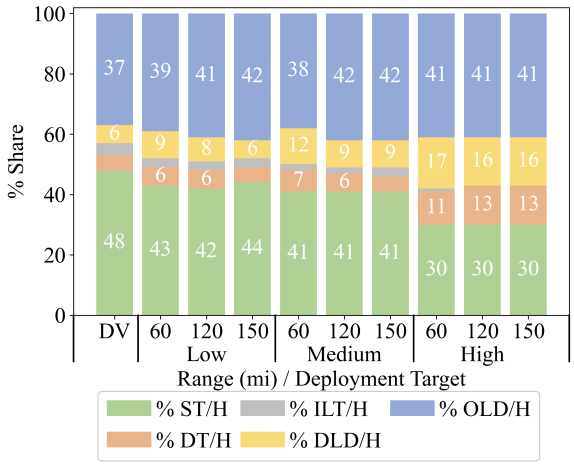

(c) CapMetro.

Figure 20: Vehicle schedule efficiency statistics. H: Horizon, ST: Service time, DT: Deadhead time, ILT: Intertrip layover time. DLD: Daytime layover at depot, OLD: Overnight layover at depot.

$\sim$35%. These results can be considered optimistic given our assumptions on depot size and charger availability. On the other hand, we do not consider opportunistic charging at the terminal stops, which would increase the schedule efficiency.

The SDEVSP is quite complex, and there are yet more aspects that are not considered in this study. Some of these are i) charger availability, ii) charger choice, e.g., pantograph or traditional, iii) charger level selection, e.g., 150 kW and 450 kW, iv) charger location including en-route charging, v) non-linear charge and discharge profiles, and vi) vehicle sizes, e.g., 40 ft and 60 ft. The readily difficult problem can easily become intractable considering a combination of these aspects. Therefore, we may tackle these problems in stages. The proposed two-step solution approach only finds a solution to the dauntingly challenging problem, and it can be enhanced. The greedy solution method is flexible to incorporate charger availability, charger level selection, and non-linear charge profiles. Future studies will improve the greedy algorithm and propose methods to address a subset of these aspects.

CHAPTER 4

ELECTRIC BUS SCHEDULING AND CHARGER LOCATION

4.1 Introduction and Background

Transit bus electrification holds significant importance in the broader context of sustainable urban transportation. The transition from traditional fossil fuel-powered buses to battery electric buses (BEBs) offers a range of benefits, encompassing environmental, economic, and social aspects The White House (2021). Some of these are reduced greenhouse gas emissions, energy efficiency, lower operating costs, and noise reduction. Yet, electrification in the transit bus context revives essential infrastructural and operational problems as well.

One such challenge is the need to reassign buses for revenue-generating service trips, referred to as the *vehicle scheduling problem* (VSP), due to the limited driving range of BEBs. Additionally, there is the task of strategically placing charging locations to accommodate charging activities. The use of pantograph chargers, which supply power from the top of the bus through scissor-like arms, introduces issues related to space occupancy and cost Daliah (2023). A growing concern is the optimal placement of these chargers across the transit service network, including terminal garages, to ensure seamless BEB operations.

A *service trip*, or simply a *trip*, is defined as a series of stop visits along a bus route that generates revenue. While bus garages are primary locations for housing chargers, placing chargers at trip end locations could facilitate charging activities. Regular recharging at these

locations could make BEBs function similarly to conventional diesel-powered buses. Resolving this necessitates solving a facility location problem (FLP) to identify optimal locations from a candidate set for housing these chargers. FLP decisions often have strategic implications, as altering or retracting them can be challenging and costly. Identifying the candidate facility set requires consideration of vehicle schedules as well. Perumal, Lusby, and Larsen (2022b) approached the VSP as a tactical planning problem, recognizing the need to address it whenever changes occur in the transit system, such as alterations in driving schedules, bus maintenance requirements, and spatial or temporal adjustments to bus routes. To address both concerns concurrently, we introduce the electric bus scheduling and charger location (EBSCL) problem.

In the existing literature, numerous studies have extensively explored the planning of charging facilities for BEBs. For instance, Liu, Song, and He (2018) presented a robust optimization model aimed at minimizing the total investment costs associated with deploying charging infrastructure for BEBs. Expanding on this work, Liu, Qu, and Ma (2021) broadened the scope by incorporating seasonality and power matching into charger deployment. This extension highlighted the significant impact of BEB energy consumption characteristics on the optimal selection of charging station locations. A comprehensive approach was adopted in An (2020) by integrating charging facility planning and fleet scheduling, addressing uncertainties in charging demand through a stochastic integer optimization model. Meanwhile, Uslu and Kaya (2021) proposed a model that focuses on determining optimal charging station locations and capacities, with an assumption of limited waiting time. Lin et al. (2019) and Li et al. (2022) approached

BEB charger deployment as a multi-stage planning problem, optimizing station locations at various stages of the planning process.

In addition to determining optimal charger locations, the scheduling of the BEB fleet emerges as a critical concern. Niekerk, Akker, and Hoogeveen (2017) made significant contributions by incorporating BEBs into the classical VSP, taking into account driving range limitations and linear charging. A more recent study by Cokyasar, Verbas, and Auld (2023b) has further delved into BEB fleet scheduling, addressing the single depot VSP and proposing a heuristic solution approach. This innovative approach involves generating short tours that a BEB can serve, employing a mixed-integer non-linear program to combine tour tuples and ultimately generate bus runs. Various aspects of BEB fleet scheduling, such as charging event time, uncertainty in travel time, and energy consumption, have also been addressed by other studies Bie et al. (2021), Wen et al. (2016), Xiong et al. (2022), Yildirim and Yildiz (2021).

Existing optimization approaches often fall short by either assuming predetermined charging facility locations or neglecting the intricacies of the BEB scheduling. This gap in the literature underscores the need for more comprehensive models that consider both charger location and fleet scheduling in an integrated manner. Recognizing this critical interdependence, certain studies have introduced integrated models to address this synergy effectively Alwesabi et al. (2021), Liu and (Avi) Ceder (2020), Wang, Liao, and Lu (2022). Nonetheless, limited attention has been given to EBSCL problem. Our research seeks to bridge this gap by focusing on optimizing the scheduling of BEBs and strategically determining charging locations, taking into account the dynamic nature of routes. By acknowledging and addressing the EBSCL problem,

our study aims to contribute novel insights and pave the way for more comprehensive and effective solutions, thereby advancing the current understanding of sustainable urban transit systems.

In the subsequent sections of the paper, Section 4.2 formally describes the EBSCL problem and presents the mixed-integer linear programming (MILP) model formulation. Next, we provide details about the data used for numerical experiments in Section 4.3. Following that, we present a comprehensive overview of the case study design and discuss parametric choices to evaluate the performance of our proposed solution algorithm in Section 4.4. Finally, Section 4.5 concludes the study by summarizing the key findings and contributions of our work and discussing potential future research directions.

4.2 Problem definition

We now formally describe the EBSCL problem, which we model as an MILP. To ease reading, we use calligraphic letters to represent sets (e.g., $\mathcal{A}$), uppercase Roman letters for parameters (e.g., $\overline{B}$), lowercase Roman letters for variables and indices (e.g., y_{ij}), and Greek letters (e.g., α) as superscripts to modify parameters. Let $\mathcal{T}$ represent the set of timetabled bus trips, and let $\mathcal{E}$ denote the set of all feasible arcs connecting consecutive trips. The binary variable y_{ij} takes the value 1 if trip j is scheduled to follow trip i, forming valid sequences of bus trips. Chargers can be located at a set of candidate facilities, denoted by $\mathcal{F}$ that includes the garage denoted by d. This set is further partitioned into a subset $\mathcal{F}_{ij} \subseteq \mathcal{F}$ representing the candidate facilities which could be used in connection of trips i and j, and $\cup_{(i,j)\in\mathcal{A}}\mathcal{F}_{ij} = \mathcal{F}$. The binary variable e_{ijf} indicates whether recharging occurs between trips i and j at facility

f. We symbolize the single garage with two indices s and t, that is every bus run starts from s and ends at t. Table XV and Table XVI provide definition of sets, parameters, and variables used in the MILP model. The model to solve the EBSCL problem is formulated as follows.

$$\min \sum_{f \in \mathcal{F}} C_f^{\mu} x_f + \sum_{i \in \mathcal{T}} C^{\nu} y_{si} + \sum_{(i,j) \in \mathcal{E}} C^{\rho} \left(T_j^{\alpha} - T_i^{\beta} \right) y_{ij} \tag{4.1}$$

subject to,

$$\sum_{j:(i,j) \in \mathcal{A}} y_{ij} = 1 \qquad \forall i \in \mathcal{T} \tag{4.2}$$

$$\sum_{i:(i,j) \in \mathcal{A}} y_{ij} = 1 \qquad \forall j \in \mathcal{T} \tag{4.3}$$

$$\sum_{f \in \mathcal{F}_{ij}} e_{ijf} \leq y_{ij} \qquad \forall (i,j) \in \mathcal{A} \tag{4.4}$$

$$u_{ijf} \leq \overline{B} e_{ijf} \qquad \forall (i,j) \in \mathcal{A}, f \in \mathcal{F}_{ij} \tag{4.5}$$

$$\sum_{(i,j) \in \mathcal{A}} e_{ijf} \leq \mathbb{M} x_f \qquad \forall f \in \mathcal{F} \tag{4.6}$$

$$\begin{aligned} v_{ij} = \max \Bigg\{ b_i - B_i - E_{ij} y_{ij} - \sum_{f \in \mathcal{F}_{ij}} \left(E_{if} + E_{fj} - E_{ij} \right) e_{ijf} + \sum_{f \in \mathcal{F}_{ij}} u_{ijf} \\ - \mathbb{M} \left(1 - y_{ij} \right), 0 \Bigg\} \qquad \forall (i,j) \in \mathcal{A} \end{aligned} \tag{4.7}$$

$$b_j = \sum_{i:(i,j) \in \mathcal{A}} v_{ij} \qquad \forall j \in \mathcal{T} \tag{4.8}$$

$$b_i - B_i - \sum_{j:(i,j)\in\mathcal{A}} E_{ij} y_{ij} \geq -\mathbb{M} \sum_{j:(i,j)\in\mathcal{A}, f\in\mathcal{F}_{ij}} e_{ijf} \qquad \forall i \in \mathcal{T} \tag{4.9}$$

$$b_i - B_i - \sum_{j:(i,j)\in\mathcal{A}, f\in\mathcal{F}_{ij}} E_{if} e_{ijf} \geq 0 \qquad \forall i \in \mathcal{T} \tag{4.10}$$

$$b_i - B_i - \sum_{j:(i,j)\in\mathcal{A}, f\in\mathcal{F}_{ij}} E_{if} e_{ijf} + \sum_{j:(i,j)\in\mathcal{A}, f\in\mathcal{F}_{ij}} u_{ijf} \leq \overline{B} \qquad \forall i \in \mathcal{T} \tag{4.11}$$

$$b_s - B_s - \sum_{f\in\mathcal{F}_{sj}} E_{sf} e_{sjf} \geq 0 \qquad \forall j \in \mathcal{T} \tag{4.12}$$

$$b_s - B_s - \sum_{f\in\mathcal{F}_{sj}} E_{sf} e_{sjf} + \sum_{f\in\mathcal{F}_{sj}} u_{sjf} \leq \overline{B} \qquad \forall j \in \mathcal{T} \tag{4.13}$$

$$b_s \leq \overline{B} \tag{4.14}$$

$$\begin{aligned} 0 \leq \left(T_j^{\alpha} - T_i^{\beta}\right) y_{ij} - \left(E_{ij} y_{ij} + \sum_{f\in\mathcal{F}_{ij}} \left(E_{if} + E_{fj} - E_{ij}\right) e_{ijf} + \frac{\sum_{f\in\mathcal{F}_{ij}} u_{ijf}}{R^{\delta}} \right) \\ \leq D + \mathbb{M} e_{ijd} \qquad \forall (i,j) \in \mathcal{E} \end{aligned} \tag{4.15}$$

The objective function (4.1) minimizes the weighted total cost, including the cost of overall time between two consecutive trips, the vehicle costs associated with each scheduled run, and the charger facility costs. Constraints (4.2) and (4.3) ensure that each trip is both preceded and succeeded by exactly one other trip, forming a valid sequence. Constraints (4.4) guarantee that a BEB can recharge between trips $i \in \mathcal{T}$ and $j \in \mathcal{T}$ if they are connected. Constraints (4.5) ensure that the charging amount between consecutive trips does not exceed the battery capacity. Constraints (4.6) enforce that a charging facility must be located at $f \in \mathcal{F}$ if it is used

TABLE XV: Sets and parameters used in the MILP for the EBSCL.

Set	**Definition**
$\mathcal{A}$	set of all feasible arcs connecting two consecutive trips within the horizon, $\mathcal{A} = \mathcal{E} \bigcup (\{s\} \times \mathcal{T}) \bigcup (\mathcal{T} \times \{t\})$, where s and t indices denote the garage buses are dispatched from and return to, respectively
$\mathcal{E}$	set of arcs connecting consecutive trips $i \in \mathcal{T}$ (first) and $j \in \mathcal{T}$ (second), $\mathcal{E} = \left\{ (i,j) \,\middle|\, i,j \in \mathcal{T} \wedge i \neq j \wedge L \leq \left(T_j^{\alpha} - T_i^{\beta} - E_{ij}\right) \leq U \right\}$
$\mathcal{F}$	set of candidate charging facilities $f \in \mathcal{F}$, and $\mathcal{F}$ includes d, that represents the garage charging
$\mathcal{F}_{ij}$	subset of candidate charging facilities that provide reasonable deflection between trips $i \in \mathcal{T}$ and $j \in \mathcal{T}$, $\cup_{(i,j)\in\mathcal{A}} \mathcal{F}_{ij} = \mathcal{F}$
$\mathcal{T}$	set of timetabled bus trips
Parameter	**Definition**
$\overline{B}$	battery capacity in time units
B_i	energy consumption of trip $i \in \mathcal{T} \cup \{s\}$ measured in time units, and $B_s = 0$
C^{ν}	vehicle cost in time units
C^{ρ}	weight for time spent between service trips
C_f^{μ}	charging facility cost at candidate location $f \in \mathcal{F}$ in time units
D	maximum duration a BEB is allowed to spend in layover between two trips, anywhere other than garage, measured in time units
E_{ij}	energy consumption of traveling from last stop of trip $i \in \mathcal{T} \cup \mathcal{F} \cup \{s,t\}$ to first stop of trip $j \in \mathcal{T} \cup \mathcal{F} \cup \{s,t\}$ measured in time units, e.g., for every minute a bus drives, it consumes one minute of energy
L	minimum admitted recharging and/or layover time between two consecutive trips
$\mathbb{M}$	big number
R^{δ}	rate of recharge, i.e., energy (in time units) gained by recharging in one unit of time, e.g., R^{δ} minutes of driving range is gained by recharging a bus for one minute
T_i^{α}	start time of trip $i \in \mathcal{T}$
T_i^{β}	end time of trip $i \in \mathcal{T}$
U	maximum admitted recharging and/or layover time between two consecutive trips

by at least one BEB. Constraints (4.7) and (4.8) calculate the state of charge (SOC) before each trip, while constraints (4.9) – (4.11) maintain the SOC within feasible bounds. Constraints (4.12) – (4.14) regulate the SOC at the beginning of each run. Constraints (4.15) set bounds on the *layover time* between two consecutive trips. Here, layover time is defined as the time that a BEB is not serving a trip, not deadheading between two trips, and not charging. To

TABLE XVI: Variables used in the MILP for the EBSCL.

Variable	Definition
b_i	state of charge (SOC) at the beginning of trip $i \in \mathcal{T} \cup \{s\}$ measured in time units, $b_i \in \mathbb{R}_{\geq 0}$
e_{ijf}	$\begin{cases} 1 & \text{if BEB recharges between trips } i \in \mathcal{T} \text{ and } j \in \mathcal{T} \text{ at facility } f \in \mathcal{F}_{ij},\ (i,j) \in \mathcal{A} \\ 0 & \text{otherwise} \end{cases}$
u_{ijf}	energy gained between trips i and j at facility $f \in \mathcal{F}_{ij}$ measured in time units, $u_{ijf} \in \mathbb{R}_{\geq 0},\ (i,j) \in \mathcal{A},\ f \in \mathcal{F}_{ij}$
v_{ij}	SOC at the beginning of trip j after serving trip i measured in time units, $v_{ij} \in \mathbb{R}_{\geq 0},\ (i,j) \in \mathcal{A}$
x_f	$\begin{cases} 1 & \text{if a charging facility is placed at candidate location } f \in \mathcal{F} \\ 0 & \text{otherwise} \end{cases}$
y_{ij}	$\begin{cases} 1 & \text{if trip } j \text{ is served after trip } i,\ (i,j) \in \mathcal{A} \\ 0 & \text{otherwise} \end{cases}$
z_{ij}	auxiliary binary variable used to linearize the max function, $(i,j) \in \mathcal{A}$

linearize constraint (4.7), involving a non-linear term with the max function, we introduce an auxiliary binary variable, z_{ij}. The linearization is achieved through the following constraints (4.16) – (4.18).

$$v_{ij} \geq b_i - B_i - E_{ij} y_{ij} - \sum_{f \in \mathcal{F}_{ij}} \left(E_{if} + E_{fj} - E_{ij}\right) e_{ijf} + \sum_{f \in \mathcal{F}_{ij}} u_{ijf} - \mathbb{M}\left(1 - y_{ij}\right) \qquad \forall (i,j) \in \mathcal{A} \tag{4.16}$$

$$v_{ij} \leq b_i - B_i - E_{ij} y_{ij} - \sum_{f \in \mathcal{F}_{ij}} \left(E_{if} + E_{fj} - E_{ij}\right) e_{ijf} + \sum_{f \in \mathcal{F}_{ij}} u_{ijf} - \mathbb{M}\left(1 - y_{ij} - z_{ij}\right) \qquad \forall (i,j) \in \mathcal{A} \tag{4.17}$$

$$v_{ij} \leq \mathbb{M}\left(1 - z_{ij}\right) \qquad \forall (i,j) \in \mathcal{A} \tag{4.18}$$

$$e_{ijf},\ y_{ij},\ x_f,\ z_{ij} \in \{0,1\}, b_i,\ u_{ijf},\ v_{ij} \in \mathbb{R}_{\geq 0}$$

TABLE XVII: Parametric values used.

C_f^{μ} (s)	C^{ρ}	V (mph)	R^{κ} (kWh/mile)	P (kW)	D (s)	$\mathbb{M}$	L (s)	U (s)
$1,000$	1	20	7.33	450	$6,000$	10^6	0	$10,800$

4.3 Data

Our experiments use Chicago metropolitan region as a testbed. We randomly select a bus garage of the transit agency Pace Suburban Bus that serves 60 trips. The trip information, i.e. T_i^{α} and T_i^{β} are obtained from the General Transit Feed Specification (GTFS) data (General Transit Feed Specification 2022). Figure 21 shows the location of the garage, the roadway links used in these trips, and five candidate charging facilities. The parameters used are summarized in Table XVII. We assumed an average speed of 20 mph and used Manhattan distances as a basis for estimating deadheading energy consumption E_{ij} in time units. The energy consumption B_i is calculated as the time difference between T_i^{β} and T_i^{α}. We consider a bus with battery capacity $B^{\kappa} = [60, 90, 120]$ miles. To determine the BEB capacity in time units, we calculate $\overline{B} = \frac{B^{\kappa}}{V}$, which yields a battery capacity of three hours for $B^{\kappa} = 60$ miles.

Regarding the charging infrastructure, we consider fast charging. The power for fast charging is $P = 450$ kW. To determine the rates of recharge, we calculate $R^{\delta} = \frac{P}{VR^{\kappa}}$, where R^{κ} is bus energy consumption rate in kWh/mile. These calculations yield recharge rates of $R^{\delta} = 3.068$, that is charging a bus for one unit of time increases the SOC by 3.068 time unit.

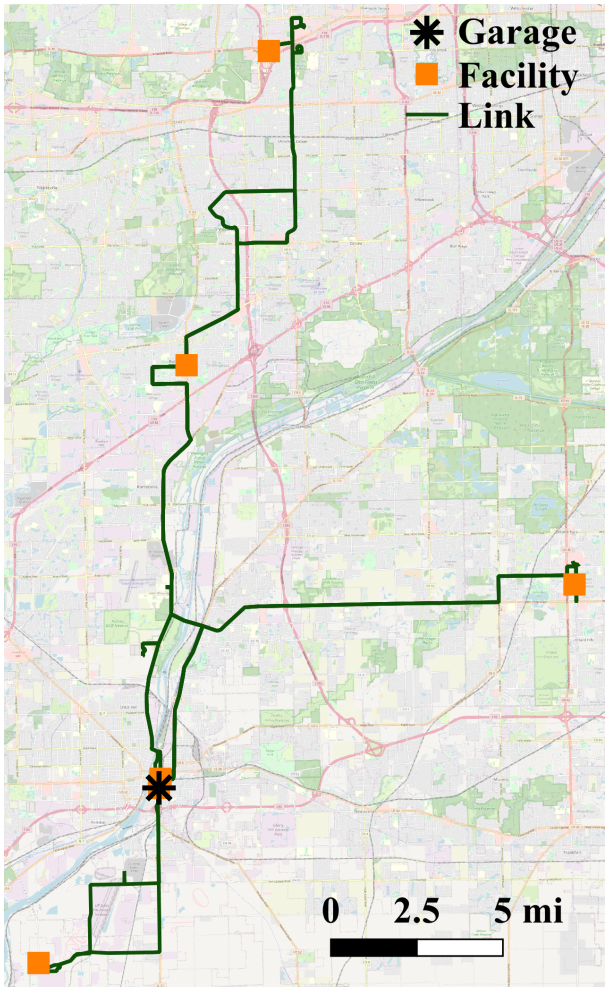

Figure 21: Candidate facility, garage, and trip locations in the case study.

4.4 Case study

In the case study, we run 15 instances of the problem considering $B^{\kappa} = [60, 90, 120]$ miles and $C^{\nu} = [1, 1K, 10K, 50K, 100K]$, where K denotes a thousand. The instances are solved using the Python 3.6.9 interface to interface with the commercial solver Gurobi 10.0 (Gurobi

Optimization, LLC 2020). Number of open facilities and the number of bus runs found by the optimization shown in Figure 22 are key performance indicators. In Figure 22a, we observe that the number of bus runs considerably decreases as vehicle cost C^{ν} increases. On the other hand, the bus range B^{κ} does not always impact the number of bus runs.

Figure 22b demonstrates the change in number of open facilities for different B^{κ} and C^{ν}. A strong correlation between C^{ν} and the number of open facilities is not found, however the number of facilities often increases as C^{ν} moves up. We observe that the number of facilities can decrease when the range increases. When B^{κ} changes from 60 to 90 and 120 miles at $C^{\nu} = 1$, we observe that the number of open facilities drops from two to one. In the case when it is one, the only open facility is the garage, while an additional candidate facility is chosen in the other case. We observe two open facilities in many cases because the combined travel time from garage to a trip's origin, servicing the trip, and from trip's destination to the garage is larger than $\overline{B}$. This finding shows that more facilities can be needed when trip times are close to the vehicle range.

In these results, we also analyze the magnitude of times spent for service, deadhead, charging, and layover. Figure 23 shows the percent share of a day spent for these four activities in these 15 scenarios. As C^{ν} increases, we observe a larger service share indicating a higher vehicle utilization.

4.5 Conclusion

The electrification trend, aimed at fostering a cleaner and sustainable environment, places particular emphasis on transitioning from diesel buses due to their significant contribution to

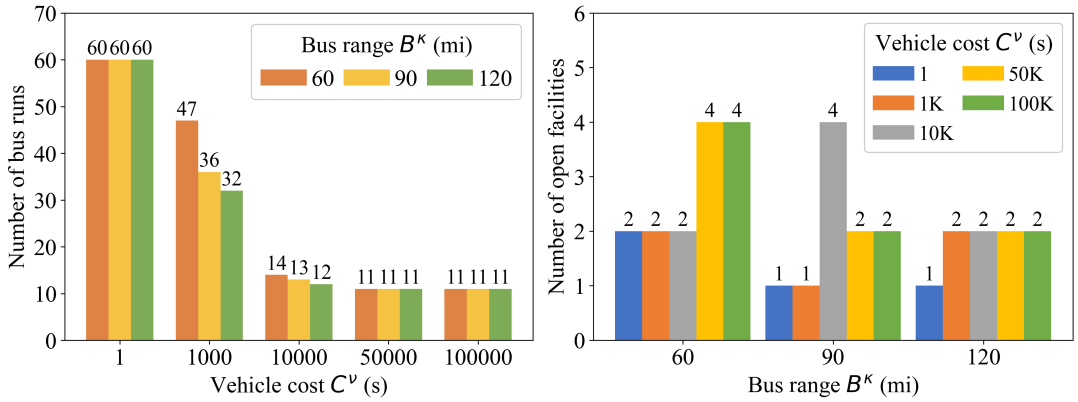

(a) (b)

Figure 22: Vehicle cost and bus range impact on fleet size.

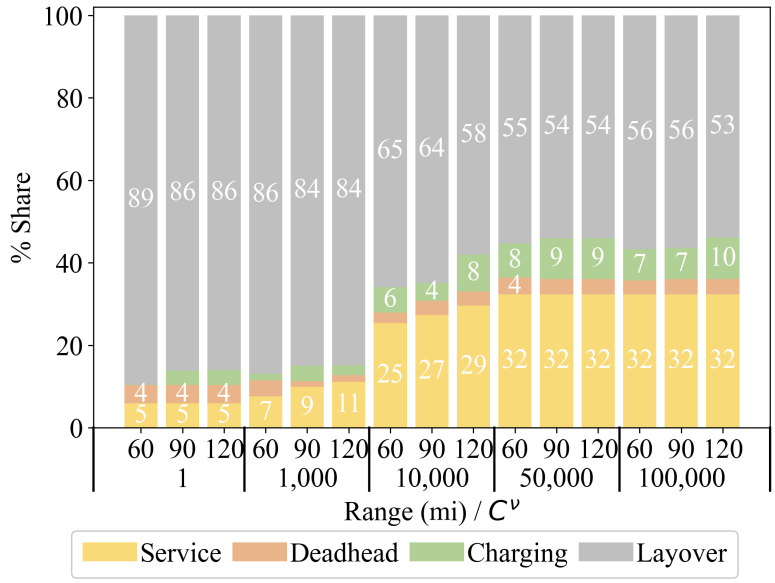

Figure 23: Vehicle schedule efficiency statistics.

emissions. However, the conversion of these buses is a challenge owing to their long ranges and fast refueling times. In this research, we tackle the EBSCL problem by formulating an MILP model. Our objective is to optimize BEB schedules and strategically identify charging facilities, especially at trip end locations. We illustrate the linearization process of the model, offer comprehensive insights into the utilized data, and present case studies to showcase the practicality of our proposed model.

The case study specifically examines a bus garage of Pace Suburban Bus in Chicago region, encompassing 60 trips and considering five potential charging locations that coincide with the terminal stops of the analyzed trips. While we can achieve optimality for this scenario, it is evident that the problem scale is not merely substantial but reaches a magnitude that exceeds the capabilities of off-the-shelf solvers. Addressing the scalability of the problem necessitates the incorporation of heuristic or metaheuristic solution methods.

This investigation concentrates exclusively on the location aspect, assuming that each identified site has the capacity to accommodate sufficient charging infrastructure. In essence, the study does not determine the charging capacity or schedule. Even with these simplifications, we highlight the inherent complexity of the problem, and introducing these factors would only amplify its intricacy. Moreover, the decision-making process for locations could be aggregated across different garages within a single transit service agency, allowing vehicles from various garages to recharge at locations overlapping with another garage's service area. In conclusion, our study marks an initial step in modeling and solving a substantial and intricate electrification problem, leaving numerous avenues for future research and exploration.

CHAPTER 5

CONCLUSION AND POLICY IMPLICATIONS

5.1 Summary

The dissertation comprises three comprehensive papers addressing critical challenges in the electrification of trucks and buses, offering insights into optimizing charging infrastructure, vehicle scheduling, and electrification strategies.

The first paper introduces the Electric Vehicle Shortest Electric Charging Location-Allocation (EVSELCA) problem, focusing on optimizing the charging infrastructure for electrified trucks. By proposing a Mixed-Integer Linear Programming (MILP) model and innovative solution approaches such as clustering and Genetic Algorithms, the study provides a versatile framework for strategically planning charging facilities. The paper emphasizes the significance of balancing economic opportunities with the freight industry's operational philosophy, addressing scalability challenges and uncovering key factors influencing the electrification decision-making process.

The second paper addresses the Stochastic Electric Demand Vehicle Scheduling Problem (SDEVSP), presenting a two-stage solution framework. Utilizing traditional methods like MILP alongside dynamic and greedy approaches, the study compares solution quality and computational time trade-offs. The research reveals that the Greedy method offers efficient solutions for large-scale instances, presenting a viable alternative to traditional methods. The paper's

findings underscore the importance of considering both electrification rates and vehicle schedule efficiency in achieving optimal transit fleet electrification.

The third paper tackles the Electrification of Bus Scheduling and Charging Location (EB-SCL) problem, formulating an MILP model to optimize Battery Electric Bus (BEB) schedules and strategically identify charging facilities. While presenting a case study focused on a bus garage in the Chicago region, the paper delves into the inherent complexity of the problem, necessitating the incorporation of heuristic or metaheuristic solution methods for scalability. The study's insights highlight the need for strategic charging infrastructure planning, considering factors such as charger locations, capacities, and types, and serves as an initial step in modeling and solving intricate electrification challenges for buses.

5.2 Policy Implacations

The government's commitment to electrification is crucial for fostering sustainable transportation, with a particular emphasis on the planning and development of electric bus and truck infrastructure. A key policy initiative involves the establishment of a dedicated fund to strategically invest in charging infrastructure planning for both trucks and buses. This fund aims to address the intricate challenges associated with the electrification process by incentivizing the adoption of innovative technologies, especially in the realm of charging infrastructure. For instance, transit agencies and freight companies that strategically plan their charging infrastructure, considering factors such as optimal locations, charger types, and capacities, could qualify for financial incentives. These incentives may encompass grants for fast-charging infrastructure, allowing for the efficient electrification of both buses and trucks.

In recognizing the pivotal role of charger costs in determining the feasibility of electrification projects, policymakers are urged to prioritize measures that reduce financial barriers hindering the widespread adoption of electric vehicles. Financial incentives, subsidies, and tax credits will be introduced to alleviate upfront costs for charger installation, fostering public-private partnerships to share financial burdens and encourage collaboration between government entities and private enterprises. Additionally, the policymakers should allocate funds for research and development initiatives aimed at advancing charger technologies, seeking to reduce manufacturing costs and enhance charging efficiency. Standardization and interoperability guidelines will be promoted to ensure compatibility with various electric vehicles, fostering accessibility and reducing overall costs.

Balancing electrification goals with operational efficiency is a crucial consideration for policymakers, especially in the context of the SDEVSP. As the study reveals trade-offs between high electrification rates and vehicle schedule efficiency, policy frameworks should emphasize a harmonious blend of environmental and operational considerations when establishing electrification targets for transit agencies. This requires a nuanced approach that appreciates the multifaceted challenges posed by electrification and strives to strike a delicate balance.

Strategic charging infrastructure planning, specifically for battery electric buses, is a targeted policy initiative that can significantly impact the efficiency of electrification. Policymakers are urged to develop comprehensive policies that encourage transit agencies to optimize charging locations, considering factors such as terminal stops, charger types, and capacities. The proposed Electrification of EBSCL model provides a foundation for such strategies. Finan-

cial incentives and supportive frameworks can motivate transit agencies to strategically plan charging infrastructure, leading to more efficient electrification outcomes for bus fleets.

5.3 Limitations

While the dissertation makes significant contributions to the electrification discourse, it is essential to acknowledge certain limitations that provide avenues for future research and refinement. Firstly, the exclusion of stochastic demand in the analysis constitutes a notable limitation. Real-world transportation systems often face uncertain and dynamic demand patterns, and the absence of stochastic considerations may impact the models' ability to accurately reflect the complexities associated with fluctuating charging needs. Future research endeavors could explore stochastic demand models to provide a more comprehensive understanding of the electrification challenges in the face of unpredictable usage patterns.

Secondly, the dissertation relies on linear profiles for charge and discharge, overlooking the potential nonlinearity inherent in electric vehicle charging and discharging processes. The simplification to linear profiles may not fully capture the intricacies of real-world charging behaviors and could impact the precision of optimization outcomes. Future studies could delve into nonlinear charge and discharge profiles to refine models and enhance their applicability, accounting for variations in charging rates and battery behaviors that linear approximations might overlook.

It is crucial to recognize the specific limitations related to charger allocation, particularly in the context of electric buses. While the EVSELCA chapter successfully determines optimal charger allocation for electric trucks, the subsequent chapters (SDEVSP and EBSCL) focus

on charger location optimization without explicitly addressing the charger allocation aspect for electric buses. In these chapters, the assumption that a sufficient number of chargers are available leads to zero waiting times for buses during the charging process. While this assumption facilitates a simplified modeling approach, it introduces a limitation by not delving into the critical aspect of charger allocation for electric buses. Charger allocation, determining how many buses each charger serves and the optimal distribution of charging resources, is a crucial consideration to ensure efficient and realistic electrification planning. This limitation signals an opportunity for future research to build upon the existing foundation and extend the optimization framework to explicitly address charger allocation for electric buses.

REFERENCES

Alwesabi Y, Liu Z, Kwon S, Wang Y, 2021 *A novel integration of scheduling and dynamic wireless charging planning models of battery electric buses. Energy* 230:120806, URL http://dx.doi.org/10.1016/j.energy.2021.120806.

Alwesabi Y, Wang Y, Avalos R, Liu Z, 2020 *Electric bus scheduling under single depot dynamic wireless charging infrastructure planning. Energy* 213:118855, URL http://dx.doi.org/https://doi.org/10.1016/j.energy.2020.118855.

An K, 2020 *Battery electric bus infrastructure planning under demand uncertainty. Transportation Research Part C: Emerging Technologies* 111:572–587, URL http://dx.doi.org/10.1016/j.trc.2020.01.009.

Auld J, Hope M, Ley H, Sokolov V, Xu B, Zhang K, 2016 *POLARIS: Agent-based modeling framework development and implementation for integrated travel demand and network and operations simulations. Transportation Research Part C: Emerging Technologies* 64:101–116, URL http://dx.doi.org/10.1016/j.trc.2015.07.017.

Bennett J, Mishra P, Miller E, Borlaug B, Meintz A, Birky A, 2021 *Estimating the breakeven price of delivered electricity to charge class 8 electric vehicles.* Available at www.nrel.gov/publications accessed on Dec. 22, 2022.

Bie Y, Ji J, Wang X, Qu X, 2021 *Optimization of electric bus scheduling considering stochastic volatilities in trip travel time and energy consumption. Computer-Aided Civil and Infrastructure Engineering* 36(12):1530–1548, URL http://dx.doi.org/10.1111/mice.12684.

Blahut RE, 2010 *Fast algorithms for signal processing* (New York: Cambridge University Press), ISBN 9780521190497.

Bodin L, 1983 *Routing and scheduling of vehicles and crews. Computer & Operations Research* 10(2):69–211, URL http://dx.doi.org/10.1016/0305-0548(83)90030-8.

Bunte S, Kliewer N, 2009 *An overview on vehicle scheduling models. Public Transport* 1(4):299–317, URL http://dx.doi.org/10.1007/s12469-010-0018-5.

Ceder A, Wilson NH, 1986 *Bus network design. Transportation Research Part B: Methodological* 20(4):331–344, URL http://dx.doi.org/https://doi.org/10.1016/0191-2615(86)90047-0.

Chao Z, Xiaohong C, 2013 *Optimizing battery electric bus transit vehicle scheduling with battery exchanging: Model and case study. Procedia - Social and Behavioral Sciences* 96:2725–2736, URL http://dx.doi.org/https://doi.org/10.1016/j.sbspro.2013.08.306, intelligent and Integrated Sustainable Multimodal Transportation Systems Proceedings from the 13th COTA International Conference of Transportation Professionals (CICTP2013).

Chicago Transit Authority, 2022 *Charging forward CTA bus electrification planning report.* URL https://www.transitchicago.com/assets/1/6/Charging_Forward_Report_2-10-22_(FINAL).pdf.

ChicagoBus, 2023 *Bus garages.* URL https://www.chicagobus.org/garages/.

Cokyasar T, Davatgari A, Mohammadian A, 2023 *An optimization model for solving the route clustering problem. The 14th International Conference on Ambient Systems, Networks and Technologies (ANT)*, volume 220, 180–186 (Procedia Computer Science, Elsevier), URL http://dx.doi.org/10.1016/j.procs.2023.03.025.

Cokyasar T, Subramanyam A, Larson J, Stinson M, Sahin O, 2022 *Time-constrained capacitated vehicle routing problem in urban e-commerce delivery. Transportation Research Record* URL http://dx.doi.org/10.1177/03611981221124592.

Cokyasar T, Verbas O, Auld J, 2023a *Electric vehicle scheduling problem with tour combinations. Procedia Computer Science* 220:413–420, URL http://dx.doi.org/10.1016/j.procs.2023.03.053.

Cokyasar T, Verbas O, Auld J, 2023b *Electric vehicle scheduling problem with tour combinations. Procedia Computer Science* 220:413–420, URL http://dx.doi.org/10.1016/j.procs.2023.03.053, the 14th International Conference on Ambient Systems, Networks and Technologies Networks (ANT) and The 6th International Conference on Emerging Data and Industry 4.0 (EDI40).

Cokyasar T, Verbas O, Davatgari A, Mohammadian A, 2023 *Solving the electric vehicle scheduling problem at large-scale. The 26th IEEE Intelligent Transportation Systems Conference*, in press for publication.

Daliah DR, 2023 *Pantograph for electric buses: From opportunity charging to depot charging.* Available at https://www.linkedin.com/pulse/pantograph-electric-buses-from-opportunity-charging-depot-daliah/ (accessed December 11, 2023).

Davatgari A, 2021 *Location planning for electric charging stations and wireless facilities in the era of autonomous vehicle operations.* URL http://dx.doi.org/10.25394/PGS.14512059.v1.

Diefenbach H, Emde S, Glock CH, 2023 *Multi-depot electric vehicle scheduling in in-plant production logistics considering non-linear charging models. European Journal of Operational Research* 306(2):828–848, URL http://dx.doi.org/https://doi.org/10.1016/j.ejor.2022.06.050.

Electrify America, 2022 *Pricing and plans for EV charging.* Available at https://www.electrifyamerica.com/pricing/ accessed on Aug. 1, 2022.

Ellis DR, 2017 *Value of Delay Time for Use in Mobility Monitoring Efforts. Texas Transportation Institute* Available at https://static.tti.tamu.edu/tti.tamu.edu/documents/TTI-2017-10.pdf accessed on Aug. 1, 2022.

Freling R, Wagelmans AP, Paixão JMP, 2001 *Models and algorithms for single-depot vehicle scheduling. Transportation Science* 35(2):165–180, URL http://dx.doi.org/10.1287/trsc.35.2.165.10135.

FTA, 2010 *Public transportation's role in responding to climate change*. URL https://www.transit.dot.gov/sites/fta.dot.gov/files/docs/PublicTransportationsRoleInRespondingToClimateChange2010.pdf.

General Transit Feed Specification, 2022 *Gtfs schedule reference*. URL https://gtfs.org/schedule/reference/.

Ghamami M, Kavianipour M, Zockaie A, Hohnstadt LR, Ouyang Y, 2020 *Refueling infrastructure planning in intercity networks considering route choice and travel time delay for mixed fleet of electric and conventional vehicles. Transportation Research Part C: Emerging Technologies* 120:102802, URL http://dx.doi.org/10.1016/j.trc.2020.102802.

Ghamami M, Zockaie A, Nie YM, 2016 *A general corridor model for designing plug-in electric vehicle charging infrastructure to support intercity travel. Transportation Research Part C: Emerging Technologies* 68:389–402, URL http://dx.doi.org/10.1016/j.trc.2016.04.016.

Guihaire V, Hao JK, 2008 *Transit network design and scheduling: A global review. Transportation Research Part A: Policy and Practice* 42(10):1251–1273, URL http://dx.doi.org/https://doi.org/10.1016/j.tra.2008.03.011.

Gurobi Optimization, LLC, 2020 *Gurobi optimizer reference manual*. Available at https://www.gurobi.com/wp-content/plugins/hd_documentations/documentation/9.0/refman.pdf accessed on Jun. 14, 2021.

Hof J, Schneider M, Goeke D, 2017 *Solving the battery swap station location-routing problem with capacitated electric vehicles using an AVNS algorithm for vehicle-routing problems with intermediate stops. Transportation Research Part B: Methodological* 97:102–112, URL http://dx.doi.org/10.1016/j.trb.2016.11.009.

Hovland Consulting LLC, 2020 *Zero-emissions road freight strategy.* Available at https://hewlett.org/library/zero-emissions-road-freight-strategy/ accessed on Jul. 7, 2022.

Illinois State Police, 2022 *Speed limit enforcement.* Available at https://www.isp.illinois.gov/TrafficSafety/SpeedLimitEnforcement accessed on Aug. 1, 2022.

Katoch S, Chauhan SS, Kumar V, 2021 *A review on genetic algorithm: past, present, and future. Multimedia Tools and Applications* 80:8091–8126, URL http://dx.doi.org/10.1007/s11042-020-10139-6.

Kernighan BW, Lin S, 1970 *An efficient heuristic procedure for partitioning graphs. The Bell System Technical Journal* 49(2):291–307, URL http://dx.doi.org/10.1002/j.1538-7305.1970.tb01770.x.

Li M, Tang P, Lin X, He F, 2022 *Multistage planning of electric transit charging facilities under build-operate-transfer model. Transportation Research Part D: Transport and Environment* 102:103118, URL http://dx.doi.org/10.1016/j.trd.2021.103118.

Li S, Huang Y, Mason SJ, 2016 *A multi-period optimization model for the deployment of public electric vehicle charging stations on network. Transportation Research Part C: Emerging Technologies* 65:128–143, URL http://dx.doi.org/10.1016/j.trc.2016.01.008.

Li X, Wang T, Li L, Feng F, Wang W, Cheng C, 2020 *Joint optimization of regular charging electric bus transit network schedule and stationary charger deployment considering partial charging policy and time-of-use electricity prices. Journal of Advanced Transportation* 2020:8863905, URL http://dx.doi.org/10.1155/2020/8863905.

Lightning eMotors, 2022 *Lightning electric class 6 low cab forward.* Available at https://lightningemotors.com/ accessed on Aug. 1, 2022.

Lin Y, Zhang K, Shen ZJM, Ye B, Miao L, 2019 *Multistage large-scale charging station planning for electric buses considering transportation network and power grid. Transportation Research Part C: Emerging Technologies* 107:423–443, URL http://dx.doi.org/10.1016/j.trc.2019.08.009.

Liu H, Wang DZ, 2017 *Locating multiple types of charging facilities for battery electric vehicles. Transportation Research Part B: Methodological* 103:30–55, URL http://dx.doi.org/10.1016/j.trb.2017.01.005.

Liu T, (Avi) Ceder A, 2020 *Battery-electric transit vehicle scheduling with optimal number of stationary chargers. Transportation Research Part C: Emerging Technologies* 114:118–139, URL http://dx.doi.org/https://doi.org/10.1016/j.trc.2020.02.009.

Liu X, Qu X, Ma X, 2021 *Optimizing electric bus charging infrastructure considering power matching and seasonality. Transportation Research Part D: Transport and Environment* 100:103057, URL http://dx.doi.org/10.1016/j.trd.2021.103057.

Liu Z, Song Z, 2018 *Dynamic charging infrastructure deployment for plug-in hybrid electric trucks. Transportation Research Part C: Emerging Technologies* 95:748–772, URL http://dx.doi.org/10.1016/j.trc.2018.08.011.

Liu Z, Song Z, He Y, 2018 *Planning of fast-charging stations for a battery electric bus system under energy consumption uncertainty. Transportation Research Record* 2672(8):96–107, URL http://dx.doi.org/10.1177/0361198118772953.

Londoño AA, Granada-Echeverri M, 2019 *Optimal placement of freight electric vehicles charging stations and their impact on the power distribution network. International Journal of Industrial Engineering Computations* 10, URL http://dx.doi.org/10.5267/j.ijiec.2019.3.002.

Metz B, Davidson O, Bosch P, Dave R, Meyer L, 2007 *Climate change 2007: Mitigation of climate change.* Available at https://agris.fao.org/agris-search/search.do?recordID=XF2008415344 ac-

cessed on Aug. 1, 2022.

Muñoz P, Franceschini EA, Levitan D, Rodriguez CR, Humana T, Correa Perelmuter G, 2022 *Comparative analysis of cost, emissions and fuel consumption of diesel, natural gas, electric and hydrogen urban buses. Energy Conversion and Management* 257:115412, URL http://dx.doi.org/https://doi.org/10.1016/j.enconman.2022.115412.

Niekerk MEK, Akker JM, Hoogeveen JA, 2017 *Scheduling electric vehicles. Public Transport* 9(1):155–176, URL http://dx.doi.org/10.1007/s12469-017-0164-0.

NumPy, 2022 *NumPy Reference*. Available at https://numpy.org/doc/stable/reference/index.html accessed on Dec. 22, 2022.

Perumal SS, Dollevoet T, Huisman D, Lusby RM, Larsen J, Riis M, 2021 *Solution approaches for integrated vehicle and crew scheduling with electric buses. Computers & Operations Research* 132:105268, URL http://dx.doi.org/https://doi.org/10.1016/j.cor.2021.105268.

Perumal SS, Lusby RM, Larsen J, 2022a *Electric bus planning & scheduling: A review of related problems and methodologies. European Journal of Operational Research* 301(2):395–413, URL http://dx.doi.org/https://doi.org/10.1016/j.ejor.2021.10.058.

Perumal SS, Lusby RM, Larsen J, 2022b *Electric bus planning & scheduling: A review of related problems and methodologies. European Journal of Operational Research* 301(2):395–413, URL http://dx.doi.org/10.1016/j.ejor.2021.10.058.

Rinaldi M, Picarelli E, D'Ariano A, Viti F, 2020 *Mixed-fleet single-terminal bus scheduling problem: Modelling, solution scheme and potential applications. Omega* 96:102070, URL http://dx.doi.org/https://doi.org/10.1016/j.omega.2019.05.006.

Schiffer M, Schneider M, Laporte G, 2018 *Designing sustainable mid-haul logistics networks with intra-route multi-resource facilities. European Journal of Operational Research* 265(2):517–532, URL

http://dx.doi.org/10.1016/j.ejor.2017.07.067.

Schiffer M, Walther G, 2017 *The electric location routing problem with time windows and partial recharging. European Journal of Operational Research* 260(3):995–1013, URL http://dx.doi.org/10.1016/j.ejor.2017.01.011.

Schiffer M, Walther G, 2018 *An adaptive large neighborhood search for the location-routing problem with intra-route facilities. Transportation Science* 52(2):331–352, URL http://dx.doi.org/10.1287/trsc.2017.0746.

Shojaei MS, Fakhrmoosavi F, Zockaie A, Ghamami M, Mittal A, Fishelson J, 2022 *Sustainable transportation networks incorporating green modes for urban freight delivery. Journal of Transportation Engineering, Part A: Systems* 148(6), URL http://dx.doi.org/10.1061/jtepbs.0000669.

Sistig HM, Sauer DU, 2023 *Metaheuristic for the integrated electric vehicle and crew scheduling problem. Applied Energy* 339:120915, URL http://dx.doi.org/https://doi.org/10.1016/j.apenergy.2023.120915.

Smith M, Castellano J, 2015 *Costs associated with non-residential electric vehicle supply equipment.* Published by the U.S. Department of Energy, available at https://afdc.energy.gov/files/u/publication/evse_cost_report_2015.pdf accessed on Aug. 1, 2022.

Speth D, Plötz P, Funke S, Vallarella E, 2022 *Public fast charging infrastructure for battery electric trucks—a model-based network for Germany. Environmental Research: Infrastructure and Sustainability* 2(2):025004, URL http://dx.doi.org/10.1088/2634-4505/ac6442.

Sule DR, 2007 *Production planning and industrial scheduling: examples, case studies and applications* (CRC press), ISBN 1-4200-4420-6.

Talebian H, Herrera OE, Tran M, Mérida W, 2018 *Electrification of road freight transport: Policy implications in British Columbia. Energy Policy* 115:109–118, URL http://dx.doi.org/10.1016/

j.enpol.2018.01.004.

The White House , 2022 *Fact sheet: Vice President Harris announces actions to accelerate clean transit buses, school buses, and trucks*. URL https://www.whitehouse.gov/briefing-room/statements-releases/2022/03/07/fact-sheet-vice-president-harris-announces-actions-to-accelerate-clean-transit-buses-school-buses-and-trucks/.

The White House, 2021 *Fact Sheet: President Biden Announces Steps to Drive American Leadership Forward on Clean Cars and Trucks*. Available at https://www.whitehouse.gov/briefing-room/statements-releases/2021/08/05/fact-sheet-president-biden-announces-steps-to-drive-american-leadership-forward-on-clean-cars-and-trucks/ (accessed December 11, 2023).

US Environmental Protection Agency, 2020 *Sources of greenhouse gas emissions*. Available at https://www.epa.gov/ghgemissions/sources-greenhouse-gas-emissions accessed on Jul. 7, 2022.

Uslu T, Kaya O, 2021 *Location and capacity decisions for electric bus charging stations considering waiting times. Transportation Research Part D: Transport and Environment* 90:102645, URL http://dx.doi.org/10.1016/j.trd.2020.102645.

Wang IL, Wang Y, Lin PC, 2016 *Optimal recharging strategies for electric vehicle fleets with duration constraints. Transportation Research Part C: Emerging Technologies* 69:242–254, URL http://dx.doi.org/10.1016/j.trc.2016.06.010.

Wang Y, Liao F, Lu C, 2022 *Integrated optimization of charger deployment and fleet scheduling for battery electric buses. Transportation Research Part D: Transport and Environment* 109:103382, URL http://dx.doi.org/10.1016/j.trd.2022.103382.

Wen M, Linde E, Ropke S, Mirchandani P, Larsen A, 2016 *An adaptive large neighborhood search heuristic for the electric vehicle scheduling problem. Computers & Operations Research* 76:73–83,

URL http://dx.doi.org/https://doi.org/10.1016/j.cor.2016.06.013.

Whitehead J, Whitehead J, Kane M, Zheng Z, 2021 *Exploring public charging infrastructure requirements for short-haul electric trucks. International Journal of Sustainable Transportation* 16(9):775–791, URL http://dx.doi.org/10.1080/15568318.2021.1921888.

Williams K, 2020 *How many hours can a truck driver drive?* Available at https://www.cdljobs.com/news-notes/news/how-many-hours-can-a-truck-driver-drive accessed on Aug. 1, 2022.

Worley O, Klabjan D, Sweda TM, 2012 *Simultaneous vehicle routing and charging station siting for commercial electric vehicles. International Electric Vehicle Conference*, 1–3 (IEEE), URL http://dx.doi.org/10.1109/IEVC.2012.6183279.

Wu W, Lin Y, Liu R, Jin W, 2022 *The multi-depot electric vehicle scheduling problem with power grid characteristics. Transportation Research Part B: Methodological* 155:322–347, URL http://dx.doi.org/https://doi.org/10.1016/j.trb.2021.11.007.

Xiong J, Bai C, Guan W, Chen Y, Xu Y, 2022 *Mixed optimization on vehicle scheduling and recharge scheduling of plug-in electric buses with consideration of partial recharge. Journal of Transportation Engineering, Part A: Systems* 148(2):04021111, URL http://dx.doi.org/10.1061/JTEPBS.0000643.

Xu X, Yu Y, Long J, 2023 *Integrated electric bus timetabling and scheduling problem. Transportation Research Part C: Emerging Technologies* 149:104057, URL http://dx.doi.org/https://doi.org/10.1016/j.trc.2023.104057.

Yang J, Sun H, 2015 *Battery swap station location-routing problem with capacitated electric vehicles. Computers & Operations Research* 55:217–232, URL http://dx.doi.org/10.1016/j.cor.2014.07.003.

Yao E, Liu T, Lu T, Yang Y, 2020 *Optimization of electric vehicle scheduling with multiple vehicle types in public transport. Sustainable Cities and Society* 52:101862, URL http://dx.doi.org/https://doi.org/10.1016/j.scs.2019.101862.

Yildirim S, Yildiz B, 2021 *Electric bus fleet composition and scheduling. Transportation Research Part C: Emerging Technologies* 129:103197, URL http://dx.doi.org/10.1016/j.trc.2021.103197.

Yilmaz M, Krein PT, 2013 *Review of battery charger topologies, charging power levels, and infrastructure for plug-in electric and hybrid vehicles. IEEE Transactions on Power Electronics* 28(5):2151–2169, URL http://dx.doi.org/10.1109/TPEL.2012.2212917.

Zhang A, Li T, Tu R, Dong C, Chen H, Gao J, Liu Y, 2021 *The effect of nonlinear charging function and line change constraints on electric bus scheduling. Promet - Traffic&Transportation* 33(4):527–538, URL http://dx.doi.org/10.7307/ptt.v33i4.3730.

Zhu ZH, Gao ZY, Zheng JF, Du HM, 2016 *Charging station location problem of plug-in electric vehicles. Journal of Transport Geography* 52:11–22, URL http://dx.doi.org/10.1016/j.jtrangeo.2016.02.002.

APPENDICES

Appendix Proofs

Proof of Lemma 1. We divide the proof of Lemma 1 into two parts: first we prove $z^*_{fk} \leq \sum_{c_{ir} \in C_{rft}, r \in \mathcal{R}} q_{c_{ir}fk}$, then $z^*_{fk} \geq 1$. To prove $z^*_{fk} \leq \sum_{c_{ir} \in C_{rft}, r \in \mathcal{R}} q_{c_{ir}fk}$, we use proof by contradiction. We suppose $z^*_{fk} > \sum_{c_{ir} \in C_{rft}, r \in \mathcal{R}} q_{c_{ir}fk}$. From Constraint (2.10) we have $x_{c_{ir}fkt} \leq q_{c_{ir}fk}$, which if we aggregate both sides of inequality on c_{ir}, $\sum_{c_{ir} \in C_{rft}, r \in \mathcal{R}} x_{c_{ir}fkt} \leq \sum_{c_{ir} \in C_{rft}, r \in \mathcal{R}} q_{c_{ir}fk}$ holds. Then, we can conclude that $z^*_{fk} > \sum_{c_{ir} \in C_{rft}, r \in \mathcal{R}} x_{c_{ir}fkt}$, which indicates that for a given $f \in \mathcal{F}$ and $k \in \mathcal{K}$, at all $t \in \mathcal{T}_{c_{ir}f}$ there exist unused chargers. This is in contradiction with the optimality of the z^*_{fk}, and therefore our assumption that $z^*_{fk} > \sum_{c_{ir} \in C_{rft}, r \in \mathcal{R}} q_{c_{ir}fk}$ is false, so $z^*_{fk} \leq \sum_{c_{ir} \in C_{rft}, r \in \mathcal{R}} q_{c_{ir}fk}$ holds. To prove $z^*_{fk} \geq 1$, from the condition of the Lemma 1, we have $\sum_{c_{ir} \in C_{rft}, r \in \mathcal{R}} q_{c_{ir}fk} \geq 1$ and from Constraint (2.10) we know $q_{c_{ir}fk} \leq \sum_{t \in \mathcal{T}_{c_{ir}f}} x_{c_{ir}fkt}$, which if we aggregate both sides of inequality on c_{ir}, $\sum_{c_{ir} \in C_{rft}, r \in \mathcal{R}} \sum_{t \in \mathcal{T}_{c_{ir}f}} x_{c_{ir}fkt} \geq \sum_{c_{ir} \in C_{rft}, r \in \mathcal{R}} q_{c_{ir}fk}$ holds. Then, we can conclude that $\sum_{c_{ir} \in C_{rft}, r \in \mathcal{R}} \sum_{t \in \mathcal{T}_{c_{ir}f}} x_{c_{ir}fkt} \geq 1$. This indicates at least for one $t \in \mathcal{T}_{c_{ir}f}$, $\sum_{c_{ir} \in C_{rft}, r \in \mathcal{R}} x_{c_{ir}fkt} \geq 1$. So from Constraints (2.3), we can conclude that for a given $f \in \mathcal{F}$ and $k \in \mathcal{K}$, if $\sum_{c_{ir} \in C_{rft}, r \in \mathcal{R}} q_{c_{ir}fk} \geq 1$, then $z^*_{fk} \geq 1$; otherwise, $\sum_{c_{ir} \in C_{rft}, r \in \mathcal{R}} q_{c_{ir}fk} = 0$, and from first part of the proof we know $z^*_{fk} \leq \sum_{c_{ir} \in C_{rft}, r \in \mathcal{R}} q_{c_{ir}fk}$, so $z^*_{fk} = 0$. □

Proof of Lemma 2. To prove Lemma 2, we aggregate Constraint (2.10) on c_{ir}, and we get

$$\sum_{\substack{c_{ir} \in C_{rft} \\ r \in \mathcal{R}}} x_{c_{ir}fkt} = \sum_{\substack{c_{ir} \in C_{rft} \\ r \in \mathcal{R}}} x^{\beta}_{c_{ir}fkt} - \sum_{\substack{c_{ir} \in C_{rft} \\ r \in \mathcal{R}}} x^{\alpha}_{c_{ir}fkt}.$$

If we suppose that all routes recharge at charger k in facility f at time t, then we have

$$\sum_{\substack{c_{ir}\in C_{rft}\\ r\in\mathcal{R}}} x^{\beta}_{c_{ir}fkt} - \sum_{\substack{c_{ir}\in C_{rft}\\ r\in\mathcal{R}}} x^{\alpha}_{c_{ir}fkt} = \sum_{\substack{c_{ir}\in C_{rft}\\ r\in\mathcal{R}}} q_{c_{ir}fk}.$$

Based on the definition of $x^{\alpha}_{c_{ir}fkt}$ and $x^{\beta}_{c_{ir}fkt}$, if a route recharges at charger k in facility f at time t after serving customer c_{ir}, $x^{\alpha}_{c_{ir}fkt} = 0$ and $x^{\beta}_{c_{ir}fkt} = 1$. Therefore, in the case that all routes are recharging at the same charger and time, $\sum_{\substack{c_{ir}\in C_{rft}\\ r\in\mathcal{R}}} x^{\alpha}_{c_{ir}fkt} = 0$ and $\sum_{\substack{c_{ir}\in C_{rft}\\ r\in\mathcal{R}}} x^{\beta}_{c_{ir}fkt} = 1$.

If we aggregate Constraints (2.22) and Constraints (2.23) on c_{ir}, we get

$$\sum_{\substack{c_{ir}\in C_{rft}\\ r\in\mathcal{R}}} d_{c_{ir}} + \sum_{\substack{c_{ir}\in C_{rft}\\ r\in\mathcal{R}}} T^{\tau}_{c_{ir}f} q_{c_{ir}fk} + \sum_{\substack{c_{ir}\in C_{rft}\\ r\in\mathcal{R}}} w_{c_{ir}fk} \leq \sum_{\substack{c_{ir}\in C_{rft}\\ r\in\mathcal{R}}} t + \sum_{\substack{c_{ir}\in C_{rft}\\ r\in\mathcal{R}}} T^{\Delta} - \sum_{\substack{c_{ir}\in C_{rft}\\ r\in\mathcal{R}}} \epsilon + \mathbb{M} \sum_{\substack{c_{ir}\in C_{rft}\\ r\in\mathcal{R}}} \left(1 - q_{c_{ir}fk} + x^{\alpha}_{c_{ir}fkt}\right)$$

and

$$\sum_{\substack{c_{ir}\in C_{rft}\\ r\in\mathcal{R}}} \left(t + T^{\Delta}\right) - \mathbb{M} \sum_{\substack{c_{ir}\in C_{rft}\\ r\in\mathcal{R}}} \left(2 - q_{c_{ir}fk} - x^{\alpha}_{c_{ir}fkt}\right) \leq \sum_{\substack{c_{ir}\in C_{rft}\\ r\in\mathcal{R}}} d_{c_{ir}} + \sum_{\substack{c_{ir}\in C_{rft}\\ r\in\mathcal{R}}} T^{\tau}_{c_{ir}f} q_{c_{ir}fk} + \sum_{\substack{c_{ir}\in C_{rft}\\ r\in\mathcal{R}}} w_{c_{ir}fk},$$

where $\sum_{\substack{c_{ir}\in C_{rft}\\ r\in\mathcal{R}}} x^{\alpha}_{c_{ir}fkt} = 0$. If we assume T^{Δ} is small ($T^{\Delta} \to 0$), then we can eliminate T^{Δ} and ϵ. Based on $\sum_{\substack{c_{ir}\in C_{rft}\\ r\in\mathcal{R}}} d_{c_{ir}} + \sum_{\substack{c_{ir}\in C_{rft}\\ r\in\mathcal{R}}} w_{c_{ir}fk} + \sum_{\substack{c_{ir}\in C_{rft}\\ r\in\mathcal{R}}} T^{\tau}_{c_{ir}f} q_{c_{ir}fk} \leq \sum_{\substack{c_{ir}\in C_{rft}\\ r\in\mathcal{R}}} t$ and $\sum_{\substack{c_{ir}\in C_{rft}\\ r\in\mathcal{R}}} d_{c_{ir}} + \sum_{\substack{c_{ir}\in C_{rft}\\ r\in\mathcal{R}}} w_{c_{ir}fk} + \sum_{\substack{c_{ir}\in C_{rft}\\ r\in\mathcal{R}}} T^{\tau}_{c_{ir}f} q_{c_{ir}fk} \geq \sum_{\substack{c_{ir}\in C_{rft}\\ r\in\mathcal{R}}} t - \mathbb{M}$ we can conclude that

$\sum_{\substack{c_{ir}\in C_{rft}\\ r\in\mathcal{R}}} w_{c_{ir}fk} \leq \sum_{\substack{c_{ir}\in C_{rft}\\ r\in\mathcal{R}}} t - \sum_{\substack{c_{ir}\in C_{rft}\\ r\in\mathcal{R}}} d_{c_{ir}} - \sum_{\substack{c_{ir}\in C_{rft}\\ r\in\mathcal{R}}} T^{\tau}_{c_{ir}f} q_{c_{ir}fk}$. Since t is a non-negative variable and the model minimizes the $w_{c_{ir}fk}$, $w_{c_{ir}fk} = 0$. □

Proof of Lemma 3. If each subproblem $p \in \mathscr{P}$ has a feasible solution X_p, then it means that blocks in $\mathcal{B}_p$ form one or more feasible bus runs. Each run in a given subproblem $p \in \mathscr{P}$ on the current horizon is connected to at least one run in the next horizon within the same subproblem $p \in \mathscr{P}$. Since there are no constraints on charging capacity or garage space, merging the solutions X_p into $X_{\mathcal{M}}$ is analogous to solving separate problems for separate garages. □

Appendix Pseudocodes

Algorithm A.1: Preliminary functions (see e.g., NumPy (2022) for details)

Function Abs(a):

    /* finds absolute value of a. */

return absolute value of a

Function Enumerate($\mathcal{A}$):

    /* returns index and item of $\mathcal{A}$. */

return index and item of $\mathcal{A}$

Function Int(a):

    /* finds integer part of a. */

return integer part of a

Function Rand(a, b):

    /* finds a pseudo-random real number c between a and b. */

return c, such that $a \leq c \in \mathbb{R} \leq b$

Function RandChoice($\mathcal{A}$, $\mathcal{B}$ *(optional)*, n):

    /* choose n elements from list (or set) $\mathcal{A}$ given a list of weights $\mathcal{B}$. */

return $\mathcal{Z}$, that is $\mathcal{Z} \subseteq \mathcal{A}$ and $|\mathcal{Z}| = n$

Function SortGiven($\mathcal{A}$, $\mathcal{B}$, R *(optional)*):

    /* sorts $\mathcal{A}$ descending given $\mathcal{B}$ if $R = True$, otherwise sorts $\mathcal{A}$ ascending given $\mathcal{B}$. */

return $\mathcal{A}$ sorted

Algorithm A.2: Pseudocode for INITIALIZATION

Input : $\mathcal{C}_r$, $\mathcal{F}_{c_{ir}}$, $\mathcal{K}$, $\mathcal{R}$, $\overline{B}$, B^{ι}, B^{ω}, $C^{\alpha=0}$, T_r^{μ}, $T_{c_{ir}f}^{\delta}$

Output: $\widehat{\mathcal{F}}_{c_{ir}}$, $\widehat{\mathcal{K}}_{c_{ir}}$

Function INITIALIZATION():

/* Parameter $C^{\alpha=0}$ is the probability that a recharging will not occur after servicing a given cluster, and T_r^{ρ} is the travel time for route r excluding service and recharging times. */

$f^{closest} \leftarrow \{\}$; $\widehat{\mathcal{F}}_{c_{ir}} \leftarrow \{\}$;

/* $\widehat{\mathcal{F}}_{c_{ir}}$ stores the facility that will be visited after serving c_{ir}; visiting 0 denotes no recharging. */

for $r \in \mathcal{R}$, **do**

  for $c_{ir} \in \mathcal{C}_r$, **do**

    $W \leftarrow$; // a list of weights in $[0, 1]$ based on $\mathcal{F}_{c_{ir}}$

    $f^{closest}(c_{ir}) \leftarrow$RANDCHOICE(SORTGIVEN($\mathcal{F}_{c_{ir}}, T_{c_{ir}f}^{\delta}$), W, 1);

    $\widehat{\mathcal{F}}_{c_{ir}} \leftarrow$RANDCHOICE($[0, f^{closest}(c_{ir})]$, $[C^{\alpha=0},\ 1 - C^{\alpha=0}]$, 1);

for $r \in \mathcal{R}$, **do**

  if $\widehat{\mathcal{F}}_{c_{ir}} = 0\ \forall c_{ir} \in \mathcal{C}_r$, **then**

    $\mathcal{C}^{select} \leftarrow$RANDCHOICE($\mathcal{C}_r$, $\lceil$(ABS($(B_r^{\iota} - B_r^{\omega} - T_r^{\mu})/\overline{B}$))$\rceil$);

    /* $\lceil$(ABS($(B_r^{\iota} - B_r^{\omega} - T_r^{\mu})/\overline{B}$))$\rceil$ denotes the minimum number of charging facilities need to be visited. */

  for $c' \in \mathcal{C}^{select}$, **do**

    $\widehat{\mathcal{F}}_{c_{ir}}(c') \leftarrow f^{closest}(c')$;

$\widehat{\mathcal{K}}_{c_{ir}} \leftarrow \{\}$;

/* $\widehat{\mathcal{K}}_{c_{ir}}$ stores the charger type that will be used after c_{ir}; 0 refers to not visiting a recharging station. */

$W \leftarrow$; // a list of weights in $[0, 1]$ based on charger type

for $r \in \mathcal{R}$, **do**

  for $c_{ir} \in \mathcal{C}_r$, **do**

    if $\widehat{\mathcal{F}}_{c_{ir}} \neq 0$, **then**

      $\widehat{\mathcal{K}}_{c_{ir}} \leftarrow$RANDCHOICE($\mathcal{K}$, W, 1);

    else

      $\widehat{\mathcal{K}}_{c_{ir}} \leftarrow 0$;

Algorithm A.3: Pseudocode for CROSSOVER

Input : $Sols$, i, j

Output: $newSols$

Function `CROSSOVER()`:

```
newSols ← {};
for element ← 1 to |Sols(i)|, do
    if RANDCHOICE([i, j], 1) = i, then
        newSols(element) ← Sols(i)(element);
    else
        newSols(element) ← Sols(j)(element);
```

Algorithm A.4: Pseudocode for MUTATION

Input : $Sols$, P^{mutate}

Output: $newSols$

Function `MUTATION()`:

```
N^mutate ← INT(|Sols|P^mutate);
/* The percent of solution to be mutated is denoted by P^mutate, and N^mutate is the number of
   elements to mutate.                                                                        */
newSols ← {};
for i ∈RANDCHOICE(Sols, N^mutate), do
    if Sols(i) indicates not recharging after visiting i, then
        newSols(i) ←; // Closest facility in terms of travel time and charger type 1
    else
        newSols(i) ←; // Next closest facility in terms of travel time and charger type
           incremented by 1
```

Algorithm A.5: Pseudocode for EVALUATOR

Input : $\mathcal{C}_r$, $\mathcal{F}$, $\mathcal{K}$, $\mathcal{R}$, $\mathcal{T}$, $\overline{B}$, B^{ι}_r, B^{ω}_r, C^{ρ}, C^{ξ}_k, C^{ν}_k, C^{ϕ}_f, $\underline{N}$, $\bar{N}$, R_k, $T^{\tau}_{c_{ir}c_{jr}}$, $T^{\kappa}_{c_{ir}}$, $T^{\delta}_{c_{ir}f}$, T^{ρ}_r, $q_{c_{ir}fk}$

Output: $\mathbf{C}$

Function EVALUATOR():

$\bar{z}_{fk} \leftarrow \sum_{c_{ir} \in \mathcal{C}_{rft}} q_{c_{ir}fk}$;

for $f \in \mathcal{F}$, **do**

  for $k \in \mathcal{K}$, **do**

    if $\sum_{c_{ir} \in \mathcal{C}_{rft}} q_{c_{ir}fk} \geq 0$, **then**

      $\underline{z}_{fk} \leftarrow 1$;

$(\underline{b}_{c_{ir}}, \underline{b}'_{c_{ir}f}, \underline{\mathbf{C}}, \underline{d}_{c_{ir}}, \underline{u}_{c_{ir}fk}, \underline{w}_{c_{ir}fk}, \underline{x}_{c_{ir}fkt}, \underline{y}_f) \leftarrow$ LOWERLEVELEVALUATOR($\mathcal{C}_r$, $\mathcal{F}$, $\mathcal{K}$, $\mathcal{R}$, $\mathcal{T}$, $\overline{B}$, B^{ι}_r, B^{ω}_r, C^{ρ}, C^{ξ}_k, C^{ν}_k, C^{ϕ}_f, R_k, T^{ρ}_r, $T^{\tau}_{c_{ir}c_{jr}}$, $T^{\kappa}_{c_{ir}}$, $T^{\delta}_{c_{ir}f}$, $q_{c_{ir}fk}$, $\underline{z}_{fk}$);

$(\bar{b}_{c_{ir}}, \bar{b}'_{c_{ir}f}, \bar{\mathbf{C}}, \bar{d}_{c_{ir}}, \bar{u}_{c_{ir}fk}, \bar{w}_{c_{ir}fk}, \bar{x}_{c_{ir}fkt}, \bar{y}_f) \leftarrow$ LOWERLEVELEVALUATOR($\mathcal{C}_r$, $\mathcal{F}$, $\mathcal{K}$, $\mathcal{R}$, $\mathcal{T}$, $\overline{B}$, B^{ι}_r, B^{ω}_r, C^{ρ}, C^{ξ}_k, C^{ν}_k, C^{ϕ}_f, R_k, T^{ρ}_r, $T^{\tau}_{c_{ir}c_{jr}}$, $T^{\kappa}_{c_{ir}}$, $T^{\delta}_{c_{ir}f}$, $q_{c_{ir}fk}$, $\bar{z}_{fk}$);

$\bar{z}_{fk} \leftarrow \sum_{c_{ir} \in \mathcal{C}_{rft}, t \in \mathcal{T}} \bar{x}_{c_{ir}fkt}$;

while $\underline{\mathbf{C}}$ is infeasible, **do**

  $\mathcal{L} \leftarrow \{\}$;

  for $f \in \mathcal{F}$, **do**

    for $k \in \mathcal{K}$, **do**

      if $\underline{z}_{fk} \geq 0$, **then**

        $\mathcal{L} \leftarrow \mathcal{L} \cup \{(f,k)\}$;

  SORT($\mathcal{L}$, $\sum_{c_{ir} \in \mathcal{C}_{rft}} \underline{w}_{c_{ir}fk}$, $R = True$);

  $N \leftarrow$ RAND $\left(\underline{N}, \bar{N}\right)$;

  for $(f,k) \in \mathcal{L}$, **do**

    $\underline{z}_{fk} \leftarrow \underline{z}_{fk} + 1$;

  $\bar{N} \leftarrow 1/2 \left(\bar{N} + \underline{N}\right)$;

if $\bar{\mathbf{C}} \leq \underline{\mathbf{C}}$, **then**

  $z_{fk} \leftarrow$ ZUUPDATER($\mathcal{C}_r$, $\mathcal{F}$, $\mathcal{K}$, $\mathcal{R}$, $\mathcal{T}$, $\overline{B}$, B^{ι}_r, B^{ω}_r, C^{ρ}, C^{ξ}_k, C^{ν}_k, C^{ϕ}_f, $\underline{N}$, $\bar{N}$, R_k, T^{ρ}_r, $T^{\tau}_{c_{ir}c_{jr}}$, $T^{\kappa}_{c_{ir}}$, $T^{\delta}_{c_{ir}f}$, $q_{c_{ir}fk}$, $\underline{z}_{fk}$, $\bar{z}_{fk}$);

else

  $z_{fk} \leftarrow$ ZLUPDATER($\mathcal{C}_r$, $\mathcal{F}$, $\mathcal{K}$, $\mathcal{R}$, $\mathcal{T}$, $\overline{B}$, B^{ι}_r, B^{ω}_r, C^{ρ}, C^{ξ}_k, C^{ν}_k, C^{ϕ}_f, $\underline{N}$, $\bar{N}$, R_k, T^{ρ}_r, $T^{\tau}_{c_{ir}c_{jr}}$, $T^{\kappa}_{c_{ir}}$, $T^{\delta}_{c_{ir}f}$, $q_{c_{ir}fk}$, $\underline{z}_{fk}$, $\bar{z}_{fk}$);

$(b_{c_{ir}}, b'_{c_{ir}f}, \mathbf{C}, u_{c_{ir}fk}, d_{c_{ir}}, w_{c_{ir}fk}, x_{c_{ir}fkt}, y_f) \leftarrow$ LOWERLEVELEVALUATOR($\mathcal{C}_r$, $\mathcal{F}$, $\mathcal{K}$, $\mathcal{R}$, $\mathcal{T}$, $\overline{B}$, B^{ι}_r, B^{ω}_r, C^{ρ}, C^{ξ}_k, C^{ν}_k, C^{ϕ}_f, R_k, T^{ρ}_r, $T^{\tau}_{c_{ir}c_{jr}}$, $T^{\kappa}_{c_{ir}}$, $T^{\delta}_{c_{ir}f}$, $q_{c_{ir}fk}$, z_{fk});

Algorithm A.6: Pseudocode for LowerLevelEvaluator

Input : $\mathcal{C}_r$, $\mathcal{F}$, $\mathcal{K}$, $\mathcal{R}$, $\mathcal{T}$, $\overline{B}$, B^{ι}_r, B^{ω}_r, C^{ρ}, C^{ξ}_k, C^{ν}_k, C^{ϕ}_f, R_k, T^{ρ}_r, $T^{\tau}_{c_{ir}c_{jr}}$, $T^{\kappa}_{c_{ir}}$, $T^{\delta}_{c_{ir}f}$, $q_{c_{ir}fk}$, z_{fk}

Output: *Out*

Function LowerLevelEvaluator():

$y_f \leftarrow$ yCalculation$\big(\mathcal{F},\ \mathcal{K},\ z_{fk}\big)$;

$\Big(\mathcal{L}_{fk}, b'_{c_{ir}f}, u_{c_{ir}fk}\Big) \leftarrow$ uCalculation($\mathcal{C}_r$, $\mathcal{F}$, $\mathcal{K}$, $\mathcal{R}$, $\overline{B}$, B^{ι}_r, B^{ω}_r, R_k, T^{ρ}_r, $T^{\tau}_{c_{ir}c_{jr}}$, $T^{\kappa}_{c_{ir}}$, $q_{c_{ir}fk}$;

$\Big(b_{c_{ir}}, d_{c_{ir}}, d'_{c_{ir}f}d''_{c_{ir}f}, w_{c_{ir}fk}\Big) \leftarrow$ wCalculation($\mathcal{C}_r$, $\mathcal{F}$, $\mathcal{K}$, $\mathcal{L}_{fk}$, $\mathcal{R}$, $T^{\delta}_{c_{ir}f}$, $T^{\tau}_{c_{ir}c_{jr}}$, $T^{\kappa}_{c_{ir}}$, $q_{c_{ir}fk}$, $u_{c_{ir}fk}$);

$x_{c_{ir}fkt} \leftarrow$xCalculation$\Big(\mathcal{C}_r,\ \mathcal{F},\ \mathcal{K},\ \mathcal{T},\ d'_{c_{ir}f},\ d''_{c_{ir}f},\ q_{c_{ir}fk},\ u_{c_{ir}fk}\Big)$;

$\mathbf{C} \leftarrow \sum_{\substack{c_{ir}\in\mathcal{C}_r, r\in\mathcal{R},\\ f\in\mathcal{F}_{c_{ir}}, k\in\mathcal{K}}} \Big[C^{\rho}\Big(T^{\delta}_{c_{ir}f}q_{c_{ir}fk} + w_{c_{ir}fk}\Big) + (C^{\rho} + C^{\xi}_k)u_{c_{ir}fk}\Big] + \sum_{f\in\mathcal{F}} C^{\phi}_f y_f + \sum_{f\in\mathcal{F}, k\in\mathcal{K}} C^{\nu}_k z_{fk}$;

if ??–?? hold, **then**

  $Out \leftarrow (b_{c_{ir}}, b'_{c_{ir}f}, \mathbf{C}, d_{c_{ir}}, u_{c_{ir}fk}, w_{c_{ir}fk}, x_{c_{ir}fkt}, y_f)$;

else

  $Out \leftarrow None$;

Algorithm A.7: Pseudocode for calculating $\bar{z}_{fk}$

Input : $\mathcal{C}_r$, $\mathcal{F}$, $\mathcal{K}$, $\mathcal{R}$, $\mathcal{T}$, $\overline{B}$, B^{ι}_{r}, B^{ω}_{r}, C^{ρ}, C^{ξ}_{k}, C^{ν}_{k}, C^{ϕ}_{f}, $\underline{N}$, $\bar{N}$, R_k, T^{ρ}_{r}, $T^{\tau}_{c_{ir}c_{jr}}$, $T^{\kappa}_{c_{ir}}$, $T^{\delta}_{c_{ir}f}$, $q_{c_{ir}fk}$, $\underline{z}_{fk}$, $\bar{z}_{fk}$

Output: z_{fk}

Function zuUpdater():

```
while True, do
    ℒ ← {};
    for f ∈ ℱ, do
        for k ∈ 𝒦, do
            if z̄_fk − z_fk ≥ 1 and z_fk ≥ 0 , then
                ℒ ← ℒ ∪ {(f, k)};
    Sort(ℒ, z̄_fk, R = True);
    N ← Rand(N̲, N̄);
    z̿_fk ← z̄_fk;
    for (f, k) ∈ ℒ, do
        z̿_fk ← z̄_fk − 1;
    N̄ ← 1/2 (N̄ + N̲);
    (b̿_{c_ir}, b̿'_{c_irf}, C̿, d̿_{c_ir}, ū̿_{c_irfk}, w̿_{c_irfk}, x̿_{c_irfkt}, ȳ̿_f) ← LowerLevelEvaluator(𝒞_r, ℱ, 𝒦, ℛ, 𝒯, B̄, B^ι_r,
      B^ω_r, C^ρ, C^ξ_k, C^ν_k, C^φ_f, R_k, T^ρ_r, T^τ_{c_ir c_jr}, T^κ_{c_ir}, T^δ_{c_irf}, q_{c_irfk}, z̿_fk);
    if C̿ ≤ C̄, then
        z̄_fk ← z̿_fk;
    else
        z_fk ← z̄_fk;
        Break;
```

Algorithm A.8: Pseudocode for calculating $\underline{z}_{fk}$

Input : $\mathcal{C}_r$, $\mathcal{F}$, $\mathcal{K}$, $\mathcal{R}$, $\mathcal{T}$, $\overline{B}$, B^{ι}_{r}, B^{ω}_{r}, C^{ρ}, C^{ξ}_{k}, C^{ν}_{k}, C^{ϕ}_{f}, $\underline{N}$, $\bar{N}$, T^{ρ}_{r}, $T^{\tau}_{c_{ir}c_{jr}}$, $T^{\kappa}_{c_{ir}}$, $T^{\delta}_{c_{ir}f}$, R_k, $q_{c_{ir}fk}$, $\underline{z}_{fk}$, $\bar{z}_{fk}$

Output: z_{fk}

Function zlUpdater():

while True, **do**

$\mathcal{L} \leftarrow \{\}$;

for $f \in \mathcal{F}$, **do**

for $k \in \mathcal{K}$, **do**

if $\bar{z}_{fk} - \underline{z}_{fk} \geq 1$ and $\underline{z}_{fk} \geq 0$, **then**

$\mathcal{L} \leftarrow \mathcal{L} \cup \{(f,k)\}$;

Sort($\mathcal{L}$, $\sum_{c_{ir} \in \mathcal{C}_{rft}} \underline{w}_{c_{ir}fk}$, $R = True$);

$N \leftarrow$ Rand $\left(\underline{N}, \bar{N}\right)$;

$\underline{\underline{z}}_{fk} \leftarrow \underline{z}_{fk}$;

for $(f,k) \in \mathcal{L}$, **do**

$\underline{\underline{z}}_{fk} \leftarrow \underline{\underline{z}}_{fk} + 1$;

$\bar{N} \leftarrow 1/2\left(\bar{N} + \underline{N}\right)$;

$(\underline{\underline{b}}_{c_{ir}}, \underline{\underline{b}}'_{c_{ir}f}, \underline{\underline{\mathbf{C}}}, \underline{\underline{d}}_{c_{ir}}, \underline{\underline{u}}_{c_{ir}fk}, \underline{\underline{w}}_{c_{ir}fk}, \underline{\underline{x}}_{c_{ir}fkt}, \underline{\underline{y}}_{f}) \leftarrow$ LowerLevelEvaluator($\mathcal{C}_r$, $\mathcal{F}$, $\mathcal{K}$, $\mathcal{R}$, $\mathcal{T}$, $\overline{B}$, B^{ι}_{r}, B^{ω}_{r}, C^{ρ}, C^{ξ}_{k}, C^{ν}_{k}, C^{ϕ}_{f}, R_k, T^{ρ}_{r}, $T^{\tau}_{c_{ir}c_{jr}}$, $T^{\kappa}_{c_{ir}}$, $T^{\delta}_{c_{ir}f}$, $q_{c_{ir}fk}$, $\underline{\underline{z}}_{fk}$);

if $\underline{\underline{\mathbf{C}}} \leq \underline{\mathbf{C}}$, **then**

$\underline{z}_{fk} \leftarrow \underline{\underline{z}}_{fk}$;

else

$z_{fk} \leftarrow \underline{z}_{fk}$;

Break;

Algorithm A.9: Pseudocode for calculating y_f

Input : $\mathcal{F}$, $\mathcal{K}$, z_{fk}

Output: y_f

Function yCalculation():

```
for f ∈ F, do
    if Σ_{k∈K} z_fk ≥ 0, then
        y_f ← 1;
    else
        y_f ← 0;
```

Algorithm A.10: Pseudocode for calculating $u_{c_{ir}fk}$

Input : $\mathcal{C}_r$, $\mathcal{F}$, $\mathcal{K}$, $\mathcal{R}$, $\overline{B}$, B^{ι}_r, B^{ω}_r, T^{ρ}_r, $T^{\tau}_{c_{ir}c_{jr}}$, $T^{\kappa}_{c_{ir}}$, $q_{c_{ir}fk}$

Output: $\mathcal{L}_{fk}, b'_{c_{ir}f}, u_{c_{ir}fk}$

Function uCalculation():

- **for** $r \in \mathcal{R}$, **do**
  - **for** $f \in \mathcal{F}$, **do**
    - **for** $k \in \mathcal{K}$, **do**
      - $\mathcal{L}_{fk} \leftarrow \{\}$;
  - $e_r \leftarrow \textsc{Int}\left(\textsc{Abs}\left(B^{\iota}_r - B^{\omega}_r - T^{\rho}_r\right) + 1\right)$;
  - $\mathcal{L} \leftarrow \{\}$;
  - **for** $c_{ir} \in \mathcal{C}_r$, **do**
    - **for** $f \in \mathcal{F}$, **do**
      - **for** $k \in \mathcal{K}$, **do**
        - **if** $q_{c_{ir}fk} = 1$ **then**
          - $\mathcal{L} \cup \{(c_{ir}fk)\}$;
          - $\mathcal{L}_{fk} \cup \{(rc_{ir})\}$;
  - $m \leftarrow 1$;
  - **while** $e_r \geq 0$, **do**
    - **if** $m = 1$, **then**
      - $(c_{ir}fk) \leftarrow \mathcal{L}\{m\}$;
      - $b'_{c_{ir}f} \leftarrow B^{\iota}_r - \sum_{c_{jr} \leftarrow c_{0r}}^{c_{jr} \leftarrow c_{i-1,r}} T^{\tau}_{c_{jr}c_{j+1,r}} - T^{\tau}_{c_{ir}f}$;
      - $u_{c_{ir}fk} \leftarrow \min\{e_r, \overline{B} - b'_{c_{ir}f}\}$;
    - **else**
      - $(c_{ir}fk) \leftarrow \mathcal{L}\{m\}$;
      - $\left(c'_{ir}f'k'\right) \leftarrow \mathcal{L}\{m-1\}$;
      - $b'_{c_{ir}f} \leftarrow b'_{c'_{ir}f'} + u_{c'_{ir}f'k'} - \sum_{c_{jr} \leftarrow c_{0r}}^{c_{jr} \leftarrow c_{i-1,r}} T^{\tau}_{c_{jr}c_{j+1,r}} - T^{\tau}_{c_{ir}f}$;
      - $u_{c_{ir}fk} \leftarrow \min\{e_r, \overline{B} - b'_{c_{ir}f}\}$;
    - $m \leftarrow m + 1$;
    - $e_r \leftarrow e_r - u_{c_{ir}fk}$;

Algorithm A.11: Pseudocode for calculating $w_{c_{ir}fk}$

Input : $\mathcal{C}_r$, $\mathcal{F}$, $\mathcal{K}$, $\mathcal{L}_{fk}$, $\mathcal{R}$, $T^{\delta}_{c_{ir}f}$, R_k, $T^{\tau}_{c_{ir}c_{jr}}$, $T^{\kappa}_{c_{ir}}$, $q_{c_{ir}fk}$, $u_{c_{ir}fk}$

Output: $b_{c_{ir}}, d_{c_{ir}}, d'_{c_{ir}f} d''_{c_{ir}f}, w_{c_{ir}fk}$

Function wCalculation():

- **for** $iter \leftarrow 1$ **to** $|\mathcal{L}_{fk}|$, **do**
  - **for** $r \in \mathcal{R}$, **do**
    - $d_{c_{0r}} \leftarrow 0$; $b_{c_{0r}} \leftarrow B^{t}_{r}$;
    - **for** $c_{ir} \in \mathcal{C}_r$, **do**
      - **if** $\sum_{f\in\mathcal{F},k\in\mathcal{K}} q_{c_{i-1,r}fk} = 1$, **then**
        - $d_{c_{ir}} \leftarrow d_{c_{i-1,r}} + T^{\delta}_{c_{i-1,r}f} + w_{c_{ir}fk} + u_{c_{ir}fk} + T^{\kappa}_{c_{ir}}$;
        - $b_{c_{ir}} \leftarrow b_{c_{i-1,r}} - T^{\delta}_{c_{i-1,r}f} + R_k u_{c_{ir}fk}$;
      - **else**
        - $d_{c_{ir}} \leftarrow d_{c_{i-1,r}} + T^{\tau}_{c_{i-1,r}c_{ir}} + T^{\kappa}_{c_{ir}}$;
        - $b_{c_{ir}} \leftarrow b_{c_{i-1,r}} - T^{\tau}_{c_{ir}c_{jr}}$;
      - **for** $f \in \mathcal{F}$, **do**
        - **for** $k \in \mathcal{K}$, **do**
          - **if** $q_{c_{ir}fk} = 1$, **then**
            - $d'_{c_{ir}f} \leftarrow d_{c_{ir}} + T^{\tau}_{c_{ir}f}$;
  - **for** $f \in \mathcal{F}$, **do**
    - **for** $k \in \mathcal{K}$, **do**
      - Sort($\mathcal{L}_{fk}$, $d'_{c_{ir}f}$, $R = True$);
      - **for** $j, (r, c_{ir}) \in$ Enumerate $\left(\mathcal{L}_{fk}\right)$, **do**
        - **if** $j = 0$, **then**
          - $w_{c_{ir}fk} \leftarrow 0$;
          - $d''_{c_{ir}f} \leftarrow d'_{c_{ir}f} + u_{c_{ir}fk}$;
        - **else**
          - $\left(r', c'_{ir'}\right) \leftarrow \mathcal{L}_{fk}\{j\}$;
          - $w_{c_{ir}fk} \leftarrow \max\{d''_{c'_{ir'}f} - d'_{c_{ir}f}, 0\}$;
          - $d''_{c_{ir}f} \leftarrow d'_{c_{ir}f} + w_{c_{ir}fk} + u_{c_{ir}fk}$;

Algorithm A.12: Pseudocode for calculating $x_{c_{ir}fkt}$

Input : $\mathcal{C}_r$, $\mathcal{F}$, $\mathcal{K}$, $\mathcal{T}$, $d'_{c_{ir}f}$, $d''_{c_{ir}f}$, $q_{c_{ir}fk}$, $u_{c_{ir}fk}$

Output: $x_{c_{ir}fkt}$

Function xCalculation():

```
for c_ir ∈ C_r, do
    for f ∈ F, do
        for k ∈ K, do
            for t ∈ T, do
                if t ≥ d'_{c_ir f} and t ≤ d''_{c_ir f}, then
                    x_{c_ir fkt} ← 1;
                else
                    x_{c_ir fkt} ← 0;
```

VITA

NAME Amir Davatgari

EDUCATION

Ph.D. in Transportation Engineering and Planning 2021-2024
Department of Civil, Material, and Environmental Engineering, University of Illinois at Chicago (UIC)

M.S. in Transportation Engineering 2019-2021
Lyles School of Civil Engineering, Purdue University

B.S. in Civil Engineering 2014-2018
Department of Civil Engineering, Sharif University of Technology

PUBLICATIONS

Davatgari, A., Cokyasar, T., Subramanyam, A., Larson, J., Mohammadian, A. "Electric Vehicle Supply Equipment Location and Capacity Allocation for Fixed-Route Networks." Under Review In European Journal of Operational Research.

Davatgari, A., Cokyasar, T., Verbas, O., Mohammadian, A. "Heuristic Approach for Single Depot Electric Vehicle Scheduling Problem with Next Day Operability Constraints." Under Review In Transportation Research Part C: Emerging Technologies.

Davatgari, A., Verbas, O., Cokyasar, T., Mohammadian, A. "Optimization of Electric Bus Scheduling and Charger Location" Under Review In The 15th International Conference on Ambient Systems, Networks and Technologies (ANT, 2024).

Davatgari, A., Mohammadi, M., Cokyasar, T., Mohammadian, A., Auld, J. "A Label-correcting Algorithm for Constrained One-to-Many K-shortest Path Problem with Replenishment" Under Review In The 15th International Conference on Ambient Systems, Networks and Technologies (ANT, 2024).

Mohammadi, M., Davatgari, A., Shabanpour, R., Asgharpour, S., Mohammadian, A., Derrible, S., Pendyala, R. M., Salon, D. "The Interaction between the Recent Evolution of Working from Home and Online Shopping." Under Review In Transportation Research Part C: Emerging Technologies.

Arefin, N., Gurumurthy, K., Davatgari, A., Auld, J., Mohammadian, A. "Exploring the Shared E-Scooter Adoption Behavior: A Case Study of Chicago."Under Review In Transportation Research Record

Javadinasr, M., Davatgari, A., Rahimi, E., Mohammadi, M., Mohammadian, A., Auld, J. "Coupling Shared E-scooters and Public Transit: A Spatial and Temporal Analysis." In Transportation Letters (2023).

Cokyasar, T., Davatgari, A., Mohammadian, A. "An optimization model for solving the route clustering problem." In Procedia Computer Science (2023), DOI: 10.1016/j.procs.2023.03.025.

Miralinaghi, M., Davatgari, A., Seilabi, S., Labi, S. "Contract Bundling Considerations in Urban Road Project Scheduling: A Bi-level Multi-Objective Optimization Methodology." In Computer-Aided Civil and Infrastructure Engineering (2022), DOI: 10.1111/mice.12740.

Mohammadi, M., Rahimi, E., Davatgari, A., Javadinasr, M., Mohammadian, A., Bhagat-Congway, M. W., Salon, D., Derrible, S., Pendyala, R. M., Khoeini S. "Examining the Persistence of Telecommuting after the COVID-19 Pandemic." In Transportation Letters (2023), DOI: 10.1080/19427867.2022.2077582.

Seilabi, S., T. Tabesh, M., Davatgari, A., Miralinaghi, M., Labi, S. "Promoting Autonomous Vehicles using Travel Demand and Lane Management Strategies considering AV dedicated lanes." In Frontiers in Built Environment (2021), DOI: 10.3389/fbuil.2020.560116.

Asgharpour, S., Davatgari, A., Javadinasr, M., Mohammadi, M., Mohammadian, A., Abraham, C. "Equity of Shared E-scooter Systems: Evidence from Chicago 2019 Pilot Program." In International Conference on Transportation and Development, Austin, Texas, 2023.

Javadinasr, M., Magassy, T., Rahimi, E., Mohammadi, M., Davatgari, A., Mohammadian, A., Chauhan, R., Bhagat-Conway, M., Pendyala, R., Salon, D., Derrible, S., Khoeini, S. "Observed and Expected Impacts of COVID-19 on Travel Behavior in the United States: A Panel Study Analysis." In 101st Annual Meeting Transportation Research Board, 2022.